

**IMMOBILIZATION OF MYOGLOBIN FROM HORSE SKELETAL MUSCLE
(Mb) AND HEMOGLOBIN I (HbI) FROM *LUCINA PECTINATA* IN
HYDROPHILIC POLYMER NETWORKS FOR H₂S BIOSENSOR
APPLICATION**

By
Angelines A. Castro Forero

A thesis submitted in partial fulfillment of the requirements for the degree of

MASTER OF SCIENCE
in
CHEMICAL ENGINEERING

UNIVERSITY OF PUERTO RICO
MAYAGÜEZ CAMPUS

2005

Approved by:

Juan López Garriga, Ph.D.
Member, Graduate Committee

Date

Lorenzo Saliceti Piazza, Ph.D.
Member, Graduate Committee

Date

Madeline Torres Lugo, Ph.D.
President, Graduate Committee

Date

Joseph Bonaventura, Ph.D.
Representative of Graduate Studies

Date

Nelson Cardona Martínez, Ph.D.
Chairperson of the Department

Date

Jose A. Mari Mutt, Ph.D.
Director of Graduate Studies

Date

ABSTRACT

Hemeproteins are known for their spectroscopic properties which change during the binding of specific ligands. This project envisioned the immobilization of myoglobin from horse skeletal muscle (Mb) and hemoglobin I from *Lucina pectinata* (HbI) in hydrophilic polymer networks to use them as recognition elements in biosensor applications. Two immobilization techniques were considered, adsorption and entrapment. Hydrophilic polymer networks of various morphologies were tailored to examine the maximum encapsulation efficiency of each. Anionic hydrogels composed of methacrylic acid (MAA), cationic hydrogels composed of dimethylamino ethyl methacrylate (DMAEM) and the neutral hydrogels composed of poly(ethylene glycol) monomethylether monomethacrylate (PEGMA) (n=200, 400, 1000), all crosslinked with poly(ethylene glycol) dimethacrylate (PEGDMA) (n=200, 600, 1000), were synthesized by free radical solution polymerization. Using adsorption immobilization method, MAA based hydrogels incorporated the highest amount of Mb when compared to PEGMA or DMAEM polymers. Evaluation of the correlation length of the networks revealed that MAA hydrogels possessed the highest correlation length (15.611-26.988nm) when compared to PEGMA containing matrices (0.254-0.342nm) or DMAEM hydrogels (1.461-1.645nm). The Mb hydrodynamic radius was reported to be approximately 2.04nm indicating that neutral and cationic hydrogels may have not adsorbed significant amounts of proteins due size exclusion effect. Release experiments performed in sodium phosphate buffer (PBS) at pH 5.8 and 7.0 showed that solute transport mechanism in anionic hydrogels was a combination of Fickian diffusion and chain relaxation process. However, Fickian diffusion predominated at pH 7.0, while chain relaxation ruled at pH 5.8. Myoglobin diffusion coefficients for MAA based hydrogels at pH 7.0 were in the magnitude order of 10^{-9} cm²/s, and they increased as crosslinker lengths diminished. The amount of protein released decreased significantly as a function of pH. The diffusion coefficients for myoglobin loaded MAA hydrogels at pH 5.8 were in the order of magnitude of 10^{-9} cm²/s and 10^{-11} cm²/s for hydrogels crosslinked with PEGDMA600 and PEGDMA1000 respectively. Myoglobin loaded MAA hydrogels showed to retain its biological activity after the immobilization process. The amount of HbI incorporated by adsorption inside anionic hydrogels was considerably lower than myoglobin loaded in the same polymer configurations. HbI loaded MAA-PEGDMA hydrogels was able to bind hydrogen sulfide evidencing that was biologically active after immobilization process. Immobilization by entrapment was not possible to achieve in neutral and cationic hydrogels, because the contact between myoglobin and these polymerization solutions produced protein precipitation due to the presence of ethanol and PEG. Changes in myoglobin spectroscopic properties were observed immediately after contact with MAA-PEGDMA polymerization solution and after polymerization was performed, indicating a possible detrimental effect over myoglobin structure. Release of myoglobin incorporated by entrapment in MAA-PEGDMA hydrogels was highly influenced by chain relaxation process. The diffusion coefficients of myoglobin incorporated by entrapment in anionic hydrogels were two magnitude orders smaller than for myoglobin incorporated by adsorption, both evaluated at pH 7.0.

RESUMEN

Las hemo-proteínas son reconocidas por sus propiedades espectroscópicas las cuales cambian durante el enlace con ligandos específicos. Este proyecto se enfocó en la inmovilización de mioglobina de caballo (Mb) y hemoglobina I proveniente de la almeja *Lucina pectinata* (HbI) en redes poliméricas hidrofílicas para usarlas como elementos de reconocimiento en aplicaciones de biosensores. Se consideraron dos técnicas de inmovilización: adsorción y atrapamiento. Polímeros hidrofílicos con diversas morfologías fueron evaluados para examinar su eficiencia de inmovilización. Hidrogeles aniónicos compuestos de ácido metacrílico (MAA), hidrogeles catiónicos compuestos de dimetilaminoetil metacrilato (DMAEM) e hidrogeles neutrales compuestos glicol de polietileno monometiléter monometacrilato (PEGMA) (n=200, 400, 1000), entrecruzados con glicol de polietileno dimetacrilato (PEGMA) (n=200, 600, 1000), fueron sintetizados mediante polimerización de radicales libres. Mediante inmovilización por adsorción, hidrogeles de MAA incorporaron la mayor cantidad de Mb en comparación con los polímeros de PEGMA y DMAEM. La evaluación de la longitud de correlación de las membranas reveló su valor era mayor para los hidrogeles de MAA (15.611-26.988nm) en comparación con los hidrogeles de PEGMA (0.254-0.342nm) o de DMAEM (1.461-1.645nm). Se ha reportado que el radio hidrodinámico de Mb es aproximadamente 2.04 nm indicando que los hidrogeles catiónicos y neutrales pudieron no haber adsorbido cantidades significativas de proteína debido a efectos de exclusión por tamaño. Experimentos de liberación realizados en buffer de fosfato de sodio (PBS) a pH 5.8 y 7.0 mostraron que el mecanismo de transporte soluto en hidrogeles aniónicos combinaba los procesos de difusión Fickiana y relajación de las cadenas. Sin embargo, la difusión Fickiana predominó a pH 7.0, mientras que la relajación de las cadenas imperó a pH 5.8. Los coeficientes de difusión de Mb en hidrogeles aniónicos a pH 7.0 estuvieron en el orden de magnitud de 10^{-9} cm²/s, y aumentaron a medida que la longitud del agente entrecruzante disminuyó. La cantidad de proteína liberada disminuyó apreciablemente como función del pH. Los coeficientes de difusión de Mb en hidrogeles aniónicos a pH 5.8 estuvieron en el orden de magnitud de 10^{-9} cm²/s y 10^{-11} cm²/s para hidrogeles entrecruzados con PEGDMA600 y PEGDMA1000 respectivamente. La mioglobina incorporada en hidrogeles de MAA conservó su actividad biológica después del proceso inmovilización. La cantidad de HbI incorporada mediante adsorción en hidrogeles aniónicos fue considerablemente menor que la Mb incorporada en los mismos polímeros. HbI incorporada en hidrogeles de MAA-PEGDMA fue capaz de enlazar sulfuro de hidrógeno indicando que se encontraba biológicamente activa. No fue posible llevar a cabo la inmovilización mediante atrapamiento en hidrogeles catiónicos y neutrales debido a que el contacto entre Mb y estas soluciones de polimerización produjo la precipitación de la proteína debido a la presencia de etanol y PEG. El contacto de Mb con la solución de polimerización de MAA-PEGDMA produjo cambios en las propiedades espectroscopias de Mb. La liberación de Mb incorporada mediante atrapamiento en hidrogeles de MAA-PEGDMA fue altamente influenciada por el proceso de relajación de las cadenas. Los coeficientes de difusión de Mb incorporada por atrapamiento en hidrogeles aniónicos fueron dos órdenes de magnitud menores que los coeficientes de difusión para Mb incorporada por adsorción, ambos evaluados a pH 7.0.

*To the Almighty Lord
My steadfast love and my stronghold
Thy faithfulness is always unto me*

*To my parents, Rafael and Socorro,
for their unwavering love, endless
patience and encouragement*

ACKNOWLEDGMENTS

During the last two and a half years, numerous people have been encouraging and helping me in immeasurable ways not only to complete this project, but also to gather many unforgettable memories. I hope that I have remembered all of you.

I would like to gratefully acknowledge the enthusiastic and enduring guidance of my advisor Dr. Madeline Torres Lugo. I will like to thank the other members of my graduate committee, Dr. Juan López Garriga and Dr. Lorenzo Saliceti Piazza, for their assistance provided at all levels of the research project and for allowing me to use their laboratory facilities. I would like also to thank Dr. Joe Bonaventura for taking time out from his busy schedule to help me every time I needed. I want to thank Dr. Guillermo Colón Burgos who provided me with necessary laboratory equipment showing his concern towards research other than his.

I recognize the Puerto Rico Alliance for the Advancement of Biomedical Research Excellence (PR-AABRE) for their financial support. Also, I appreciate the opportunity given to me at the Chemical Engineering Department to accomplish my Master of Science degree. My sincere gratitude to the whole department staff. My thanks to Angel Zapata for being always available to figure out solutions to technical problems and to cordially answer all my inquisitive questions.

My true gratitude for my lab partners, the graduate students Lorena, Nilmarie and Hector. Thanks to Margarita for her assistance and kindness. I appreciate the help, hard work, and self motivation showed by my undergraduate students David, and foremost Aixa. I enjoyed the moments shared with the other undergraduate students like

Alejandro, Lymarie and very especially Giselle. A special mention to Adriana and Jimmy as we started as lab partners and we became good friends. Adriana, my best friend, Jimmy, the most annoying person I ever meet, thanks for making me laugh and be with me in the good days and in the blue days.

I would also like to thank Johnny, for his priceless friendship. My housemates Aliana and her daughter Arodí, thanks for their company, for sharing a movie and a meal on those lazy days. I had a lot fun with my quasi-housemates, Rosa the psychologist, Diana always in crisis, and Gustavo always complaining. Thanks to Kattya, my personal image advisor.

I am very grateful to the Central Presbyterian Church at Mayagüez, where I was always warmly welcomed; they became my family in Puerto Rico. I appreciate all their prayers and support. Mostly, I thank Rvdo. Eduardo Miranda, his wife Olgi and Muguette, Migdalia and Priscila.

Finally but foremost, I would like to express my gratefulness to my parents, Rafael and Socorro. Through the distance they have always been in my heart and thoughts. Thanks for their ineffable love and unconditional support. This is for them.

TABLE OF CONTENTS

List of Tables.....	x
List of Figures.....	xii
List of Appendixes.....	xvii
Chapter One	
Introduction.....	1
1.1 Motivation.....	1
1.2 Project Description.....	2
Chapter Two	
Literature Review.....	7
2.1 Hydrogen Sulfide.....	7
2.2 Hemeproteins.....	11
2.2.1 Hemoglobin I from <i>Lucina pectinata</i>	14
2.2.2 Myoglobin from Horse Skeletal Muscle.....	19
2.3 Protein Immobilization.....	23
2.3.1 Protein Immobilization Applied to Biosensor Technology.....	27
2.4 Hydrogels.....	28
2.4.1 Hydrogels Structural Parameters.....	30
2.4.2 Diffusion Theory.....	38
2.4.3 Hydrogel Partition Coefficient.....	43

2.4.4 Bioengineering Applications of Hydrogels.....	44
Chapter Three	
Previous Work.....	48
3.1 Immobilization of Hemeproteins.....	48
Chapter Four	
Objectives.....	58
Chapter Five	
Materials and Methods.....	59
5.1 Materials.....	59
5.1.1 Polymerization Materials.....	59
5.1.2 Proteins.....	61
5.2 Methods.....	62
5.2.1 Isolation of Hemoglobin I from <i>Lucina pectinata</i>	63
5.2.1.1 Ctenidia dissection.....	63
5.2.1.2 Size exclusion chromatography.....	64
5.2.1.3 Ion exchange chromatography.....	66
5.2.2 Polymerization.....	68
5.2.3 Hydrogel Characterization.....	69
5.2.3.1 Determination of $V_{g,r}$, V_P and $V_{g,s}$	69
5.2.4 Determination of Coefficient Partition.....	71

5.2.5 Release Studies.....	72
5.2.6 Activity Studies.....	72

Chapter Six

Results and Discussion.....	74
6.1 Hydrogel Structural Parameters.....	74
6.2 Myoglobin Immobilization through Adsorption.....	79
6.3 Myoglobin Release after Incorporation by Adsorption.....	92
6.4 Myoglobin Immobilization through Entrapment.....	103
6.5 Myoglobin Release after Incorporation by Entrapment.....	115
6.6 Myoglobin Activity Studies after Incorporation by Adsorption.....	119
6.7 Hemoglobin I immobilization through Adsorption.....	134
6.8 Hemoglobin I Activity Studies after Incorporation by Adsorption.....	136

Chapter Seven

Conclusions.....	138
References.....	145

LIST OF TABLES

Table 1.	Kinetic constants for the reaction of <i>Lucina pectinata</i> hemoglobins and sperm whale hemoglobin with oxygen, carbon monoxide, and hydrogen sulfide [42].....	16
Table 2.	Spectral properties of ferrous <i>Lucina pectinata</i> hemoglobins [12].....	17
Table 3.	Spectral properties of ferric <i>Lucina pectinata</i> hemoglobins [43].....	18
Table 4.	Spectral properties of ferrous myoglobin from horse [35, 36].....	20
Table 5.	Spectral properties of ferric myoglobin from horse [35, 36].....	20
Table 6.	Amino acids sequences for HbI from <i>Lucina pectinata</i> [44] and Mb from horse skeletal muscle.....	22
Table 7.	Transport mechanism of solute through a hydrophilic polymer network.....	41
Table 8.	Monomer – crosslinker arrangements used in this project.....	60
Table 9.	Monomer to crosslinker ratio and percentage of dilution used in the preparation of different hydrogel configurations.....	61
Table 10.	Values of the parameters n and k of the Stefan’s approximation for myoglobin incorporated through adsorption in MAA-PEGDMA hydrogels with various crosslinker lengths. Experiments were performed in PBS at pH = 7.0 and T = 30 °C.....	98
Table 11.	Diffusion coefficients for myoglobin incorporated through adsorption in MAA-PEGDMA hydrogels with various crosslinker lengths evaluated using the Berens and Hopfenbers model. Experiments were performed in PBS at pH = 7.0 and T = 30 °C.....	98
Table 12.	Values of the parameters n and k of the Stefan’s approximation for myoglobin incorporated through adsorption in MAA-PEGDMA hydrogels with various crosslinker lengths. Experiments were performed in PBS at pH = 5.8 and T = 30 °C.....	102
Table 13.	Diffusion coefficients for myoglobin incorporated through adsorption in MAA-PEGDMA hydrogels with various crosslinker lengths evaluated using the Berens and Hopfenbers model. Experiments were performed in PBS at pH = 5.8 and T = 30 °C.....	102

Table 14.	Values of the parameters n and k of the Stefan's approximation for myoglobin incorporated through entrapment in MAA-PEGDMA hydrogels with various crosslinker lengths. Experiments were performed at PBS at pH = 7.0 and T = 30 °C.....	118
Table 15.	Diffusion coefficients for myoglobin incorporated through entrapment in MAA-PEGDMA hydrogels with various crosslinker lengths evaluated using the Berens and Hopfenbers model. Experiments were performed at PBS at pH = 7.0 and T = 30 °C.....	118

LIST OF FIGURES

Figure 1.	Heme pocket representation. I, II, III, and IV are the four pyrrole rings. α , β , γ , and δ are the methane bridges.....	12
Figure 2.	Ribbon representation of HbI three-dimensional structure. (Taken from the Protein Data Bank).....	15
Figure 3.	Ribbon representation of Mb from horse three-dimensional structure. (Taken from the Protein Data Bank).....	19
Figure 4.	Representation of the pH changes effect over hydrogel structure.....	29
Figure 5.	Representation of the number average molecular weight between crosslinks (M_c) and the correlation length (ξ).....	31
Figure 6.	Scheme of the experimental procedures followed during this project.....	62
Figure 7.	Typical UV-VIS spectrum obtained after size exclusion chromatography. The first peak corresponds to the mixture of HbII and HbIII proteins and the second peak corresponds to HbI and cysteine.....	65
Figure 8.	Typical UV-Vis spectrum obtained after ion exchange chromatography. The first two peaks corresponds to the HbI in deoxy and metaquo state and the third peak corresponds to cysteine.....	67
Figure 9.	Molecular weight between two adjacent crosslinks for various hydrogel compositions; \square PEGMA200-PEGDMA600 (n=7), ▨ PEGMA200-PEGDMA1000 (n=9), ▩ PEGMA400-PEGDMA600 (n=8), \blacksquare PEGMA400-PEGDMA1000 (n=8), ▧ PEGMA1000-PEGDMA1000 (n=9), ▦ MAA-PEGDMA200 (n=7), ▨ MAA-PEGDMA600 (n=6), ▩ MAA-PEGDMA1000 (n=7), ▧ DMAEM-PEGDMA200 (n=7), ▦ DMAEM-PEGDMA600 (n=6), ▩ DMAEM-PEGDMA1000 (n=6). Each bar represents an average \pm one standard deviation.....	77
Figure 10.	Correlation length (nm) for various hydrogels morphologies; \square PEGMA200-PEGDMA600 (n=7), ▨ PEGMA200-PEGDMA1000 (n=9), ▩ PEGMA400-PEGDMA600 (n=8), \blacksquare PEGMA400-	

	PEGDMA1000 (n=8),  PEGMA1000-PEGDMA1000 (n=9),  MAA-PEGDMA200 (n=7),  MAA-PEGDMA600 (n=6),  MAA-PEGDMA1000 (n=7),  DMAEM-PEGDMA200 (n=7),  DMAEM-PEGDMA600 (n=6),  DMAEM-PEGDMA1000 (n=6). Each bar represents an average \pm one standard deviation.....	78
Figure 11.	MAA-PEGDMA200 hydrogel after being in contact with a horse myoglobin solution 0.481 mM. Incorporation was performed in deionized water at T = 4.0 °C	80
Figure 12.	UV-Vis spectra of MAA-PEGDMA hydrogels before and after myoglobin incorporation through adsorption.  MAA-PEGDMA without protein,  MAA-PEGDMA200,  MAA-PEGDMA600, and  MAA-PEGDMA1000 after protein incorporation.....	83
Figure 13	Partition coefficient for MAA-PEGDMA hydrogels for various crosslinker lengths;  MAA-PEGDMA200 (n=6),  MAA-PEGDMA600 (n=6),  MAA-PEGDMA1000 (n=6). Myoglobin dissolved in water, 0.481 mM at T = 4.0 °C. Each bar represents an average \pm one standard deviation.....	84
Figure 14.	UV-Vis spectra of DMAEM-PEGDMA hydrogels before and after myoglobin incorporation through adsorption,  DMAEM-PEGDMA before protein contact,  DMAEM-PEGDMA200,  DMAEM-PEGDMA600, and  DMAEM-PEGDMA1000 after protein contact.....	86
Figure 15.	Partition coefficient for DMAEM-PEGDMA hydrogels for various crosslinker lengths,  DMAEM-PEGDMA200 n=3,  DMAEM-PEGDMA600 n=3,  DMAEM-PEGDMA1000 n=3. Myoglobin dissolved in water, 0.257 mM at T = 4.0 °C. Each bar represents an average \pm one standard deviation.....	87
Figure 16.	UV-Vis spectra of PEGMA200-PEGDMA600 hydrogels before and after myoglobin incorporation through adsorption,  PEGMA200-PEGDMA600 before myoglobin incorporation,  PEGMA200-PEGDMA600 after myoglobin incorporation.....	88
Figure 17	Summary of the partition coefficients for anionic and cationic hydrogels.  MAA-PEGDMA200 (n=6),  DMAEM-PEGDMA200 (n=3),  MAA-PEGDMA600 (n=6),  DMAEM-PEGDMA600 (n=3),  MAA-PEGDMA1000 (n=6),  DMAEM-PEGDMA1000 (n=3). Incorporation was performed in deionized water at T = 4.0 °C. Each bar represents an average \pm one standard deviation.....	91

Figure 18.	Fractional release of myoglobin incorporated through adsorption in MAA-PEGDMA hydrogels for various crosslinker lengths in PBS at pH = 7.0 at T = 30 °C, ▲ MAA-PEGDMA200 (n=4), ▼ MAA-PEGDMA600 (n=5) and ◆ MAA-PEGDMA1000 (n=3). Each point represents an average ±one standard deviation.....	94
Figure 19.	Fractional release of myoglobin incorporated through adsorption in MAA-PEGDMA hydrogels for various crosslinker lengths in PBS at pH = 5.8 at T = 30 °C, ▼ MAA-PEGDMA600 (n=3) and ◆ MAA-PEGDMA1000 (n=3). Each point represents an average ±one standard deviation.....	101
Figure 20.	Comparison between the amount of myoglobin incorporated inside MAA based hydrogels with various crosslinker lengths by adsorption and entrapment. ▨ adsorbed Mb in MAA-PEGDMA200 (n=6), ▩ entrapped Mb in MAA-PEGDMA200 (n=5), ▪ adsorbed Mb in MAA-PEGDMA600 (n=6), ▫ entrapped Mb in MAA-PEGDMA600 (n=5), ▬ adsorbed Mb in MAA-PEGDMA1000 (n=6), ▭ entrapped Mb in MAA-PEGDMA1000 (n=5). Each bar represents an average ±one standard deviation.....	105
Figure 21.	Effect of MAA-PEGDMA200 polymerization solution over Soret characteristic peak of horse myoglobin. — Spectrum of MAA-PEGDMA200 polymerization solution without myoglobin, — spectrum of free myoglobin in metaquo state, — spectrum of MAA-PEGDMA200 polymerization solution immediately after addition of Mb, — spectrum of MAA-PEGDMA200 containing myoglobin after polymerization.....	106
Figure 22.	Precipitating effect of PEGMA-PEGDMA polymerization solutions over myoglobin after 10 minutes of contact, a) PEGMA200-PEGDMA600, b) PEGMA1000-PEGDMA1000, 1:1 monomer crossliker molar ratio and 1:1 dilution rate.....	108
Figure 23.	Precipitating effect of ethanol over myoglobin a) after 1 minute of contact, b) after 2 minutes of contact.....	109
Figure 24.	Precipitating effect of PEGMA-PEGDMA solutions over myoglobin after 10 minutes of contact a) PEGMA200-PEGDMA600, b) PEGMA1000-PEGDMA1000.....	110
Figure 25.	Precipitating effect of DMAEM-PEGDMA polymerization solutions containing ethanol over myoglobin after 10 minutes of contact, a) DMAEM-PEGDMA600, b) DMAEM-PEGDMA1000.....	113

Figure 26.	Precipitating effect of DMAEM-PEGDMA solutions over myoglobin after 10 minutes of contact a) DMAEM-PEGDMA600, b) DMAEM-PEGDMA1000.....	114
Figure 27.	Fractional release of myoglobin incorporated through entrapment in MAA-PEGDMA hydrogels for various crosslinker lengths in PBS at pH = 7.0 at T = 30 °C, ▲ MAA-PEGDMA200 (n=5), ▼ MAA-PEGDMA600 (n=5) and ◆ MAA-PEGDMA1000 (n=5). Each point represents an average ± one standard deviation.....	117
Figure 28.	Effect of the addition of sodium dithionite over the spectroscopic properties of myoglobin incorporated in MAA-PEGDMA200 hydrogels before release, — spectrum before addition of sodium dithionite, spectra after addition of sodium dithionite: — t=0 min, — t=5 min, — t=10 min, — t=20 min, and — t=30 min.....	122
Figure 29.	Effect of the addition of sodium dithionite over the spectroscopic properties of myoglobin incorporated in MAA-PEGDMA600 hydrogels before release, — spectrum before addition of sodium dithionite, spectra after addition of sodium dithionite: — t=0 min, — t=10 min, — t=30 min, — t=45 min.....	123
Figure 30.	Effect of the addition of sodium dithionite over the spectroscopic properties of myoglobin incorporated in MAA-PEGDMA1000 hydrogels before release, — spectrum before addition of sodium dithionite, spectra after addition of sodium dithionite: — t=0 min, — t=5 min, — t=10 min.....	124
Figure 31.	Effect of the contact with carbon monoxide over the spectroscopic properties of reduced myoglobin incorporated in MAA-PEGDMA200 hydrogels before release, — spectrum before addition of CO, spectra after addition of CO: — 0.5 cm ³ CO t=5 min, — 1.0 cm ³ CO t=5 min, — 1.0 cm ³ CO t=10 min, — 1.0 cm ³ CO t=20 min.....	125
Figure 32.	Effect of the contact with carbon monoxide over the spectroscopic properties of reduced myoglobin incorporated in MAA-PEGDMA600 hydrogels before release, — spectrum before addition of CO, spectra after addition of CO: — 0.5 cm ³ CO t=0 min, — 0.5 cm ³ CO t=5min, — 0.5 cm ³ CO t=10 min, — 1.0 cm ³ CO t=5 min.....	126
Figure 33.	Effect of the addition of carbon monoxide over the spectroscopic properties of reduced myoglobin incorporated in MAA-PEGDMA1000 hydrogels before release, — spectrum before addition of CO, spectra after addition of CO: — 1.0 cm ³ CO t=0	

	min, — 1.0 cm ³ CO t=10 min, — 1.5 cm ³ CO t=10 min, — 1.5 cm ³ CO t=30 min.....	127
Figure 34.	Effect of sodium dithionite and carbon monoxide over the spectroscopic properties of myoglobin incorporated in MAA-PEGDMA200 hydrogels after release, — spectrum before dithionite and CO, spectra after addition of sodium dithionite: — t=0 min, — t=5 min, spectra after CO — 0.5 cm ³ CO t=0 min, — 0.5 cm ³ CO t=0 min.....	131
Figure 35.	Effect of sodium dithionite and carbon monoxide over the spectroscopic properties of myoglobin incorporated in MAA-PEGDMA200 hydrogels after release, — spectrum before dithionite and CO, spectra after addition of sodium dithionite: — t=0 min, — t=5 min, — t=10 min, spectra after CO: — 0.5 cm ³ CO t=0 min and, — 0.5 cm ³ CO t=5 min.....	132
Figure 36.	Effect of sodium dithionite and carbon monoxide over the spectroscopic properties of myoglobin incorporated in MAA-PEGDMA1000 hydrogels after release, — spectrum before dithionite and CO, spectra after addition of sodium dithionite: — t=0 min, — t=5 min, — t=10 min, spectra after CO: — 0.5 cm ³ CO t=0 min, — 0.5 cm ³ CO t=5 min, — 0.5 cm ³ CO t=10 min, and — 1.0 cm ³ CO t=5 min.....	133
Figure 37.	Comparison between the amount of myoglobin and hemoglobin I incorporated by adsorption inside MAA based hydrogels with various crosslinker lengths, Mb in MAA-PEGDMA200 (n=6), HbI in MAA-PEGDMA200 (n=6), Mb in MAA-PEGDMA600 (n=6), HbI in MAA-PEGDMA600 (n=6), Mb in MAA-PEGDMA1000 (n=6), HbI in MAA-PEGDMA1000 (n=6). Each bar represents an average \pm one standard deviation.....	135
Figure 38.	Effect of the contact with a hydrogel sulfide solution over the spectroscopic properties of hemoglobin I incorporated in MAA-PEGDMA200 hydrogels, — spectrum of MAA-PEGDMA200 hydrogel containing HbI, — spectrum after 1 minute of contact with hydrogen sulfide solution.....	137

LIST OF APPENDIXES

Appendix 1.	Polymer volume fraction in the swollen state for various hydrogel compositions; □ PEGMA200-PEGDMA600 (n=7), ▨ PEGMA200-PEGDMA1000 (n=9), ▩ PEGMA400-PEGDMA600 (n=8), ■ PEGMA400-PEGDMA1000 (n=8), ▭ PEGMA1000-PEGDMA1000 (n=9), ▮ MAA-PEGDMA200 (n=7), ▯ MAA-PEGDMA600 (n=6), ▰ MAA-PEGDMA1000 (n=7), ▱ DMAEM-PEGDMA200 (n=7), ▲ DMAEM-PEGDMA600 (n=6), △ DMAEM-PEGDMA1000 (n=6). Each bar represents an average \pm one standard deviation.....	156
Appendix 2.	Volumetric swelling ratio for various hydrogel compositions; □ PEGMA200-PEGDMA600 (n=7), ▨ PEGMA200-PEGDMA1000 (n=9), ▩ PEGMA400-PEGDMA600 (n=8), ■ PEGMA400-PEGDMA1000 (n=8), ▭ PEGMA1000-PEGDMA1000 (n=9), ▮ MAA-PEGDMA200 (n=7), ▯ MAA-PEGDMA600 (n=6), ▰ MAA-PEGDMA1000 (n=7), ▱ DMAEM-PEGDMA200 (n=7), ▲ DMAEM-PEGDMA600 (n=6), △ DMAEM-PEGDMA1000 (n=6). Each bar represents an average \pm one standard deviation.....	157
Appendix 3.	Kinetic constants and efficiency of the initiator 1-Hydroxy cyclohexyl phenyl ketone.....	158
Appendix 4.	Values of the different polymer parameters used for the calculation of the molecular weight between crosslinks.....	159

Chapter One

Introduction

1.1 Motivation

The detection of hydrogen sulfide (H_2S) has a significant relevance as a means to control the undesirable effects of this gas over the health, environment, and industrial facilities [1, 2]. This colorless gas is the most toxic of the sulfur gas family and is considered a broad-spectrum poison capable of adversely affecting systems in the body [3]. The majority of the organs in the body are vulnerable to hydrogen sulfide exposure but, the most susceptible are those with high oxygen demand, since hydrogen sulfide is a strong inhibitor of the enzyme cytochrome oxidase, which participates in the mitochondrial electron transport during cellular respiration [4, 5]. Inhalation of this gas can provoke loss of consciousness and even death within a few breaths [6].

Currently, the detection of hydrogen sulfide is primarily focused in spectroscopic, electrochemical and chromatographic methods. Also, detection techniques based on

metal oxides has been investigated as solid state sensors [7]. Even though, in principle, there exists a broad range of techniques for hydrogen sulfide detection, which can be suitable for specific applications, there is still a challenge; the development of fast, inexpensive and on-site devices for monitoring hydrogen sulfide levels [8]. Moreover, the new sensors should emphasize selectivity rather than sensitivity in order to overcome the most common disadvantage of present detection methods which is fouling from other sulfur compounds such as anions and thiols [8].

Hemeproteins are known for their spectroscopic properties which change during the binding of specific ligands [9]. Consequently, the feasibility of using them as a recognition component in optical sensing devices has been investigated for different analytes and proteins [10]. Ferric hemoglobin I (HbI) from *Lucina pectinata* is a hemeprotein considered a physiological receptor for hydrogen sulfide [11]. Hemoglobin I is one of the three cytoplasmic hemoglobins that have been found in the clam *Lucina pectinata*. It has been widely reported in the literature the strong affinity of this protein toward hydrogen sulfide [12, 13]. This high affinity could allow the solution to the more pressing need of the current techniques of hydrogen sulfide detection which is selectivity.

1.2 Project Description

This project proposed to investigate the use of the hemeprotein Hemoglobin I (HbI) from *Lucina pectinata* as a recognition element that will allow the detection of hydrogen sulfide in a biosensor application. Biosensors are devices that combine the

recognition capability of biological molecules with advanced transducers which convert the biological signal into a measurable output [14, 15]. The change in spectroscopic properties that HbI exhibits when it binds hydrogen sulfide could be employed to monitor and to quantitatively evaluate the presence of H₂S through the use of an optical biosensor.

HbI from *Lucina pectinata* is not commercially available and must be isolated and purified. This process provides relatively small quantities of protein within a significant amount of time. Hence, myoglobin from horse skeletal muscle, which is commercially available, was employed to develop all the necessary experimental protocols and to compare the results obtained from HbI. Both proteins are globular characterized by hydrophilic groups located on the molecule's surface and their structure is constituted by a monomeric chain. Also, the immobilization of myoglobin has its own applications. This protein has been investigated as a recognition element of diverse analytes such as nitric oxide (NO), cyanide (CN), carbon monoxide (CO) [16, 17].

The use of a protein as a recognition element in a biosensor requires the examination of two essential considerations: operational stability and long term use. These two factors are highly influenced by the immobilization technique and the immobilization support [18]. The more common methods for protein immobilization are adsorption, entrapment and covalent binding [19]. Unlike covalent binding immobilization, adsorption, and entrapment do not involve the formation of covalent linkages that could disrupt the protein three-dimensional structure and impose more stress over the protein structure [20]. Compared with covalent binding technique, those methods are considered easier to perform and milder processes to the protein structure [21]. As a consequence, both techniques are expected to minimize the effects on protein

structure and to allow retaining a higher activity after immobilization [22]. Both methods, adsorption and entrapment, were analyzed to establish which one enables the highest permanent protein incorporation without a substantial decrease in biological activity.

Hydrophilic polymer networks, also named as hydrogels, were selected as immobilization support. Hydrogels are physically and chemically cross linked polymers capable of adsorbing and retaining great amounts of water or biological fluids [23]. These polymers have been widely investigated for the delivery of drugs, peptides, and proteins. This feature indicates that hydrogels offer protection against harsh environments and preserve the stability of these molecules over the time [24]. Even though hydrogels have been used as drug or protein controlled delivery devices, the behavior of drug release from hydrogels is influenced by many factors such as structural properties of polymer, the degree of crystallinity, degree of swelling, molecular weight between crosslinks, pH, and ionic strength of the surrounding media [25, 26]. The appropriate control and handling of these factors could allow the permanent immobilization of a protein into a hydrogel.

Three different polymer morphologies were investigated as protein support and evaluated in their capacity of better immobilization by adsorption or entrapment techniques. Hydrogel matrices were tailored to contain polar groups that were expected to produce favorable interactions with the hydrophilic groups of the proteins. Three different polymer morphologies were evaluated as protein supports. The first was methacrylic acid (MAA) crosslinked with poly(ethylene glycol) dimethacrylate (PEGDMA). The second was poly(ethylene glycol) monomethyl ether monomethacrylate

(PEGMA) crosslinked with PEGDMA. The final hydrogel tested was dimethylaminoethyl methacrylate (DMAEM) crosslinked with PEGDMA. These hydrogels are characterized by the chemical moieties that compose the structure. MAA contains carboxylic acid groups that above its pKa of 4.88 at 20°C create a negative or anionic network [27]; the amino groups of DMAEM are ionized at pH below 6.0 making a cationic network [28] and PEG is a neutral polymer [29]. By means of these polymer networks it was possible to determine which kind of hydrogel, neutral, anionic or cationic, could provide an enhanced support for the herein mentioned proteins without significantly affecting their biological activity.

The aforementioned morphologies were characterized by means of the determination of the polymer volume fraction in the swollen state ($v_{2,s}$), the number average molecular weight between crosslinks (M_c), the correlation length (ξ), and the partition coefficient (K). The partition coefficient allowed the evaluation of the affinity between the protein and the hydrogel and the amount of protein incorporated inside the hydrogel through adsorption. The correlation length determination enabled the estimation of the available space for diffusion. According to this average measure, it was possible to identify which polymer networks could hinder the diffusion of the protein due to size exclusion effect.

After the immobilization of the two heme proteins, hemoglobin I and myoglobin, was accomplished by the two proposed techniques, release studies were performed. Through these tests, it was possible to evaluate the amount of protein permanently immobilized inside the hydrogels. Also, release studies allowed us to evaluate the

diffusion mechanism that took place during the molecule release and to quantify the diffusion coefficients.

The capacity of the heme proteins immobilized into hydrogels to bind a specific ligand was assessed during activity studies. These experiments were carried out before and after release studies. In this manner, the viability of using hemoglobin I from *Lucina pectinata* immobilized into a hydrogel as a recognition element for the detection of the highly toxic gas hydrogen sulfide was evaluated.

Chapter Two

Literature Review

2.1 Hydrogen Sulfide

Hydrogen sulfide (H_2S) is a colorless gas with a very characteristic odor to rotten eggs which can be perceived organoleptically at concentrations as low as 0.025 ppm [6], but this sensitivity is lost over 150-200 ppm or after a prolonged exposure [8]. This gas can be found in some natural sources: volcanic gases, marshes, sulfur springs, putrefying vegetable and animal matter, but also, it is present as a byproduct from some industries: petroleum refining, natural gas plants, coke oven plants, knot pulp mills, and tanneries [7, 30]. The interest in the detection of hydrogen sulfide arises from the detrimental effects that exposure to this gas has in areas such as: health, environment, and industrial facilities care [1, 2].

The most severe effect of hydrogen sulfide, due to its high toxicity, is death; it is considered one of the leading causes of sudden death at occupational sites [2, 30].

Nevertheless, hydrogen sulfide can also produce deterioration on the normal function of several organs in the body including eyes, lungs, olfactory parts, nervous system, heart, brain, gastrointestinal system, and liver [5]. The US Occupational Safety and Health Administration (OSHA) has established a concentration of 10 ppm over an eight hour day as a permissible exposure limit (PEL), a considerably high level when compared with the allowed concentration established by the World Health Organization (WHO) which is as low as 0.003 ppm [31]. In addition, OSHA established a hydrogen sulfide level of 300 ppm as immediately dangerous to life and health (IDLH) [30].

Beyond the health effects, there is an increasing concern over the environmental consequences of H₂S discharges [8]. Even though hydrogen sulfide has only a small contribution to the atmospheric sulfide levels, in certain industrial locations, especially at petrochemical facilities, the emissions of H₂S are responsible for most of sulfur emissions in these areas [3]. In recent years, there has been an increase in the levels of sulfur content in the crude extract used to produce oil and natural gas. As a consequence, the released concentration of H₂S, as a by product of refining processes, has also increased [8, 30]. Furthermore, the monitoring of hydrogen sulfide has become critical to minimize health casualties in the workplace since it is by far the most toxic sulfur compound [3]. Finally, the presence of hydrogen sulfide can cause lack of ductility in pipelines making them more susceptible to hydrogen attack. This type of corrosion, known as hydrogen embrittlement, increases the risk of explosion [1].

Bearing in mind all the potentially adverse risks that the presence of hydrogen sulfide could represent, particularly that its high toxicity could provoke physiological distress or even death and the strict legislation directed to protect workers wellbeing;

hydrogen sulfide has become a target of research addressed to the development of highly sensitive and quick response sensors [7, 32]. Spectroscopic methods are the most common techniques discussed in the literature for the detection of sulfide compounds followed by electrochemical and chromatographic methods [8].

Analytical methods for the detection of hydrogen sulfide involve a collection and a preconcentration of the sample [3]. The collection of the gas can be made in liquids or on impregnated solid substrates. The collected analyte is examined by spectroscopic techniques directly or after conversion to a measurable species [30]. Problems during the collection step can arise from the interference produced due to the presence of atmospheric oxidants [3].

Within the spectroscopic methods employed for the determination of hydrogen sulfide, those that include UV/visible and fluorescence spectroscopy predominate [7]. The most common sensing method for hydrogen sulfide is the methylene blue test. The methylene blue test was first described in 1886 by Emil Fisher. In this test, aqueous sulfide reacts with N,N-dimethylphenyl-1,4 diamine in presence of ferric ions which produce a typical blue coloration. The detection of the dye is conventionally made by UV-visible spectroscopy. Also, fluorescence and high performance liquid chromatography (HPLC) techniques could be employed [8]. Moreover, several researches have studied the selectivity of other fluorescent labels such as thionine, tetraoctylammonium fluorescein mercury (II), fluorescein mercury acetate, and 2,7-dichlorofluorescein. These labels take advantage of the affinity of sulfide ions for the coordinated mercuric ion [3, 8].

The use of hydrogen sulfide sensors based on spectroscopic methods is justified not only because they are easy to perform compared to other methods but also, they allow monitoring of hazardous areas from distance using optical fiber technology [7]. The main challenge to improve these methods is to find a dye that possesses a rapid, specific, sensitive, and reversibly response in the presence of hydrogen sulfide [7, 8].

Detection of hydrogen sulfide via electrochemical methods includes four techniques: potentiometric, galvanic, coulometric, and amperometric. The most common approach for the detection of hydrogen sulfide by means of potentiometric techniques employs silver sulfide as the sensing element. However, long response time and contamination of the reference electrode component have been observed [5]. Amperometric methods, which exploit the properties of metallic sulfide deposits with silver or mercury, have been successfully applied in several applications, but their efficiency is reduced by the diffusion of the analyte through the porous membrane. As a result, long response times and loss of sensitivity could appear [5, 8].

Chromatographic techniques are highly mentioned in literature for the detection of hydrogen sulfide. Chromatographic methods are employed when the sample is constituted by different sulfur and thiol compounds and it becomes necessary to separate them for a posterior identification [1]. Ion chromatographic systems comprise from simple exchange columns to gel based separation columns. The final identification is made in several applications using UV-adsorption spectrometry [8].

An additional type of sensing method for hydrogen sulfide is constituted by solid state sensors. These sensors are employed in environmental air monitoring for the detection of low levels of H₂S. Solid state sensors make use of metal oxides which have

shown sensitivity towards the detection of low concentration of this toxic gas. Tungsten oxide (WO_3) and selenium oxide (SnO_3) are part of the metal oxides frequently reported in literature [32-34]. These systems are often less sensitive when compared to the other methods previously mentioned. In general, solid state sensors are susceptible to temperature and humidity fluctuations [8].

2.2 Hemeproteins

Hemoglobin and myoglobin are respiratory proteins. Myoglobin is found in the cytoplasm of smooth or striated muscles of all animals and participates in oxygen storage. The name hemoglobin was at first given to proteins that are present in the blood of vertebrates and participates in the oxygen transport [35, 36]. Thereinafter, proteins showing similar features to myoglobins and hemoglobins have been found in tissues other than blood and muscle. These tissural proteins have also adopted the name of hemoglobins, and are present especially in some invertebrate species such as mollusks where they can be found as monomeric, dimeric and tetrameric structures [35, 37].

Hemoglobin and myoglobin are characterized by their globular structures and are part of the globins family. Globular proteins are characterized for having the polypeptide chain folded into a spherical or globular shape and containing several types of secondary structures. Another important feature of these proteins is the positioning of amino acid side chains, which reflects a structure that derives much of its stability from hydrophobic interactions; most of their hydrophobic R groups are in the interior of the molecule,

distant from exposure to water, and most of their hydrophilic (polar) R groups are located on the external surface of the molecule [38].

The respiratory heme proteins, hemoglobin (Hb) and myoglobin (Mb), can undergo a reversible reaction with molecular oxygen by virtue of the heme group which is non-polar and consists of an organic group known as proto-porphyrin containing an iron (Fe) atom [37]. Protoporphyrin is composed by four pyrrole rings connected by methane bridges (α , β , γ , δ) and substituted by different amino acids in the external positions (position 1-8). The nature of the groups placed in positions 1-8 produce several porphyrins which have different solubility, spectrum and reactivity [35]. Figure 1. displays a representation of the heme pocket.

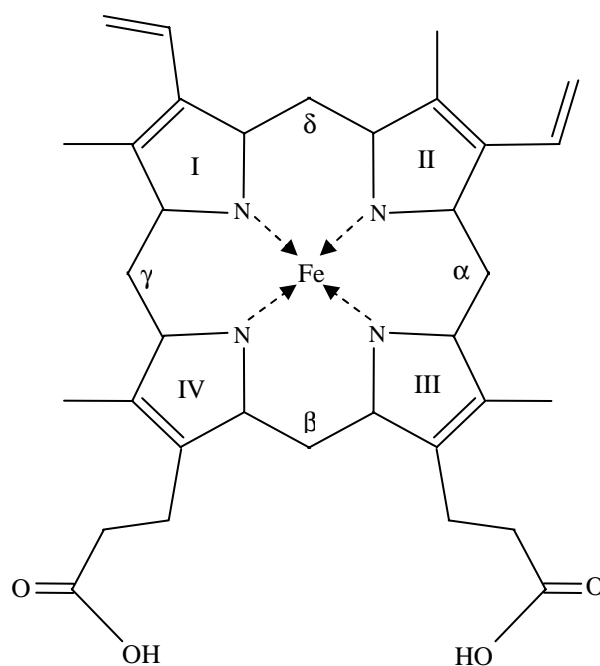


Figure 1. Heme pocket representation. I, II, III, and IV are the four pyrrole rings. α , β , γ , and δ are the methane bridges.

The heme group exists in four oxidizing states depending on the 6th coordinate position of Fe: deoxy, with empty 6th coordinate position; oxy, with its 6th coordinate position occupied by O₂; met or ferri, with its 6th coordinate position occupied by H₂O, and carboxy in which carbon monoxide binds to free heme. All of these states show specific bands in their adsorption spectrum [35].

Like other biological molecules, hemoproteins can experiment loss of biological activity caused by environmental changes or chemical treatments, which induce a disruption in the protein native conformation, a process known as denaturation [39]. The denaturated state does not imply a complete unfolding of the protein and a randomization of conformation [38, 39]. Raising or lowering the pH could change the ionic state of protein ionizable side chains, thereby breaking hydrogen bonds, creating regions of charge repulsion, and disrupting ion pairs; all of these disruptions can contribute to denaturation [39]. Heating a protein solution affects the weak interactions in a protein, primarily hydrogen bonds, which have the function to stabilize the folded conformation. It has been observed that when the temperature is slowly increased, the protein's conformation generally remains intact until an abrupt loss of structure and function occurs over a narrow temperature range [38]. Finally, proteins can also be denaturated by certain miscible organic solvents such as alcohol, acetone, and solutes such as urea and guanidine hydrochloride, or detergents [39, 39].

2.2.1 Hemoglobin I from *Lucina pectinata*

Lucina pectinata is a clam that inhabits sulfide rich tropical and semitropical muds. This mollusk has a symbiotic relation with a vast population of intracellular chemoautotrophic bacteria which fix carbon monoxide into hexoses. The bacteria employs for this function energy obtained from the oxidation of environmental hydrogen sulfide that surround the clam habitat. The host clam depends nearly completely on the symbiont for its supply of organic carbon and oxygen because it lacks mouth and guts [12, 40].

The symbiotic relationship between the host clam and the intracellular chemoautotropic bacteria is characterized by the existence of the mollusk cytoplasmic hemoglobins located probably in the cytoplasm of the bacteriocyte gill cells [41]. *Lucina pectinata* contains three types of hemoglobins: hemoglobin I (HbI), hemoglobin II (HbII) and hemoglobin III (HbIII). Each hemoglobin has its own chemical and physical properties [42].

Hemoglobins II and III bind oxygen (O₂) reversibly and non-cooperatively with an affinity similar to that observed for sperm whale myoglobin. They are responsible for the oxygen transport in the clam [41]. Hemoglobins II and III chains have an approximately relative molecular mass of 17000 Da and possess similar amino acid compositions with 75% sequence homology [40, 43].

Hemoglobin I is a monomeric protein with 142 amino acid residues in its sequence which is markedly different from HbII and HbIII [43]. Depending on the method

employed to estimate the molecular weight of HbI, it varies from 14,443 to 14,862.10 Da [44]. Figure 2. shows the three-dimensional arrangement of HbI.

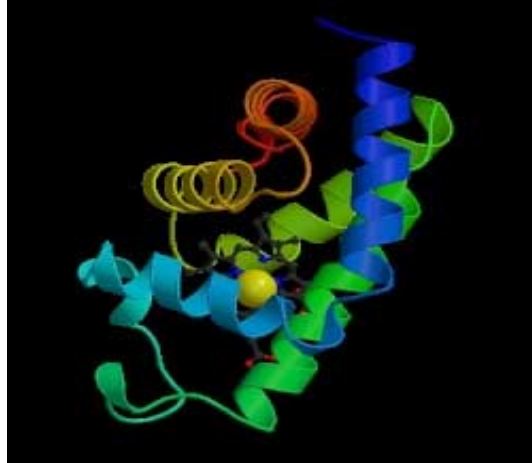
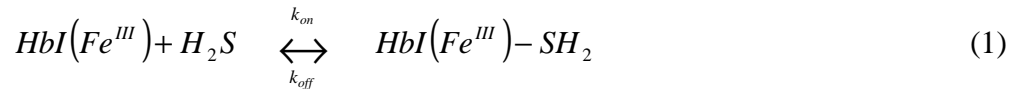


Figure 2. Ribbon representation of HbI three-dimensional structure. (Taken from the Protein Data Bank).

Hemoglobin I also binds oxygen, but in the presence of both oxygen and hydrogen sulfide, it is oxidized to the ferric HbI:sulfide complex [45]. The formation of the ferric HbI-sulfide complex could be described by the following reaction,



where k_{on} and k_{off} are the formation and the dissociation constants of the complex, respectively. The ratio between the formation and the dissociation constants represents the affinity constant.

$$k_{affinity} = \frac{k_{on}}{k_{off}} \quad (2)$$

In contrast, the other two hemoglobins (HbII and HbIII) remain oxygenated in the presence of hydrogen sulfide [45]. Hydrogen sulfide binds hemoglobin I in its ferric state

(Fe^{III}), which yields unusual results when compared to more common ligands such as oxygen (O₂), nitric oxide (NO) or carbon monoxide (CO), which bind to ferrous heme proteins (Fe^{II}) [46].

Hemoglobin I shows an extraordinary affinity for hydrogen sulfide when compared to other hemoglobins. Its affinity is about 5000 fold superior to that observed in HbII, HbII and sperm whale myoglobin [13, 41]. Table 1 presents the kinetic constants for the reaction between ligands (O₂, CO and H₂S) and HbI, HbII and HbIII from *Lucina pectinata* and myoglobin from sperm whale [42].

Table 1. Kinetic constants for the reaction of *Lucina pectinata* hemoglobins and sperm whale hemoglobin with oxygen, carbon monoxide, and hydrogen sulfide [42].

Protein	Oxygen		Carbon Monoxide		Hydrogen Sulfide	
	$k_{on} \times 10^{-6}$ ($M^{-1}s^{-1}$)	k_{off} (s^{-1})	$k_{on} \times 10^{-6}$ ($M^{-1}s^{-1}$)	k_{off} (s^{-1})	$k_{on} \times 10^{-6}$ ($M^{-1}s^{-1}$)	k_{off} (s^{-1})
HbI <i>Lucina pectinata</i>	100-200	61.1	0.780	0.0142	226	0.22
HbII <i>Lucina pectinata</i>	0.390	0.11	0.019	0.0071	11.3	17
HbIII <i>Lucina pectinata</i>	0.288	0.075	0.0072	0.0107	41.7	16
Sperm whale Mb	19	10	0.44	0.0185	8.8	48

Even though the reasons that explain the high affinity of hemoglobin I toward hydrogen sulfide are not completely understood, several unique characteristics in their amino acid sequence have been postulated as the molecular basis of this special behavior [41]. In the amino acids chain of HbI several residues are conserved concerning to other species, but some residues have been changed [95]. X-ray analysis of met-aquo HbI have shown a particular arrangement of the heme pocket residues. Positions E11, B10, and E7

in HbI are naturally mutated. See the amino acids sequence of HbI presented in Table 6. Hemoglobin I has a Phe(68) instead of Val at position E11, a Phe(29) instead of Leu at position B10, and a Gln(64) instead of His at position E7 [13, 42]. Furthermore, hemoglobin I has an unusual presence and location of aromatic residues in the heme pocket, having a total of 10 phenylalanines, four tryptophanes, two histidines and one tyrosine [41]. This peculiar distribution of phenylalanyl residues at the distal ligand binding site is atypical for a hemoglobin and has not been previously observed in the globin family [45].

Tables 2 and 3 summarize the spectral properties of the three different hemoglobins found in *Lucina pectinata* at ferrous and ferric state. The spectral properties of each hemoglobin changes when a specific hemoglobin binds a different ligand [12, 43].

Table 2. Spectral properties of ferrous *Lucina pectinata* hemoglobins [12].

Derivate	HbI		HbII		HbIII	
	λ_{\max} (nm)	ϵ (mM ⁻¹ cm ⁻¹)	λ_{\max} (nm)	ϵ (mM ⁻¹ cm ⁻¹)	λ_{\max} (nm)	ϵ (mM ⁻¹ cm ⁻¹)
Hb (deoxy)	433	119	432	120	431	116
	557	12.2	556	12.5	555	12.3
HbO ₂ (oxy)	282	48.3	277	39.6	278	44.7
	416	135	414	129	414	144
	541	13.4	540	13.3	540	14.5
	576	13.0	576	12.6	575	13.8
HbCO (carboxy)	421	189	420	178	419	178
	539	13.2	539	12.9	538	13.2
	570	12.2	570	11.8	569	12.3

Table 3. Spectral properties of ferric *Lucina pectinata* hemoglobins [43].

Derivate	HbI		HbII		HbIII	
	λ_{\max} (nm)	ϵ (mM ⁻¹ cm ⁻¹)	λ_{\max} (nm)	ϵ (mM ⁻¹ cm ⁻¹)	λ_{\max} (nm)	ϵ (mM ⁻¹ cm ⁻¹)
Hb ⁺ (H ₂ O)	407	178	403	130	405	151
(metaquo)	502	10.2	502	9.4	501	9.6
pH 7.5	633	4.2	632	3.6	630	3.6
Hb ⁺ (SH ₂)	426	102	423	79	423	72
(sulfide)	544	11.4	542	10	541	10.4
	574	8.9	574	7.9	572	8.8

The unique properties of hemoglobin I (HbI) from *Lucina pectinata* toward hydrogen sulfide make this protein an ideal candidate to be used to quantitatively evaluate the presence of H₂S. Boffi et al. [11] proposed a spectrophotometric technique for the determination of hydrogen sulfide dissolved in solution based on the reaction of H₂S with ferric HbI. They monitored the large absorbance changes that occurred when HbI binds the ligand (H₂S). Concentrations as low as 1×10⁶ were detected. In addition, the immobilization of HbI from *Lucina pectinata* as a recognition element of a biosensor was attempted using sol gels by Estrada L. [47]. A decrease in the affinity of immobilized HbI toward H₂S was observed. The affinity constant had a value six magnitude orders smaller than its respective value in solution. Further discussion will follow in section 3.1.

2.2.2 Myoglobin (Mb) from Horse Skeletal Muscle

Myoglobin (Mb) from horse skeletal muscle is a relatively small oxygen-binding protein with a molecular weight of 17,600 Da. Mb from horse contains a single polypeptide chain of 153 amino acid residues and a single iron protoporphyrin, or heme group. It does not have disulfide bridges or free –SH groups. The myoglobin backbone contains eight relatively straight segments of right-handed α helices, joined by non-ordered or random coil regions. The function of myoglobin is to store oxygen and to facilitate oxygen diffusion in rapidly contracting muscle tissue. The affinity of myoglobin for oxygen is higher than that of hemoglobin. Slight changes in the tertiary structure of myoglobin could destroy the oxygen binding function of the heme group [36, 37]. Figure 3. shows a ribbon representation of the structure of myoglobin from horse. A summary of the spectral properties of myoglobin from horse at ferrous and ferric state is displayed in Tables 4 and 5 [35, 36].



Figure 3. Ribbon representation of Mb from horse three-dimensional structure. (Taken from the Protein Data Bank).

Table 4. Spectral properties of ferrous myoglobin from horse [35, 36].

Derivate	Mb	
	λ_{\max} (nm)	ϵ (mM ⁻¹ cm ⁻¹)
Mb (deoxy)	435	121
	560	13.8
MbO ₂ (oxy)	542	13.9
	580	14.4
MbCO (carboxy)	424	207
	540	15.4
	579	13.9

Table 5. Spectral properties of ferric myoglobin from horse [35, 36].

Derivate	Mb	
	λ_{\max} (nm)	ϵ (mM ⁻¹ cm ⁻¹)
Mb ⁺ (H ₂ O)	408	188
(metaquo) pH 6.4	502	10.2
	630	3.9
Mb ⁺ (NO) (nitric oxide)	422	116
	540	11.3

Myoglobin from horse skeletal muscle, which is commercially available, has been employed to develop all the experimental protocols that were performed in this project. Hemoglobin I from *Lucina pectinata* is a protein that must be isolated in the laboratory and this process takes a considerable amount of time and provides small quantities of the purified protein. Both proteins are globular and respiratory heme proteins with a

monomeric structure, and have some similarities in their amino acid sequence. The amino acid sequence for both proteins is illustrated in Table 6.

Table 6. Amino acids sequences for HbI from *Lucina pectinata* [44] and Mb from horse skeletal muscle.

Residue number	Mb	HbI	Residue number	Mb	HbI	Residue number	Mb	HbI
1	Gly	Ser	52	Glu	Lys	103	Tyr	Ala
2	Leu	Leu	53	Ala	Gly	104	Leu	Gly
3	Ser	Glu	54	Glu	Thr	105	Glu	Gln
4	Asp	Ala	55	Met	Val	106	Phe	Leu
5	Gly	Ala	56	Lys	Lys	107	Ile	Glu
6	Glu	Gln	57	Ala	Asn	108	Ser	Ala
7	Trp	Lys	58	Ser	Thr	109	Asp	Ala
8	Gln	Ser	59	Glu	Pro	110	Ala	Phe
9	Gln	Asn	60	Asp	Glu	111	Ile	Lys
10	Val	Val	61	Leu	Met	112	Ile	Val
11	Leu	Thr	62	Lys	Ala	113	His	Leu
12	Asn	Ser	63	Lys	Ala	114	Val	Ser
13	Val	Ser	64	His	Gln	115	Leu	Gly
14	Trp	Trp	65	Gly	Ala	116	His	Phe
15	Gly	Ala	66	Thr	Gln	117	Ser	Met
16	Lys	Lys	67	Val	Ser	118	Lys	Lys
17	Val	Ala	68	Val	Phe	119	His	Ser
18	Glu	Ser	69	Leu	Lys	120	Pro	Tyr
19	Ala	Ala	70	Thr	Gly	121	Gly	Gly
20	Asp	Ala	71	Ala	Leu	122	Asp	Gly
21	Ile	Trp	72	Leu	Val	123	Phe	Asp
22	Ala	Gly	73	Gly	Ser	124	Gly	Glu
23	Gly	Thr	74	Gly	Asn	125	Ala	Gly
24	His	Ala	75	Ile	Trp	126	Asp	Ala
25	Gly	Gly	76	Leu	Val	127	Ala	Trp
26	Gln	Pro	77	Lys	Asp	128	Gln	Thr
27	Glu	Glu	78	Lys	Asn	129	Gly	Ala
28	Val	Phe	79	Lys	Leu	130	Ala	Val
29	Leu	Phe	80	Gly	Asp	131	Met	Ala
30	Ile	Met	81	His	Asn	132	Thr	Gly
31	Arg	Ala	82	His	Ala	133	Lys	Ala
32	Leu	Leu	83	Glu	Gly	134	Ala	Leu
33	Phe	Phe	84	Ala	Ala	135	Leu	Met
34	Thr	Asp	85	Glu	Leu	136	Glu	Gly
35	Gly	Ala	86	Leu	Glu	137	Leu	Glu
36	His	His	87	Lys	Gly	138	Phe	Ile
37	Pro	Asp	88	Pro	Gln	139	Arg	Glu
38	Glu	Asp	89	Leu	Cys	140	Asn	Pro
39	Thr	Val	90	Ala	Lys	141	Asp	Asp
40	Leu	Phe	91	Gln	Thr	142	Ile	Met
41	Glu	Ala	92	Ser	Phe	143	Ala	
42	Lys	Lys	93	His	Ala	144	Ala	
43	Phe	Phe	94	Ala	Ala	145	Lys	
44	Asp	Ser	95	Thr	Asn	146	Tyr	
45	Lys	Gly	96	Lys	His	147	Lys	
46	Phe	Leu	97	His	Lys	148	Glu	
47	Lys	Phe	98	Lys	Ala	149	Leu	
48	His	Ser	99	Ile	Arg	150	Gly	
49	Leu	Gly	100	Pro	Gly	151	Phe	
50	Lys	Ala	101	Ile	Ile	152	Gln	
51	Thr	Ala	102	Lys	Ser	153	Gly	

2.3 Protein Immobilization

Immobilized enzymes, which are catalytic proteins, are defined as “...enzymes physically trapped or situated in a certain space in a way which enables them to retain their activity as well as their repeated and continual use” [48]. Immobilization protects the protein against aggregation and degeneration improving its long term stability. Also, immobilization allows the repeated use of the protein [49]. The immobilization of biomolecules was approximately reported in 1916 when J. M. Nelson et al. observed that invertase absorbed into activated charcoal retained its catalytic activity. Thenceforth, the immobilization of proteins has become a broad area of research, which has allowed the development of several methods to achieve immobilization [50]. Protein immobilization techniques can be classified in three different categories based on how the molecule is retained on the carrier, by adsorption, covalent binding, or held occluded in the three dimensional network built by the chains of a polymeric carrier. Techniques combining various methods are also possible [19, 51].

Adsorption is the most antique and the easiest technique for non-covalent protein immobilization [50]. It is achieved by placing the carrier, an adsorbent surface, in a solution of the protein. The forces responsible for this kind of immobilization are relatively weak and include hydrogen bonds, van de Waals forces, and hydrophobic interactions [48]. In addition, adsorption may involve ionic binding, which is based on ionic interactions between the protein and the opposite charges of the carrier [22]. The weakness of the forces involved in protein immobilization could allow desorption of the

protein from the support. Changes in pH, ionic strength, and temperature disrupt the interactions between the protein and the carrier [50]. The conditions of the immobilization by adsorption are mild in comparison with those required in covalent immobilization techniques. Thereby, proteins immobilized by adsorption are expected to retain high activities [48].

Immobilization by adsorption has been applied to amylase and acid phosphatase utilizing various supports such as bentonite, kaolin, celite, hydroxyapatite, and tricalcium phosphate. Among the diverse immobilization matrices, tricalcium phosphate showed the highest capability to bind amylase (84% specific activity retention) and acid phosphatase (83% specific activity retention). This result is believed to be caused by the large amount of hydroxyl groups [22].

Another enzyme that has been successfully immobilized by adsorption is pullulanase. In this case, glass beads, porous glass, ceramics, and chitosan have been employed as support. Chitosan provide the highest immobilization capability. The hydrophilic character of this natural polymer could be the cause of this performance [22].

One of the techniques that makes use of a three dimensional network built by polymer chains to retain the protein inside the carrier is entrapment. The network should be tight enough to avoid protein release, whereas allows the diffusion of the ligand or substrate through the carrier [50]. The principal advantage of this immobilization method is that it produces a minor loss of biological activity when compared with chemical methods of immobilization [48]. The diffusional limitations resulting from the high degree of crosslinking required to minimize the release of the protein account for the major disadvantage of this technique [22].

The most common support used to immobilize enzymes by entrapment is polyacrylamide (PAM). The pH profile characteristic of the enzyme immobilized in PAM resembles those of the free enzyme. The list of enzymes that have been immobilized using polyacrylamide is considerably large and include glucose oxidase, L-aminoacid oxidase, xantin oxidase, alcohol dehydrogenase, lactic dehydrogenase, catalase, peroxidase, and hexokinase among others [19, 50].

In addition, immobilization by entrapment has been investigated for the immobilization of lipases. These enzymes are the most frequently used in organic synthesis. Different supports such as silica and polyvinyl chloride (PVC) have been employed. The lipases immobilized by entrapment have shown to maintain a higher activity when compared to lipases immobilized by adsorption [22, 52].

Besides polyacrylamide, another hydrogel used for the entrapment of drugs, enzymes, and cells was based on poly(2-hydroxyethyl methacrylate) (HEMA) which is versatile and biocompatible. Among the enzymes, cells, and drugs that have been immobilized in this kind of hydrogel are penicilin acylase, arginase, glucose oxidase, yeast cells, and narciclasine. It was observed that the use of hydrogels built from HEMA and PEG enhanced the protein release at larger molecular weights of PEG [53].

Finally, the third widespread technique employed for protein immobilization is covalent binding. This method is based on the development of covalent bonds between the protein and the matrix. Covalent linkages are strong; thereby the protein will not be released from the support material even in the presence of a ligand or a substrate solution, or in high ionic strength solutions [22, 48]. The required conditions to perform covalent immobilization are more complicated and less mild than the ones used in others carrier

binding methods. The covalent bond formed between the protein and the matrix should not involve amino acid residues placed in the active center of the protein to maintain protein biological activity [21].

Covalent binding requires the activation of specific functional groups of the support; glutaraldehyde has been extensively used to achieve this objective in organic and inorganic supports [22]. It is also possible to introduce into the protein being immobilized additional reactive groups by chemical modification. These two conformational changes in both protein and support are performed to obtain an extent and specific attachment between the protein and the support [54].

Covalent immobilization can use a diversity of supports, which can be classified as inorganics, organics, naturals or synthetics [21]. Inorganic carriers including glass, silica gel, alumina, bentonine, hydroxyapatite, titania, and zirconia have shown good mechanical properties, thermal stability, and resistance against microbial attack and organic solvents [54]. Among the natural organic carriers are keratin, collagen, albumin, carbohydrates. From this group, carbohydrates have been extensively studied because they are highly hydrophilic which provides an attractive media for many proteins [21]. Synthetic polymers constitute the largest numbers of supports available for protein immobilization. These include polystyrene, polyacrylates, polyacrylamides, hydroxyalkyl methacrylates, and polyamides, among others. Synthetic carriers present several advantages: they are inert to microbial attack and their degree of porosity and chemical composition can be manipulated [54].

2.3.1 Protein Immobilization Applied to Biosensor Technology

In 1962, Clark and Lyons demonstrated that an enzyme, glucose oxidase, could be immobilized on an oxygen sensing electrode. This became the first enzyme-based sensor system. Since then, biosensors technology has made considerable progresses [55, 56]. The term biosensor refers to a small, portable and analytical device that couples a biomolecule with an appropriate transducer to produce a signal proportional to the target analyte concentration [57, 58]. The four principal types of transducers traditionally used in biosensor technology are: electrochemical, optical, thermometric, and piezoelectric [14]. A biosensor should have the capacity to respond to changes in analyte concentration in a manner direct, reversible, continuous, rapid and accurate [59].

Some of the most widely investigated biosensors take advantage of the protein properties. Proteins can be successfully used as a recognition element for biosensors because they are highly sensitive and specific [20, 60]. Protein immobilization can be achieved by one of the described methods: adsorption, entrapment, or covalent binding. From these, one of the most convenient methods is entrapment because it is rapid, simple, and the protein is maintained inside the support without chemical reaction. However, this method can be only applied to systems where the ligands or substrates are small enough to diffuse through the matrix. In the case of large ligands or substrates is necessary to employ covalent binding [61].

Health care and environmental monitoring are two of the of the most relevant application fields for biosensor technology [62]. Concerning to medical applications, glucose sensing has dominated the biosensor research and has achieved commercial

success. Currently, the uses of devices that allow people to self-test the levels of glucose have been extended [63]. Also, systems that permit to evaluate glucose levels in vivo have been further investigated [64]. Other analytes that have received considerable attention for the development of devices to monitor their levels are creatinine, urea and lactate [14].

Traditional methods commonly employed to environmental monitoring exhibit some problems: time consuming, cost, sample analysis and preparation are required in many applications. In counterview, biosensors are portable, economic, highly selective and sensitive [62, 65]. Biosensor technology has been employed in the measurement of pollutants and other environmental hazards such as pesticides, biochemical oxygen demand (BOD), phenols, heavy metals and polluting gases (NO_x , SO_x , CO_2 , methane and ozone) [65, 66].

Maintaining the stability of the biological recognition element is the most important challenge to address to extend the applications of biosensor technology. This problem can be avoided by improving the immobilization techniques or using semisynthetic or synthetic analogs of biological molecules [20, 57].

2.4 Hydrogels

Hydrogels are hydrophilic polymer networks which have the capacity of absorbing and retaining large amounts of water and physiological fluids [67, 68]. This three dimensional network can be constituted for homopolymers or copolymers and the

presence of chemical (tie-point, junctions) and physical (entanglements, crystallites) crosslinking render them insoluble [25, 69]. Hydrogels have received great attention in the past forty years because their ability to absorb water (swelling behavior) could be dependent on external environmental conditions. The swelling behavior could be controlled through changes in pH, temperature, ionic strength, nature of the swelling media and electromagnetic radiation depending on the presence of specific ionic moieties [26]. Figure 4. shows a representation of the effect of pH changes over hydrogel structure.

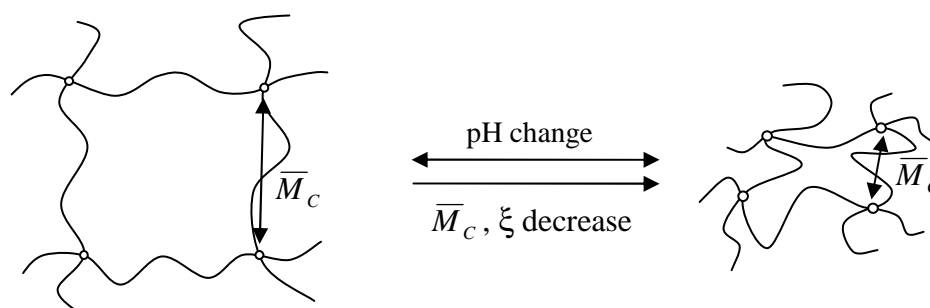


Figure 4. Representation of the pH changes effect over hydrogel structure.

Hydrogels are classified according to the nature of the charges of their pendant groups as neutral or ionic [70]. The swelling behavior of neutral hydrogels is only influenced by two forces: the thermodynamic force of mixing and the retractive force of the polymer chain. The equilibrium is reached when the two forces are equal [25]. In contrast, in ionic hydrogels, the swelling process is promoted not only by the forces already mentioned but also by the interactions between the charged polymer and the free ions of the solvent. When pendant groups such as carboxylic acid, sulphonic acid, or

amine are ionized, the hydrogel becomes more hydrophilic and the capacity to absorb water increases [71].

Depending on the type of pendant groups of the moieties, ionic hydrogels can be anionic or cationic. Anionic hydrogels, which contain negatively charged groups, shows a notorious increase in the swelling at higher pH caused by the electrostatic interactions between the anions formed along the chains [72]. Cationic hydrogels, which have positive charges in their pendant groups, exhibit an increase in their swelling behavior at low pH [73]. This swelling enhancement in cationic hydrogels is the result of two phenomena: first the augmentation in the hydrophilicity of the polymer and second the electrostatic repulsion between the positively charged groups [74].

2.4.1 Hydrogel Structural Parameters

The network structure of hydrogels can be characterized as a function of three main parameters: the polymer volume fraction in the swollen state ($\nu_{2,s}$), the number average molecular weight between crosslinks (M_C) and the correlation length (ξ), the last one also known as the mesh (or pore) size [70].

The polymer volume fraction in the swollen state ($\nu_{2,s}$) evaluates the amount of fluid absorbed and retained by the hydrogel. The molecular weight between two adjacent crosslinks (M_C) is a measure of the degree of crosslinking of the polymer. The correlation length between two subsequent crosslinks (ξ) is a measure of the space available for diffusion between two macromolecular chains. Due to the extent of

randomization produced during the polymerization, both the molecular weight between crosslinks and the correlation length can be only evaluated as an average value. The determination of these parameters can be performed through theoretical methods and experimental techniques. Equilibrium swelling and rubber elasticity theory are two experimental techniques frequently used in the literature for the determination of hydrogel mechanical parameters [25]. Figure 5. illustrates the physical meaning of (M_c) and (ξ).

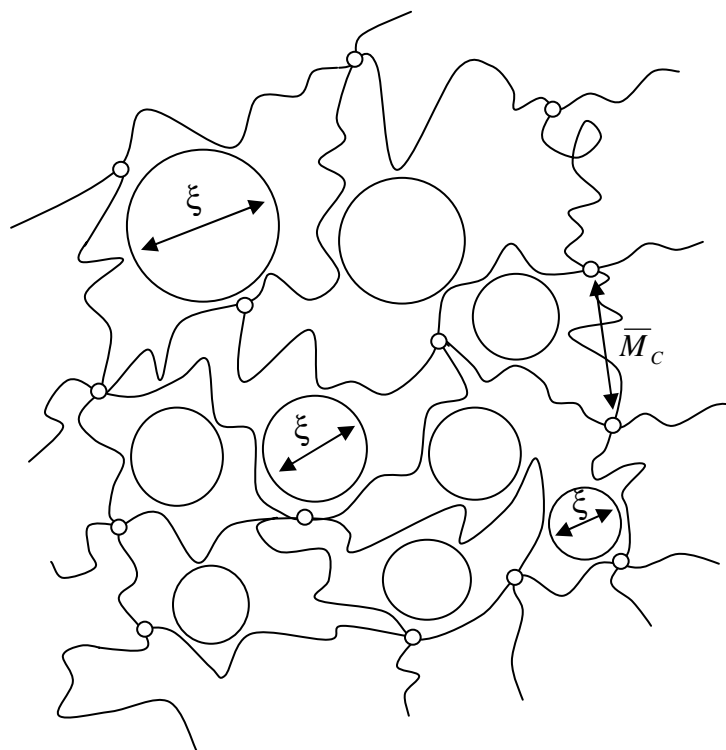


Figure 5. Representation of the number average molecular weight between crosslinks (M_c) and the correlation length (ξ).

Hydrogels swelling highly deviate from the ideal thermodynamic behavior. As a consequence, classical thermodynamics can not describe their exact behavior.

Nevertheless, the Flory-Rehner theory and its later variations have been employed with considerable success [25]. The Flory-Rehner theory assumed hydrogels as neutral networks, tetra-functionally crosslinked, with polymer chains showing a Gaussian distribution [75]. This theory applies when the crosslinking of the polymer chains occurs in the solid state [76]. As mentioned earlier, the thermodynamic force of mixing and the retractive force of polymer chains are the only forces that affect the swelling behavior of neutral hydrogels. When equilibrium is reached, the contribution of the two forces is equal, and this physical situation can be expressed in terms of the free energy of Gibbs [70, 77].

$$\Delta G_{Total} = \Delta G_{Elastic} + \Delta G_{Mixing} \quad (3)$$

where $\Delta G_{Elastic}$ is the contribution of the elastic retractive forces developed inside the gel and ΔG_{Mixing} is the contribution of the spontaneous mixing of the fluid molecules with the polymer chains.

Equation (1) can be differentiated with respect to the number of molecules of swelling agent, keeping the pressure and the temperature constant.

$$\mu_1 - \mu_{1,0} = \Delta\mu_{Elastic} + \Delta\mu_{Mixing} \quad (4)$$

where $\Delta\mu_{Elastic}$ and $\Delta\mu_{Mixing}$ are the elastic and mixing contributions to the chemical potential change respectively, μ_1 is the chemical potential of the solvent in the polymer gel and, $\mu_{1,0}$ is the chemical potential of the pure solvent.

The difference between the chemical potentials of the solvent outside and inside the gel must be zero during swelling equilibrium. The change in chemical potential due to mixing can be evaluated from the entropy change of mixing and the heat of mixing.

The chemical potential change due to elastic contributions can be determined from the rubber elasticity theory [70, 77]:

$$\Delta\mu_{Mixing} = RT(\ln(1 - v_{2,s}) + v_{2,s} + \chi_1 v_{2,s}^2) \quad (5)$$

and

$$\Delta\mu_{Elastic} = \frac{RTV_1}{\bar{v}\bar{M}_c} \left(1 - \frac{2\bar{M}_c}{\bar{M}_n}\right) \left(v_{2,s}^{1/3} - \frac{v_{2,s}}{2}\right) \quad (6)$$

where χ_1 is the Flory-Huggins polymer-water interaction parameter, V_1 is the molar volume of water, \bar{v} is the specific volume of the polymer, $v_{2,s}$ is the volume fraction of the swollen gel, \bar{M}_c is the number average molecular weight between the crosslinks, \bar{M}_n is the molecular weight of linear polymer chains prepared at the same conditions without crosslinking, R is the gas constant and T is the temperature.

Equating these two contributions, an expression for the determination of the molecular weight between two adjacent crosslinks can be written as [78]:

$$\frac{1}{\bar{M}_c} = \frac{2}{\bar{M}_n} - \frac{\left(\frac{\bar{v}}{V_1}\right) [\ln(1 - v_{2,s}) + v_{2,s} + \chi_1 v_{2,s}^2]}{v_{2,s}^{1/3} - \frac{v_{2,s}}{2}} \quad (7)$$

Equation (8) gives an expression to evaluate the molecular weight of linear polymer chains prepared under identical conditions but in the absence of the crosslinking

$\left(\bar{M}_n\right)$ [69]:

$$\bar{M}_n = M_0 \frac{k_p [M]}{(fk_d k_t [I])^{1/2}} \quad (8)$$

where M_0 is the molecular weight of the monomer unit, k_p and k_t are the kinetic constants of propagation and termination respectively, k_d is the kinetic constant of the initiator decay, f is the efficiency of the initiator, $[M]$ and $[I]$ are the concentrations of the monomer and initiator respectively

Peppas and Merrill [78] introduced a modification to the Flory-Rehner theory to extend its applications to hydrogels in which the solvent is present during the crosslinking reaction of the macromolecular chains. The chemical potential change due to elastic contributions is affected by the presence of solvent. Therefore, $\Delta\mu_{Elastic}$ must account for the volume fraction density of the chains during crosslinking. According to this model, the molecular weight between two subsequent crosslinks in neutral hydrogels prepared in the presence of water is evaluated by equation (9).

$$\frac{1}{\bar{M}_c} = \frac{2}{\bar{M}_n} - \frac{\left(\bar{v}/V_1\right)\left[\ln(1-v_{2,s}) + v_{2,s} + \chi_1 v_{2,s}^2\right]}{v_{2,r} \left[\left(\frac{v_{2,s}}{v_{2,r}}\right)^{1/3} - \left(\frac{v_{2,s}}{2v_{2,r}}\right) \right]} \quad (9)$$

where $v_{2,r}$ is the polymer volume fraction in the relaxed state, immediately after crosslinking, but prior to swelling.

The polymer volume fractions of the hydrogel in both relaxed and swollen state, $v_{2,r}$, and $v_{2,s}$ can be evaluated from swelling studies using the following relationship [79]:

$$v_{2,r} = \frac{V_p}{V_{g,r}} \quad (10)$$

$$v_{2,s} = \frac{V_p}{V_{g,s}} \quad (11)$$

where V_p is the volume of the dry polymer, $V_{g,r}$ is the volume of the hydrogel after crosslinking but before swelling and $V_{g,s}$ is the volume of the hydrogel after equilibrium swelling. In addition, the reciprocal of polymer volume fraction of the hydrogel in swollen state $v_{2,s}$ is known as the volumetric swelling ratio Q [73].

$$Q = \frac{1}{v_{2,s}} \quad (12)$$

The hydrogel volume before and after swelling can be evaluated applying the Archimedes buoyancy principle which states that every solid body immersed in a fluid loses weight by an equal amount to the fluid displaced [79]. Using this principle, the following expressions are obtained:

$$V_{g,r} = \frac{W_{a,r} - W_{n,r}}{\rho_n} \quad (13)$$

$$V_{g,s} = \frac{W_{a,s} - W_{n,s}}{\rho_n} \quad (14)$$

where $W_{a,r}$ is the hydrogel weight in air after crosslinking, $W_{n,r}$ is the hydrogel weight in a non-solvent after crosslinking, $W_{a,s}$ is the hydrogel weight in air after swelling, $W_{n,s}$ is the hydrogel weight in a non-solvent after swelling, and ρ_n is the density of the non-solvent.

The volume of the dry polymer V_p can be evaluated using the next expression:

$$V_p = \frac{W_{a,d}}{\rho_n} \quad (15)$$

where $W_{a,d}$ is the hydrogel weight in air after drying.

The thermodynamic analysis of the swelling behavior in ionic hydrogels is much more complicated. A chemical potential due to the ionic character of the hydrogel must be included. The nature of the ions present in the solvent and the ionic strength of the surrounding media have a marked influence in the ionic chemical potential [80, 81]. Equations (16) and (17) have been derived for the swelling of anionic and cationic hydrogels in the presence of a solvent respectively [76, 78].

$$\begin{aligned} \frac{V_1}{4I} \left(\frac{v_{2,s}^2}{\bar{v}} \right) \left(\frac{K_a}{10^{-pH} - K_a} \right)^2 = & \left[\ln(1 - v_{2,s}) + v_{2,s} + \chi_1 v_{2,s}^2 \right] \\ & + \left(\frac{V_1}{\bar{v} \bar{M}_c} \right) \left(1 - \frac{2\bar{M}_c}{\bar{M}_n} \right) v_{2,r} \left[\left(\frac{v_{2,s}}{v_{2,r}} \right)^{1/3} - \left(\frac{v_{2,s}}{2v_{2,r}} \right) \right] \end{aligned} \quad (16)$$

and

$$\begin{aligned} \frac{V_1}{4I} \left(\frac{v_{2,s}^2}{\bar{v}} \right) \left(\frac{K_b}{10^{pH-14} - K_b} \right)^2 = & \left[\ln(1 - v_{2,s}) + v_{2,s} + \chi_1 v_{2,s}^2 \right] \\ & + \left(\frac{V_1}{\bar{v} \bar{M}_c} \right) \left(1 - \frac{2\bar{M}_c}{\bar{M}_n} \right) v_{2,r} \left[\left(\frac{v_{2,s}}{v_{2,r}} \right)^{1/3} - \left(\frac{v_{2,s}}{2v_{2,r}} \right) \right] \end{aligned} \quad (17)$$

where I is the ionic strength, K_a and K_b are the acid dissociation constant and the base dissociation constant of the polymer chains respectively.

After the molecular weight between crosslinks is determined using the swelling theory, the correlation length or pore size can be evaluated through equation (18) [25, 69].

$$\xi = \alpha \left(\bar{r}_0^2 \right)^{1/2} \quad (18)$$

where α is the elongation ratio of the polymer chains, $\left(\bar{r}_0^2\right)^{1/2}$ is the root mean squared end-to-end distance of the polymer chain in freely jointed state.

The elongation ratio (α) is related to the swollen polymer volume fraction ($v_{2,s}$) by equation (16).

$$\alpha = v_{2,s}^{-1/3} \quad (19)$$

The unperturbed end-to-end distance of the polymer chain between two adjacent crosslinks can be determinate using the following equation.

$$\left(\bar{r}_0^2\right)^{1/2} = l(C_n N)^{1/2} \quad (20)$$

where C_n is the Flory characteristic ratio of the polymer, l is the length of the bond along the polymer backbone and, N is the number of links along the polymer chain.

This last parameter can be calculated by equation (21)

$$N = \frac{2\bar{M}_c}{M_r} \quad (21)$$

where M_r is the molecular weight of the repeating unit.

In summary, coupling equations from (18) to (21), the mesh network pore size can be obtained.

$$\xi = v_{2,s}^{-1/3} \left(\frac{2C_n \bar{M}_c}{M_r} \right)^{1/2} l \quad (22)$$

The correlation length allows classifying the hydrogels as macro-porous, micro-porous and non-porous, depending on the sizes of the pores [25]. Macroporous hydrogels

are those with pore size in a range of 100 nm-10 μm . Microporous hydrogels are characterized by a pore size in the range of 10-100 nm. Finally, non-porous hydrogels has a typical correlation length of 10–100 Å [82, 83].

2.4.2 Diffusion Theory

Solute diffusion is an essential characteristic for several applications of hydrogels in bioengineering [70]. Diffusion is the mass transport across a chemical potential which is caused mainly by random molecular motions [84]. This process correlates the mass transfer rate of a substance through a unit area to the concentration gradient normal to the section by a proportionality constant, D (cm^2/s), also known as diffusion coefficient [85]. Polymer diffusion is complex and the diffusion rates lie between those in liquids and in solids. Polymer diffusion rates are strongly influenced by the concentration and the swelling degree of the polymers [83].

The first mathematical approach for diffusion in one dimension was made by Fick [83]. The Fick's law can be employed to describe the drug or protein diffusion through a hydrogel, assuming that the diffusion coefficient (D) is constant [85].

$$\frac{\partial C_d}{\partial t} = D \left(\frac{\partial^2 C_d}{\partial x^2} \right) \quad (23)$$

where C_d is the concentration of the solute, t is the time and, x is the distance.

The solution of Fick law for a plane sheet of the sample of thickness (L) with surfaces maintained at constant concentration was given by Crank [84]:

$$\frac{M_t}{M_\infty} = 1 - \frac{8}{\pi^2} \sum_{n=0}^{\infty} \frac{1}{(2n+1)^2} \times \exp\left[-\frac{D(2n+1)^2 \pi^2 t}{4L^2}\right] \quad (24)$$

where M_t is the accumulative mass of solute released at time and, M_∞ is amount of solute released at infinite time.

At short times when $t \rightarrow 0$, the last equation can be simplified to the Stefan approximation [86].

$$\frac{M_t}{M_\infty} = \frac{2}{\sqrt{\pi}} \left[\frac{Dt}{L^2} \right]^{1/2} \quad (25)$$

Equation (17) was derived assuming that the diffusion coefficient (D) is constant. Plotting the mass release ratio (M_t/M_∞) versus the root square of the time ($t^{1/2}$), the diffusion coefficient can be evaluated from the slope of the curve for the 60% of the total release with an accuracy of 1% [85, 86].

The preceding analysis is valid for systems where Fick's law applies. However, transport of organic molecules in glassy polymers often does not follow the Fickian diffusion model [87]. When a solid polymer is placed in contact with a penetrating solution loaded with a solute, the solute diffuses into the polymer and the polymer swells. Diffusion requires the transport of solute molecules through pre-existing or dynamically formed spaces of the polymeric chains. Polymer swelling involves the motion of the polymer chains resulting in an increased separation between polymer molecules [88]. Both the diffusion process controlled by the concentration gradient and the relaxation process controlled by a time dependent response of the polymer to the swelling stress, contribute to the rate and extent of molecule penetration in glassy polymers [88, 89].

The following features characterize the relaxation controlled transport [90]:

- a) When the solvent penetrates into the polymer, a sharp advancing boundary separates the glassy inert core from the swollen shell.
- b) The boundary between the swollen gel and the glassy core advances toward the film mid-plane at a constant velocity.
- c) The initial weight gain for the polymer is directly proportional to time.
- d) The swollen gel behind the advancing front is at a uniform state of swelling.

The interactions between the diffusion and chain relaxation process allow that different behaviors occur during solute transportation in polymers. A more general expression of the Stefan approximation permits the evaluation of the different solute transport mechanisms [91]:

$$\frac{M_t}{M_\infty} = kt^n \quad \text{for } 0 < \frac{M_t}{M_\infty} < 0.60 \quad (26)$$

where k is the characteristic constant of the polymer/solute system and n is the diffusional exponent.

The value of the diffusional exponent allows the determination of the type of predominating diffusion mechanism in the system. Generally, for $n = 0.5$ transport follows Fickian behavior and for $n = 1$ transport is relaxation controlled. A value of (n) between 0.5 and 1 indicates anomalous transport. In this case, there are contributions from Fickian diffusion and relaxation processes [86, 91, 92]. Table 7. summarizes the different types of transport based on the values of the diffusional exponent.

Table 7. Transport mechanism of solute through a hydrophilic polymer network [85, 93].

Diffusional Exponent, n	Type of Transport
0.5	Fickian Diffusion (Case I)
$0.5 < n < 1.0$	Non-Fickian (anomalous) transport
1.0	Relaxation Controlled (Case II)

In situations when the sorption kinetic is not completely Fickian, the use of the Berens and Hopfenberg model (dual-mode sorption model) is regularly reported in the literature. For this model, the sorption process is considered as a linear superposition of independent contributions from Fickian diffusion and polymer relaxation. The following equation gives an expression for the total amount of sorption at time t [88].

$$M_t = M_{t,F} + M_{t,R} \quad (27)$$

where $M_{t,F}$ is the contribution of the Fickian diffusion and, $M_{t,R}$ is the contribution from the relaxation process.

Fickian diffusion for polymer disks of thickness (L) is described by equation (24). Berens and Hopfenbers proposed equation (28) as the differential equation for the relaxation process. This equation was based upon the assumption that the relaxation process was first order in the concentration difference which drives the relaxation [88].

$$\frac{dM_{t,R}}{dt} = k(M_{\infty,R} - M_{t,R}) \quad (28)$$

where k is relaxation rate constant and, $M_{\infty,R}$ is the ultimate amount of sorption due to relaxation.

Integration of the previous equation leads to:

$$M_{t,R} = M_{\infty,R} [1 - \exp(-kt)] \quad (29)$$

Substituting equation (24) and (28) into equation (27) and rearranging result in an expression that consider the contributions of Fickian diffusion and relaxation process to the sorption process for a disk of thickness (L) [85, 88, 92].

$$\frac{M_t}{M_\infty} = \phi_F \left[1 - \sum_{n=1}^{\infty} \frac{8}{(2n+1)^2 \pi^2} \exp\left(-\frac{D(2n+1)^2 \pi^2 t}{L^2}\right) \right] + \phi_R (1 - \exp(-kt)) \quad (30)$$

where ϕ_F is the fraction of sorption contributed by Fickian diffusion, ϕ_R is the fraction of sorption contributed by relaxation chains, k is the first order relaxation constant and, D is the diffusion coefficient.

At later times, the sorption process is dominated by the relaxation of polymer chains, and the Fickian contribution of equation (27) can be neglected. For this conditions, a semilog plot of $(1 - M_t/M_\infty)$ versus time can be used to evaluate k , ϕ_F and ϕ_R [92].

$$\text{Ln}\left(1 - \frac{M_t}{M_\infty}\right) = \text{Ln}(\phi_R) - kt \quad (31)$$

Expanding the equation (27) for $n = 3$ and taking natural logarithm in both sides, the following equation is obtained:

$$\text{Ln}\left(1 - \frac{M_t}{M_\infty}\right) = \text{Ln}(4.8305 \times 10^{-5} \phi_F^3) + \text{Ln}(\phi_R) + \left(\frac{-204.7943D}{L^2} - k\right)t \quad (32)$$

At short times, the relaxation process can be neglected. Using the latter equation for the 60% of sorption process, a plot of $\ln(1 - M_t/M_\infty)$ versus time could be used to determine the diffusion coefficient.

$$D = \left(\frac{L^2}{-204.58} \right) (\text{slope} + k) \quad (33)$$

2.4.3 Hydrogel Partition Coefficient

After polymerization, proteins, peptides, or drugs can be introduced into a hydrogel using a suitable solvent. The capability of the solvent to act as a swelling agent for the hydrogel and its ability to dissolve the molecule are relevant features that should be considered when selecting the solvent [85]. Molecule loading is performed by placing the hydrogel in a solution of the protein or drug. The hydrogel is allowed to reach the equilibrium with the surrounding media to evaluate the equilibrium distribution or partition coefficient between the gel and the solution [91].

The partition coefficient is a measure of the solute's affinity toward to diffuse inside the polymer membrane or to remain in solution. The value of this parameter is related to characteristics of the molecule to be loaded such as: size, shape, and net charge. If a protein to be loaded into a hydrogel has an opposite net charge, the protein can plug the pores at the surface of the hydrogel during the incorporation. If the net charge of the protein is the same as that of the hydrogel, Donnan exclusion effect can cause the exclusion of the protein from the hydrogel. Also the ionic strength, pH, and solvent

employed to prepare the protein solution may affect the amount and the distribution of the protein into the gel [23].

The following equation allows the calculation of the partition coefficient [69, 73].

$$K_d = \frac{C_m}{C_s} = \frac{V_s(C_i - C_0)}{V_m C_0} \quad (34)$$

where C_m and C_s are the concentrations of the solute in the membrane and in the solution respectively, C_i is the initial concentration of the solute in the solution, C_0 is the concentration of the solute in the solution after equilibrium, V_s and V_m are the volumes of the solution and the membrane respectively.

2.4.4 Bioengineering Applications of Hydrogels

Through the years, hydrogels have found applications in different fields including controlled release devices, tissue engineering, separation systems, and sensor components [94-96]. Hydrogels have been used for applications in the controlled administration of drugs by several different routes: oral, nasal, buccal, rectal, vaginal, ocular and parental [25]. Ionic hydrogels exhibit dramatic changes in swelling behavior, network structure, permeability or mechanical strength as a consequence to different stimuli internal and external to the body [97]. In drug delivery applications, these changes are exploited to design systems that can release a drug or a protein at predetermined rates for predefined periods of time in response to variable demand conditions at specific sites of the body [98].

Within the environmental sensitive hydrogels, two categories that have been further investigated are those in which their response is controlled by temperature and pH [70]. In thermosensitive hydrogels, swelling behavior can be controlled by a temperature change in the swelling media. This attribute has been utilized to regulate the drug release [36, 106]. The most studied temperature sensitive hydrogel is poly (N-isopropylacrylamide) (PNIPAAm) [70]. The pH dependent swelling behavior of hydrogels have been useful in the design of novel drug delivery systems due to known pH variations that naturally occur in several body sites such as the gastrointestinal tract, vagina and blood vessels [98]. These type of hydrogels has been investigated mainly for oral drug delivery systems [24]. The most extensively pH sensitive hydrogels used are poly(acrylic acid) (PAA), poly(methacrylic acid) (PMAA), poly(diethylaminoethyl methacrylate) (PDEAEM) and poly(dimethylaminoethyl methacrylate) (PDMAEM), and their copolymers [70].

The most recent application of hydrogels is in tissue engineering. Tissue engineering is a challenging method for treating patients who need a new organ or a new tissue. This technique requires the utilization of a porous scaffold which behaves as a three dimensional template for the cell attachment and subsequent tissue formation [23, 93]. The structural similarity to the macromolecular based components of the body and the biocompatibility are the relevant features of hydrogels that make them appropriate to be used as scaffolds to construct new tissues [99].

Hydrogels have been also investigated for sensor applications even though in a lesser proportion than for drug delivery systems. In this area, hydrogels have been investigated for the development of long-term implantable biosensors [100]. The

deleterious effect of biofouling and lack of poor in vivo biocompatibility has limited the application of implantable biosensors to academic studies. The use of hydrogels emerges as an alternative to overcome these difficulties because they are considered biocompatible and have shown to act as effective antifouling sensor components [101].

Glucose responsive insulin release devices couple two applications of hydrogels: sensing and drug delivery. These systems involve the immobilization of glucose oxidase in a pH responsive hydrogel enclosed in a saturated insulin solution [26]. When glucose diffuses into the hydrogel, glucose oxidase catalyses its conversion to gluconic acid. The acid formation diminishes the pH in the microenvironment surrounding the hydrogel [97]. In anionic hydrogels, the decrease in pH causes a reduction in the mesh size as a consequence; insulin is squeezing out from the matrix. In cationic hydrogels, the fall in pH increases the mesh size. In this case insulin is released from the network by diffusion [72]. For this application, hydrogels built from polyacrylamide, poly(2-hydroxyethyl methacrylate) (HEMA), poly (dimethylaminoethyl methacrylate) (DMAEM), poly(diethylaminoethyl methacrylate) (DEAEM), poly(ethylene glycol) (PEG) and copolymers have been investigated [74].

In addition, pH sensitive hydrogels have also been investigated for the development of carbon dioxide (CO₂) sensors. This sensor combines hydrogel microspheres with a pressure sensor. By means of measuring pressure versus pH it is possible to estimate the hydrogel pK_a. Then, when measurement in a specific pH range is required, such as induced by CO₂, a hydrogel with a pK_a in that range can be tailored for this sensor application. Herber and colleagues proposed for this application the

utilization of hydrogel microspheres of metacrylic acid (MAA) copolymerized with diethylenetriamide (DETA) (MAA-co-DETA) [100].

Chapter Three

Previous Work

3.1 Immobilization of Hemeproteins

The immobilization of hemeproteins has been addressed to achieve different goals, but the emphasis of the investigations has been primarily focused in the utilization of these proteins in electrochemical and optical sensing devices. Hemeproteins are considered redox proteins, which refers to their capability of undergoing electron transfer. Increasing interest has encouraged the study of protein electrochemistry to improve the understanding about the mechanisms of electron exchange between proteins and electrodes [102, 103]. Also, hemeproteins are able to perform very selective reactions which are essentially based on the electron transfer [104]. Therefore, hemeproteins have been investigated for the development of highly selective and sensitive electrochemical biosensors [105]. For electrochemical applications, the direct

electron transfer between hemeproteins and electrodes has been accomplished incorporating proteins in films [106], SP Sephadex [107], and gold nanoparticles [108-111].

Protein incorporation into modified electrode surface films is a fairly new strategy to improve the protein electrochemistry. Thin films are expected to provide a well-defined microenvironment for proteins and facilitate the electron transfer between proteins and electrodes [103]. Three types of film forming materials have been investigated: surfactant film, polyion-surfactant or clay-surfactant composite films and amphiphilic polymers [112]. The surfactant film has been studied by Rusling and colleagues which reported the incorporation of myoglobin in surfactants films on pyrolytic graphite (PG), gold (Au), and Platinum (Pt) electrodes. The surfactant used was didodecyldimethylammonium bromide (DDAB). An increase in electron transfer for Mb in surfactant films at PG, Au, and Pt electrodes was observed when compared to bare or naked electrodes. This enhancement displayed only little dependence on the electrode material. The strong adsorption of surfactants at the electrode film interface may be the cause of the improved electron transfer. Additionally, the embedded surfactant inhibits macromolecular adsorption that would interfere with the electron transfer between Mb and the electrode. Cast Mb-surfactant films showed to be stable for weeks and can catalytically dehalogenate organohalide pollutants [102, 113].

The second type of films are composed by a polyion (clay) and an oppositely charged surfactant, both forming a neutral and water insoluble composite. The polyion-surfactant composite films have similar features to the surfactants films alone, but maybe they can provide better stability than the latter mentioned due to the introduction of

polymer or clay backbones in the films. These films may create a biomembrane-like microenvironment for proteins. Some of the polyions studied are polystyrenesulfonate (PSS), polyacrylic acid (PAA), polyvinyl sulfate (PVS), and poly(diallyldimethylammonium) (PDDA) [103, 114].

The last type of film used to immobilize hemoproteins for electrochemical applications are amphiphilic polymer films. These polymers, which can be considered as polymeric surfactants, have a hydrophobic backbone and hydrophilic groups. N. Hu and coworkers investigated the immobilization of different hemoproteins (hemoglobin, myoglobin, horseradish peroxidase (HRP), catalase (Cat)) in polyacrylamide (PAM) films [105, 115]. Mb-PAM and Hb-PAM films exhibited an enhanced electron transfer rates which were similar to those observed in other films and much faster than those on bare PG electrodes. These films were believed to be stabilized by the hydrophobic interactions between the protein and the polymer. Polyacrylamide films can absorb large amounts of water and form a hydrogel. These hydrogel films were water-insoluble and very stable in aqueous solution and could offer a suitable microenvironment for incorporated proteins [106, 112, 116].

SP Sephadex membranes are frequently employed in chromatographic techniques to purify proteins showing an appropriate media for the entrapment of proteins. For that reason SP Sephadex membranes have been utilized to entrap hemoglobin combined with a pyrolytic graphite electrode. Fan et al. entrapped bovine Hb in SP Sephadex membrane observing that electrons could easily exchange with the electrode. Also, hemoglobin showed a high peroxidase activity though the non-covalent interaction with SP Sephadex

membranes, making this configuration an excellent candidate for the development of hydrogen peroxidase biosensors [107]

Other supports that have gained increased interest for the immobilization of proteins for electrochemical applications are nanoparticles. Nanoparticles have demonstrated to protect the bioactivity of proteins upon adsorption. The most widely investigated nanoparticles are based on colloid gold. Gu and colleagues verified that bovine hemoglobin could be successfully immobilized by adsorption on gold nanoparticles retaining its biological activity. The hemoglobin immobilized in this manner could be used for the development of a hydrogen peroxide biosensor because the protein displayed an excellent catalytic response to the reduction of H_2O_2 . However, at a concentration of hydrogen peroxide higher than 1.0×10^{-2} M, denaturation of the immobilized Hb occurred [108]. These researchers also reported the immobilization of bovine hemoglobin in gold nanoparticles to monitor nitric oxide [110].

Liu and coworkers studied the immobilization by adsorption of hemoglobin in colloid gold nanoparticles mixed with carbon paste. In this specific investigation the pursued objective was the development of nitrogen dioxide (NO_2^-) biosensor. The sensing device displayed a good stability and it could be quickly regenerated showing reproducible measurements [117]. Lately, Liu and colleagues performed an investigation of the feasibility to immobilize hemoglobin into zirconium dioxide (ZrO_2) nanoparticles modified with pyrolytic graphite electrode. The results revealed that Hb was effectively immobilized and a fast electron transfer was achieved. A higher affinity of hemoglobin toward hydrogen peroxide was detected, which could allow the production of a H_2O_2 sensor [118].

Hemeproteins are also well known for their optical properties which change during the binding of the corresponding ligands [9]. These optical characteristics have been investigated for the development of optical biosensors to detect dissolved oxygen (DO), nitric oxide (NO), carbon monoxide (CO) [16, 17]. In optical applications, the most widely investigated material for hemeproteins immobilization has been the sol-gels [119]. Sol-gel encapsulation process has been used to immobilize hemeproteins because this mechanism allows the physical entrapment of the biomolecule without chemical modification. The sol-gel technique involves hydrolysis and condensation reactions of liquid alkoxides [16]. A porous structure is built around the biomolecule being immobilized and a small analyte molecule can diffuse through the pores. The interactions between the protein and the ligand are frequently monitored by spectroscopic methods since sol-gel matrices are optically transparent [120]. It has been observed that proteins immobilized in sol-gels retain their chemical and spectroscopic properties, probably because sol-gels are synthesized at low temperature under mild reaction conditions [121, 122].

J. Zink et al. studied the immobilization of horse heart myoglobin into silica sol-gels prepared from tetramethyl orthosilicate (TMOS) as a sensing element in a measurement method for dissolved oxygen (DO). Myoglobin was immobilized in metaquo state and subsequently reduced to deoxy state using a dithionite solution. DeoxyMb gels were found to react with dissolved oxygen to give oxyMb gels and the changes in spectroscopic properties were used to confirm the detection of DO. The optical response, which was related to the rate change absorbance after binding, was 2

minutes. Regeneration of used gels was accomplished using a dithionite solution, which reduces oxyMb gels to deoxyMb gels [16].

McCurley and colleagues also immobilized horse heart myoglobin in sol-gels based on TMOS. However, this investigation established that the use of fluorescence could allow the detection of lower concentrations of dissolved oxygen when compared to the levels detected by absorbance techniques. DeoxyMb gels were placed in the beam path between excitation monochromator and the cuvette containing the fluorophore, brilliant sulfaflavin. The emission of the fluorescent dye translated the absorbance change of myoglobin after oxygen binding into a fluorescent signal [123].

The immobilization of human hemoglobin in TMOS sol-gels were achieved by Shibayama. Oxy and deoxy hemoglobins were immobilized and it was observed that both retained their reversible oxygenation properties and spectroscopic properties. The principal conclusion of these studies was that Hb encapsulated into sol-gel matrices maintained fixed its original quaternary structure during oxygenation and deoxygenation process. Apparently, the kinetic of the structural changes was considerably diminished by sol-gel immobilization [120].

Blyth and colleagues concluded that through the immobilization of hemoglobin in sol-gel glasses it would be possible to develop a solid state material that can be used as a biological recognition element for some gases such as: oxygen (O_2), carbon monoxide (CO) and nitrogen monoxide (NO). The changes in spectroscopic properties of hemoglobin have not shown to be affected by immobilization process [17].

J. Zink and coworkers has also investigated the immobilization of another heme protein, cytochrome-c. The successful immobilization of cytochrome-c into sol-

gels silica gels using TMOS was reported. It was found that this immobilization process provides protection against external denaturing agents. Also, denaturation of immobilized cytochrome-c was reversible and the native form could be regenerated. The reactivity and chemical function of immobilized cytochrome c resembled those of the free protein [121, 122].

Estrada explored the possibility of taking advantage of the strong affinity shown by hemoglobin I from *Lucina pectinata* as recognition element for hydrogen sulfide detection. This cytoplasmic hemoglobin was immobilized inside TMOS sol-gels. The encapsulated protein in TMOS sol-gels spontaneously changed from ferrous to ferric state. Unlike HbI in solution, the treatment of immobilized HbI with sodium dithionite did not provoke a reduction in oxidation state. It was concluded that the entrapment process had an effect in oxidation state of this particular protein. The association constant for the formation of the HbI-SH₂ complex was 0.1416 M⁻¹s⁻¹. This value was six orders magnitude lower than the value reported in the literature for the association constant of HbI in solution and H₂S. Spectral changes were observed after 400 seconds of the addition of hydrogen sulfide to the sol-gels containing HbI and saturation occurred after approximately 15 minutes. In contrast, the dissociation constant was very low; the dissociation process took place in about 6 to 10 hours. This work concluded that the sol-gel matrix did not induce significant changes in the three dimensional structure and did not produce denaturation of the HbI immobilized. Also, the pores of the matrix may difficult the diffusion of hydrogen sulfide through the sol-gel provoking the decrease of both the dissociation and association constant [47].

In general, it has been widely reported that after entrapment of heme proteins in sol-gel matrices these proteins retain their spectroscopic properties and chemical functions. However, a slight perturbation of the protein conformation has been observed in cytochrome-c incorporated in sol-gel matrices. Raman studies on myoglobin have evinced that the entrapment in a sol-gel matrix hinder the conformational fluctuations necessary to open the heme pocket. At earlier steps of the incorporation process when the conformational fluctuations are still possible, partial loss of the heme group may provoke the reported partial protein inactivation [9].

Sol-gel immobilization techniques have demonstrated to allow high protein loading, control the polarity and porosity of the matrix, adapt the material composition to increase the matrix biocompatibility, and show low leaching of the incorporated biomolecule. Some disadvantages of sol-gel methods are the difficulty to predict the properties of the resultant glass, aging of the material, and protein denaturation with time which causes problems with sensor calibration. Moreover, the size of the pores must be controlled to allow the transport of the analyte inside the matrix and to avoid the leaching of the entrapped protein. Finally, aging can also produce cracking and shrinking of the matrix leading to severe drawbacks in sensor responses [10].

The use of sol-gels in optical sensing techniques can allow reaching a single molecule detection limit when fluorescent signaling is used. This advantage is not present in electrochemical methods and can be used to measure very dilute solutions. The mayor disadvantage of sol-gel based optical biosensor is the restricted range of materials that can be employed for sensor fabrication because these materials must yield optical transparent films [10].

This project has proposed the utilization of hydrogels as immobilization support for hemeproteins. Hydrogels emerge as an alternative to provide biomolecules with environments that could protect their biological function and allow their use in biosensor technology. Like sol-gels, hydrogels are also transparent which make them appropriate to be used in optical sensing applications. Hydrogels have been extensively employed in the delivery of drugs, peptides, and proteins [124]. This application indicates that hydrogels could create suitable environments which offer protection from a harsh external media and improve the stability [24, 26]. Hydrogels display variations in their swelling behavior, network structure, permeability or mechanical strength as a consequence of different stimuli. Among the various stimuli that can be used to modulate the drug delivery are changes in the pH, ionic strength of the surrounding media, temperature, electric or magnetic fields, and concentration [25, 98].

Hydrogels can be designed to possess precise features through the manipulation of specific properties. The degree of crosslinking, which determines the molecular weight between crosslinks, is a factor that may be used to modify the mechanical strength, the swelling ratio, and the diffusion characteristics of hydrogels [125]. Other hydrogel properties that can affect the diffusive behavior are hydration, surface area to volume ratio, and ionic interaction between the protein and the hydrogel. Also, the solute diffusivity is influenced by thickness and stiffness of the polymer chains. All these properties can be tailored to produce a desired release profile or an immobilization support [126, 127].

The incorporation of the drug, peptides, or proteins inside the hydrogels has been frequently performed by two methods. One method consists in entrapping the molecule

inside the hydrogel during the polymerization. The other method utilizes a preformed hydrogel which is swelled to equilibrium in a molecule solution [128]. Forming the hydrogel in the presence of the molecule can be an effective approach but polymerization conditions could provoke deleterious effects on molecule properties [93]. Besides, removing the impurities and byproducts produced from the gel formation may produce leaching of some of the incorporated molecule. Moreover, side reactions between the hydrogel and the molecule may occur [129]. In the case of protein adsorbed on hydrogels, the interactions between the protein and the hydrophilic polymer have the potential to produce irreversible adsorption [85]. However, large proteins could be excluded from the hydrogel network due to the phenomenon known as size exclusion [129].

Getting a better understanding of the relationships between hydrogel structure and exhibited properties is critical for the advance in the development and rational design of hydrogels with specific characteristics that allow the permanent protein immobilization [130]. The capacity of hydrogels to maintain the activity and to provide a long term stability of proteins will determine the feasibility of this material as biomolecule carriers in monitoring system.

Chapter Four

Objectives

The main goal of this project was the examination of various polymer morphologies which could provide the best immobilization support for HbI from *Lucina pectinata* and Mb from horse skeletal muscle, without significantly affecting their biological activity.

To achieve these goals the following specific objectives were proposed:

- Determine optimum polymer morphology for the immobilization by adsorption and by polymerization in presence of the protein.
- Examine the polymer affinity towards the protein by the calculation of the partition coefficient as a function of the network morphology.
- Evaluation of the amount of protein permanently bound inside the polymer network as a function of polymer morphology.
- Examination of the protein biological activity after immobilization.

Chapter Five

Materials and Methods

5.1 Materials

5.1.1 Polymerization Materials

Polymers with different morphologies were used in this project, but the differences are not only related with the type of polymer employed; ionic or neutral, they also refer to the several crosslinker lengths used in each polymer. Two ionic monomers were considered, an anionic: methacrylic acid (MAA), and a cationic: dimethylaminoethyl methacrylate (DMAEM). The neutral polymer employed was poly(ethylene glycol) monomethyl ether monomethacrylate (PEGMA) with different tethered chain molecular weights, 200, 400 and 1000 g/mol. Poly(ethylene glycol) dimethacrylate was employed as the crosslinker and the following molecular weights were considered: 200, 600, and 1000 g/mol. In the case of neutral hydrogels, these only

can be prepared when the crosslinker length is larger than the monomer tethered chain. Table 8 illustrates the various arrangements between monomer and crosslinker that were studied.

Table 8. Monomer – crosslinker arrangements used in this project.

Monomer	Length of PEGDMA Crosslinker		
	200	600	1000
MAA	√	√	√
PEGMA	200	√	√
	400	√	√
	1000		√
DMAEM	√	√	√

Monomers and crosslinker agent were bought from Polyscience, Inc. (Warrington, PA) and were used as received with the exception of MAA. Methacrylic acid was purified to remove the inhibitor agent hydroquinone monomethyl ether using Di-hibit resin (Polyscience, Inc. Warrington, PA). The photo-initiator was 1-hydroxy cyclohexyl phenyl ketone at 99% (SIGMA - Aldrich, Milwaukee, WI). A mixture 1:1 of ethanol and deionized water was employed to dilute the polymerization mixture (EtOH, Fisher Scientific, Fair Lawn NJ).

The monomer/crosslinker molar ratio and the percentage of dilution were different for each hydrogel configuration employed during the project. Table 9 displays the values used for each morphology.

Table 9. Monomer to crosslinker ratio and percentage of dilution used in the preparation of different hydrogel configurations.

	MAA-PEGDMA Hydrogels	PEGMA-PEGDMA Hydrogels	DMAEM-PEGDMA Hydrogels
Monomer to crosslinker molar ratio	97:3	50:50	95:5
Monomer and crosslinker mixture to solvent mass ratio	1:1	1:1	3:2
Percentage of initiator	1%	1%	1%

5.1.2 Proteins

Two proteins were used in this project. Myoglobin from horse skeletal muscle (SIGMA - Aldrich, Milwaukee, WI) which was used as received. Hemoglobin I from *Lucina pectinata* was isolated from the clam and purified using size exclusion and ion exchange chromatography. The following chemicals were used during the isolation procedure:

- HEPES (N-[2-hydroxyethyl]piperazine-N'-[2-ethanesulfonic acid]) (SIGMA - Aldrich, Milwaukee, WI).
- EDTA (ethylenediaminetetraacetic acid) (SIGMA - Aldrich, Milwaukee, WI).
- DTR (dithiothreitol) (SIGMA - Aldrich, Milwaukee, WI).
- Sodium dihydrogen phosphate (NaH_2PO_4) (Fisher Scientific, Fair Lawn NJ).
- Ammonium bicarbonate (NH_4HCO_3) (Fisher Scientific, Fair Lawn NJ).

5.2 Methods

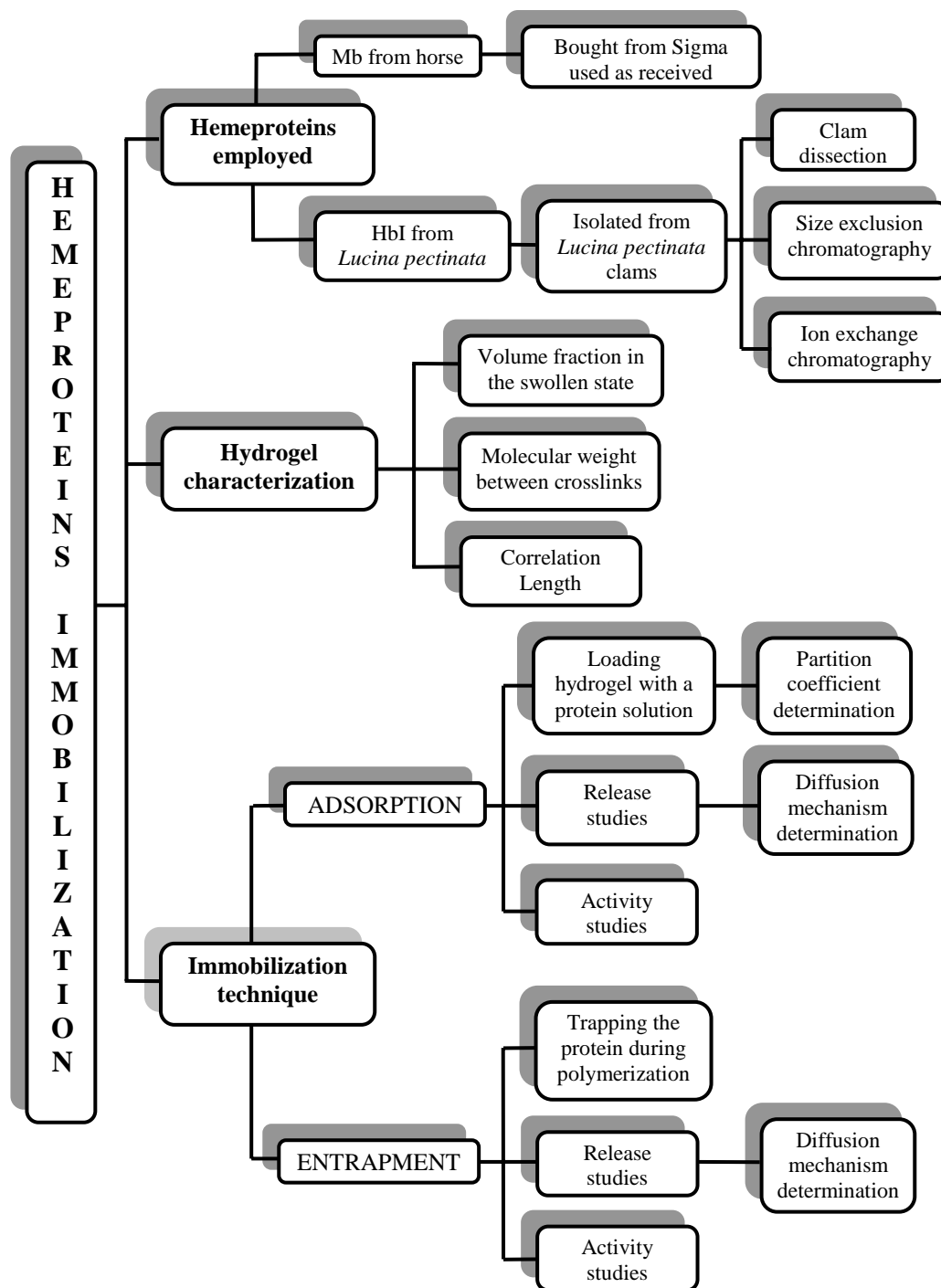


Figure 6. Scheme of the experimental procedures followed during this project.

5.2.1 Isolation of hemoglobin I from *Lucina pectinata*

5.2.1.1 Ctenidia dissection

Approximately sixty *Lucina pectinatas* were collected from the mangrove swamps of La Parguera and brought to the laboratory in seawater. The clams were opened and the ctenidia were carefully removed with a spatula. The ctenidium is the red part in the interior of the mollusk where the three hemoglobins are found. The ctenidia were pulled together in a beaker placed in an ice bath. For each 25g of ctenidia, 100 ml of extraction solution was added. The extraction solution was prepared mixing 10 mM of HEPES (N-[2-hydroxyethyl]piperazine-N'-[2-ethanesulfonic acid]), 5 mM of EDTA (ethylenediaminetetraacetic acid) and 1mM of DTR (dithiotheitol). The pH of the buffer containing the ctenidia was adjusted to 7.5 with 1 M TEA (triethylamine). Then, the sample was homogenized using a Virtis cyclone I.Q2 (Virtis Company, Gardiner, NY) at 14000 rpm until a one liquid phase was obtained. To maintain the protein in ferrous state (Fe^{II}), the sample was bubbled for 15 minutes with CO. After this, the sample was centrifuged for one hour at 19000 rpm in a Beckman model J2-HS centrifuge with a JA-20 rotor (Beckman Coulter Inc, Fullerton, CA). The supernatant was collected and the pellet was discarded. The supernatant was filtrated by vacuum through 1.6 μm filter papers (Whatman Inc, Florham Park, NJ). The filtered solution was stored at $-50\text{ }^{\circ}\text{C}$.

5.2.1.2 Size exclusion chromatography

Size exclusion chromatography allows separating Hemoglobin I from Hemoglobin II and III. This technique uses the difference in size and shape of biomolecules to separate them and establish the order in which they elute from the chromatographic column [151]. The first to elute is a mixture of Hemoglobin II and III which have a similar size. Followed, hemoglobin I elutes together with cysteine, another protein present in the sample isolated from the clam. An AKCA fast protein liquid chromatographer (FPLC) (Amersham Biosciences Corp, Piscataway, NJ) was used with a column of 5×90 cm containing Superdex200 resin (Amersham Biosciences Corp, Piscataway, NJ). The column was equilibrated with 300 ml of sodium dihydrogen phosphate (NaH_2PO_4) and EDTA buffer adjusted to pH 7.5. For each run, a sample of 5 ml of the mixture of proteins was introduced using a syringe in the column followed with 300 ml of NaH_2PO_4 /EDTA buffer adjusted to pH 7.5. The flow rate was maintained in 1.5 mL/min. Figure 7 shows a typical spectrum obtained after separation of HbI from HbII and HbIII. The eluent was collected by a FRAC950 fraction collector (Amersham Biosciences Corp, Piscataway, NJ) and re-concentrated using an Amicon ultra-filtration device (Millipore Corp., Billerica, MA).

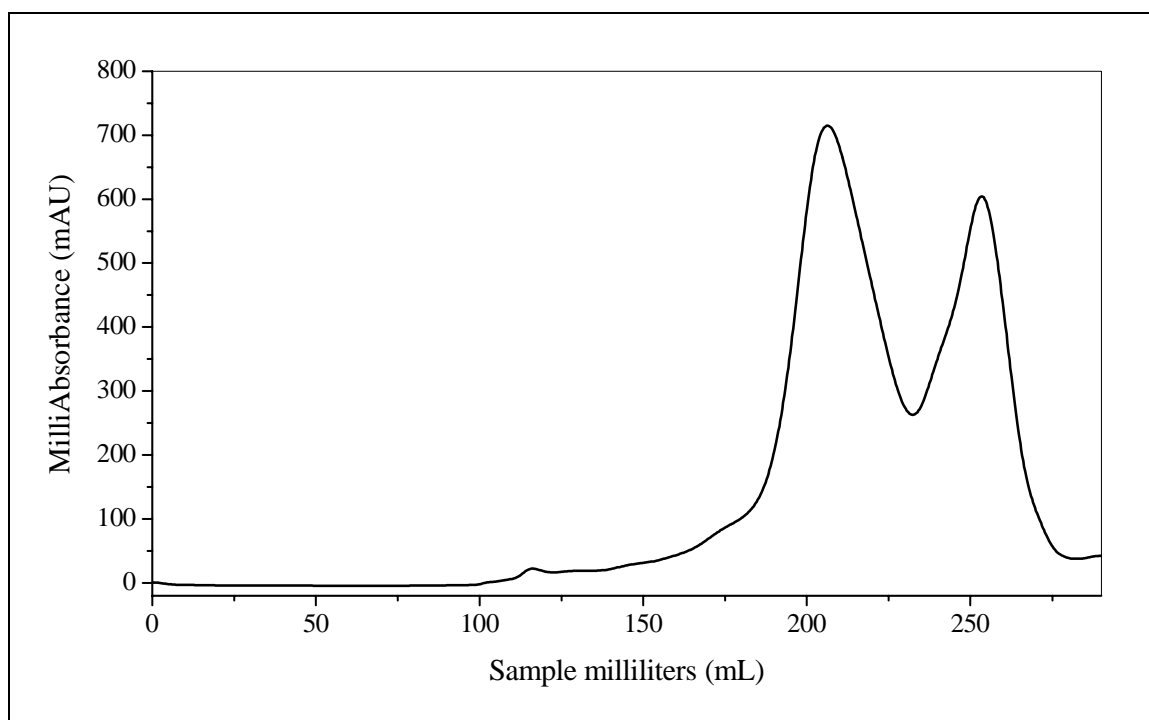


Figure 7. Typical UV-VIS spectrum obtained after size exclusion chromatography. The first peak corresponds to the mixture of HbII and HbIII proteins and the second peak corresponds to HbI and cysteine.

5.2.1.3 Ion exchange chromatography

Through ion exchange chromatography is possible to separate hemoglobin I from cysteine. An AKCA fast protein liquid chromatographer (FPLC) (Amersham Biosciences Corp, Piscataway, NJ) was used with a column of 2.5×70 cm packed with DEAE Sepharose resin (Pharmacia Biotek, Piscataway, NJ). The interactions between the protein and the resin allowed the separation. Hemoglobin I eluted first. The sample obtained from size exclusion chromatography was concentrated and the buffer was changed to 25 mM ammonium bicarbonate (NH_4HCO_3) at pH 8.3 by pressure filtration over an YM10 membrane using an Amicon ultra-filtration device (Millipore Corp., Billerica, MA). Before each run, the column was equilibrated with a NH_4HCO_3 /sodium chloride (NaCl) buffer at pH 8.3. The column was washed with this buffer until the pH of the eluting buffer was equal to 8.3. After equilibrium was reached, a sample of 10 mL was injected to the column with a syringe followed by 300 mL of 25 mM NH_4HCO_3 buffer at pH 8.3. The flow was fixed in 5 mL/min. Figure 8 shows a typical spectrum obtained after separation of HbI form cysteine. The fractions containing HbI were concentrated and changed to deionized water. The purified HbI was stored at -50°C .

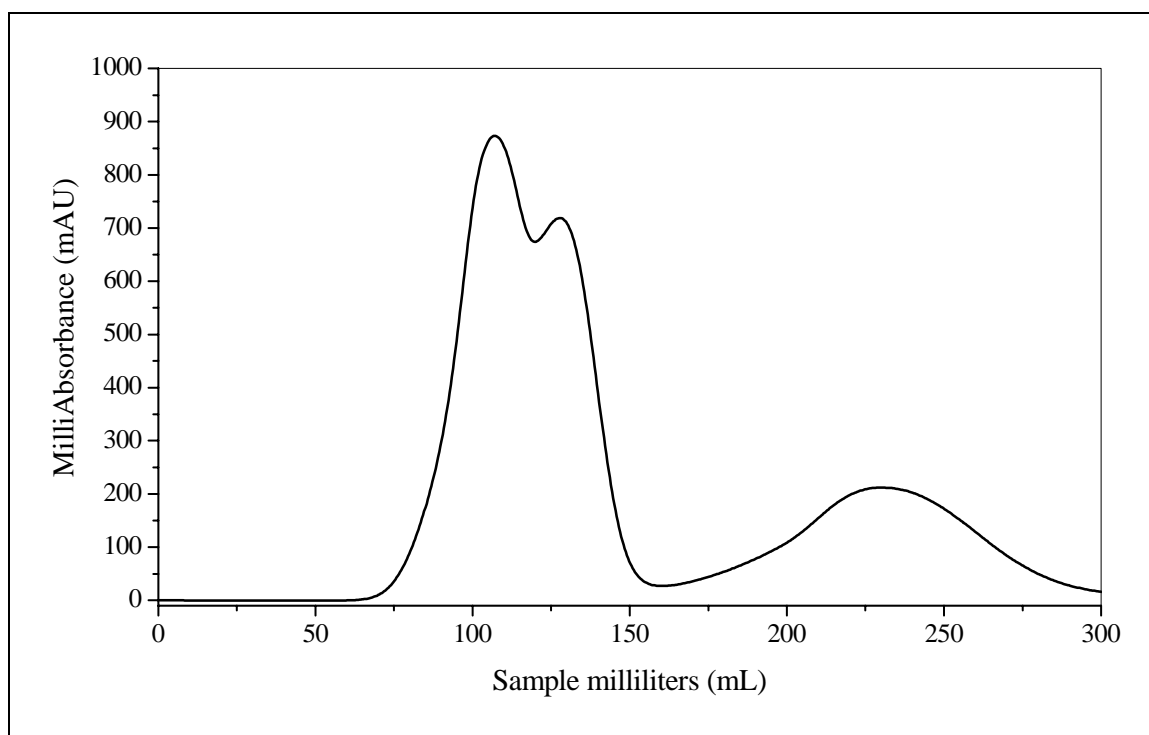


Figure 8. Typical UV-Vis spectrum obtained after ion exchange chromatography. The first two peaks corresponds to the HbI in deoxy and metaquo state and the third peak corresponds to cysteine.

5.2.2 Polymerization

The mixture of monomer, crosslinker, solvent and initiator was prepared in an amber bottle (SIGMA - Aldrich, Milwaukee, WI), placed in an inert chamber and purged for 20 minutes with nitrogen to remove the excess of oxygen that may interfere with the free radical polymerization reaction. The polymerization mixture was composed by the monomer: MAA, PEGMA (200, 400 and 1000) or DMAEM crosslinked with PEGDMA with different PEG molecular weight (200, 600 and 1000 g/mol), and the photoinitiator 1-hydroxy cyclohexyl phenyl ketone. This solution was diluted with a solution of 1:1 ethanol/deionized water. In the immobilization by entrapment method, a known concentration aliquot of the protein solution was added to the polymerization mixture.

The polymerization solution was introduced by capillarity between two pre-cleaned microscope slides (Fisher Scientific, Fair Lawn, NJ) separated by Teflon® spacers of 0.030 inches (Small Parts Inc, Miami Lakes, FL) and located under UV light for appropriate time. The intensity of the UV light fluctuated in range of 40 to 30 mW/cm². The polymer obtained was washed depending on the ionic nature of the hydrogel. For anionic polymer, the polymer was washed for two days with deionized (DI) water. After the two days, the polymer was cut in circles of 9/16 inch of diameter and washed with 0.1 M sodium phosphate buffer pH 7.00 for two more days. Finally, the polymer was washed with DI water for two more days. The buffer and the DI water were changed at least every 24 hours. For cationic hydrogels the buffer used was 0.1 M sodium phosphate buffer pH 5.8. Neutral hydrogels were only washed with deionized water. After washing, the hydrogels were cut again in circles 1 inch in diameter.

5.2.3 Hydrogel Characterization

To characterize the hydrogels, the polymer volume fraction in the swollen state ($v_{2,s}$), the number average molecular weight between crosslinks (M_C) and the correlation length (ξ) were calculated. The pathway followed to evaluate these parameters was explained in the section 2.3.1. To determine these parameters is necessary to experimentally measure the membrane volume in the relaxed state after crosslinking $V_{g,r}$, the dry membrane volume V_P and the swelled membrane volume $V_{g,s}$.

5.2.3.1 Determination of $V_{g,r}$, V_P and $V_{g,s}$

After each polymer configuration is polymerized, the membrane was cut in circles of 9/16 inches of diameter. For these experiments, the hydrogels were washed in ethanol/deionized water mixtures (EtOH/DI) to avoid swelling. PEGMA-PEGDMA hydrogels were washed in 40 %wt EtOH/DI. In the case DMAEM-PEGDMA hydrogels, 70 %wt EtOH/DI was used. Finally, for MAA-PEGDMA hydrogels 100% EtOH was employed. The cleaning media was changed twice a day for three days. After washing, the membrane volume in the relaxed state after crosslinking ($V_{g,r}$) was determined according to equation (13). To evaluate this parameter, it was necessary to measure the hydrogel weight in air after crosslinking ($W_{a,r}$) and the hydrogel weight in a non-solvent after crosslinking ($W_{n,r}$). These measurements were made using a density kit coupled to

the Voyager Balance (Ohaus Corp., Pine Brook, NJ). Heptane was used as non-solvent to avoid swelling.

Once the membrane volume in the relaxed state after crosslinking ($V_{g,r}$) was measured, the membranes were placed for two days in a desiccator containing calcium sulphate anhydrous (a desiccant agent) (Fisher Scientific, Fair Lawn, NJ) followed by one day in the vacuum oven at 35 °C and 20 mmHg (VWR International, West Chester, PA). After drying period, the membrane volume (V_p) was evaluated using equation (15). The hydrogel weight in air after drying ($W_{a,d}$) was quantified by a density kit coupled to the Voyager Balance (Ohaus Corp., Pine Brook, NJ).

The determination of the swelled membrane volume ($V_{g,s}$) required the placement of the different hydrogels in an appropriate buffer that allows the swelling. For PEGMA-PEGDMA hydrogels, sodium phosphate buffer pH 7.0 was employed. Cationic hydrogels (DMAEM-PEGDMA) and anionic hydrogels (MAA-PEGDMA) were swelled in sodium phosphate buffer pH 5.8 and pH 7.4 respectively. After the equilibrium swelling was reached, the swelled membrane volume ($V_{g,s}$) was evaluated using equation (14). The hydrogel weight in air after swelling ($W_{a,s}$), and the hydrogel weight in a non-solvent after swelling ($W_{n,s}$) were measured using once more the density kit of the Voyager Balance (Ohaus Corp., Pine Brook, NJ). Heptane was used as non-solvent.

5.2.4 Determination of Partition Coefficient

A concentrated solution of the protein (HbI or Mb) dissolved in deionized water was prepared. The concentration of this solution was estimated measuring the ultraviolet (UV) absorbance at the characteristic peak in the Soret band that these proteins exhibit. According to the Beer Lambert law the concentration can be estimated by:

$$A = \epsilon bC \quad (35)$$

where A is the absorbance, ϵ is the molar absorptivity or extinction coefficient ($\text{mM}^{-1}\text{cm}^{-1}$), C is the molar concentration (moles/L) and b is the path length (cm). The extinction coefficient for myoglobin from horse at 408 nm is $188 \text{ mM}^{-1}\text{cm}^{-1}$, and for hemoglobin from *Lucina pectinata* at 407 nm is $178 \text{ mM}^{-1}\text{cm}^{-1}$. The spectrophotometer used was a microplate PowerwaveX-I (Bio-Tek Instruments Inc, Winooski, VT). The path length for the microplates (Corning Inc., Acton, MA) used was 0.5834 cm

The volume of the membrane to be used was measured before placing it in the protein solution using a density kit which was coupled to the analytical balance (Voyager Balance Ohaus Corp., Pine Brook, NJ). A previously swelled polymer membrane was placed into a 120 ml amber bottle (Fisher Scientific, Fair Lawn NJ) containing 10 ml of the protein solution and kept it approximately at $5 \text{ }^{\circ}\text{C}$. After the equilibrium was achieved, the concentration and the volume of the remaining solution were measured. The concentration of the remaining solution was assayed in triplicate. The partition coefficient was calculated from the equation (34). The membranes were dried in a desiccator containing anhydrous calcium sulphate (a desiccant agent) (Fisher Scientific,

Fair Lawn, NJ). Membranes were placed for one day in the vacuum oven at 35 °C and 20 mmHg (VWR International, West Chester, PA) to prepare them for release studies.

5.2.5 Release Studies

A dried hydrogel with incorporated protein was placed in a bottle containing 10 ml of buffer solution. The buffer solution was continually agitated and maintained at 30°C. The buffer was changed periodically and replaced by fresh buffer. The protein concentration in the buffer solutions was determined in triplicate from spectroscopic measures at characteristic wavelengths. The test lasted until no more protein was released from the hydrogel. For the protein incorporated in MAA-PEGDMA hydrogels the buffer used was 0.1 M sodium phosphate at pH 7.00 and 5.8. Using the sorption data obtained from release experiments it was possible to estimate the diffusion coefficients. Applying the general expression of the Stefan approximation (equation 26), the predominant transport mechanism was established. The determination of the transport mechanism was performed with a confidence interval of 95%.

5.2.6 Activity Studies

The protein capacity to perform reactions with its ligand was evaluated through activity tests. These experiments were executed immediately after protein was incorporated inside hydrogels. Also, the protein activity was analyzed after release experiments to determine if the amount of protein remaining inside the hydrogel was still

biologically active and was not affected during drying and release processes. The changes in heme proteins spectroscopic properties were used to confirm the occurrence of the reactions.

The activity tests of hydrogels containing myoglobin consisted in changing its oxidation state and evaluating its capacity to bind carbon monoxide (CO). The polymer network containing ferric myoglobin was placed in a quartz cap screw cell (Starna Cells Inc., Atascadero CA), and a UV-Vis spectrum was taken. Then, a buffer solution with a small amount of sodium dithionite was added with a syringe through the septum cell. Sodium dithionite is known for its capacity to reduce heme proteins from metaquo state (Fe^{III}) to deoxy state (Fe^{II}). Spectra of the hydrogel in contact with sodium dithionite were collected over time to confirm the reduction of the protein to ferrous state. Afterward, the buffer solution was taken out from the cell with a syringe. Small quantities of CO were injected into the cell. UV-Vis spectra of the hydrogel after the addition of CO were taken in the course of time to verify the binding between myoglobin and CO.

For the case of hydrogels containing HbI from *Lucina pectinata*, a spectrum of the polymer containing HbI was taken. Then, the hydrogel was placed in a solution of hydrogen sulfide. UV-Vis spectra were taken to observe the occurrence of the binding between HbI and H_2S .

Chapter Six

Results and Discussion

6.1 Hydrogel Structural Parameters

To understand the effects and restrictions that hydrogel structure imposed over the polymer behavior during protein loading, it was necessary to characterize the structure of the networks employed. To characterize the structure of hydrogels three important parameters were evaluated, the polymer volume fraction in the swollen state ($v_{2,s}$), the number average molecular weight between crosslinks (\overline{M}_c), and the correlation length (ξ). These parameters were determined for the various hydrogel morphologies using the equilibrium swelling theory described in section 2.4.1. In this way, it was possible to establish which of the polymer configurations provided the largest space for diffusion taking in to consideration the hydrodynamic radius of the studied protein.

For the determination of the polymer volume fraction in the swollen state ($v_{2,s}$), it was necessary to experimentally measure the volume of the dry polymer (V_p), the

volume of the hydrogel after crosslinking but before swelling ($V_{g,r}$) and, the volume of the hydrogel after equilibrium swelling ($V_{g,s}$). These measurements were performed following the experimental procedure presented in section 5.2.3. As defined in equation (12), the reciprocal of polymer volume fraction of the hydrogel in swollen state ($v_{2,s}$) is the volumetric swelling ratio (Q). The results obtained for the polymer volume fraction in the swollen state ($v_{2,s}$) and the volumetric swelling ratio (Q) are presented in Appendix 1 and Appendix 2.

From the parameters mentioned above, the degree of crosslinking of the network was estimated through the determination of the molecular weight between two adjacent crosslinks. Peppas and Merrill model was employed to calculate (\overline{M}_c) [78]. Finally, the correlation length was estimated according to equation (22). The different parameters necessary to perform all the calculation are presented in Appendix 3 and Appendix 4. Figures 9 and 10 illustrate the values of the molecular weight between crosslinks and correlation length, respectively.

From Figure 9, it can be observed that the molecular weight between two adjacent crosslinkers is higher in MAA-PEGDMA hydrogels followed by DMAEM-PEGDMA and PEGMA-PEGDMA hydrogels, respectively. The evaluation of the networks correlation length revealed that methacrylic acid hydrogels possessed the highest correlation length (15.611-26.988nm at PBS buffer pH 7.4) when compared to polyethylene glycol (0.252-0.342nm at PBS buffer pH 7.0) and dimethylaminoethyl methacrylate (1.461-1.645nm at PBS buffer pH 5.8) hydrogels (see Figure 10). Also, in

MAA-PEGDMA hydrogels, the correlation length had an inverse relationship with the crosslinker length: the larger crosslinker length the smaller the correlation length.

The calculation of the correlation length is based on the determination of the molecular weight between two adjacent crosslinkers (M_c). This parameter was evaluated using the swelling theory. The results obtained for MAA based hydrogels showed that the molecular weight between crosslinks increased when the crosslinker lengths decreased. Anionic hydrogels with shorter crosslinker lengths enclosed a higher amount of monomer units between two adjacent crosslinkers. Therefore, the higher molecular weight between crosslinks produced an increment in the mesh size. The increase in the crosslinker length was not able to counterbalance this effect. In addition, the reduction in the mesh size at larger crosslinker lengths may be related to the formation of loops and heterogeneous regions in the network.

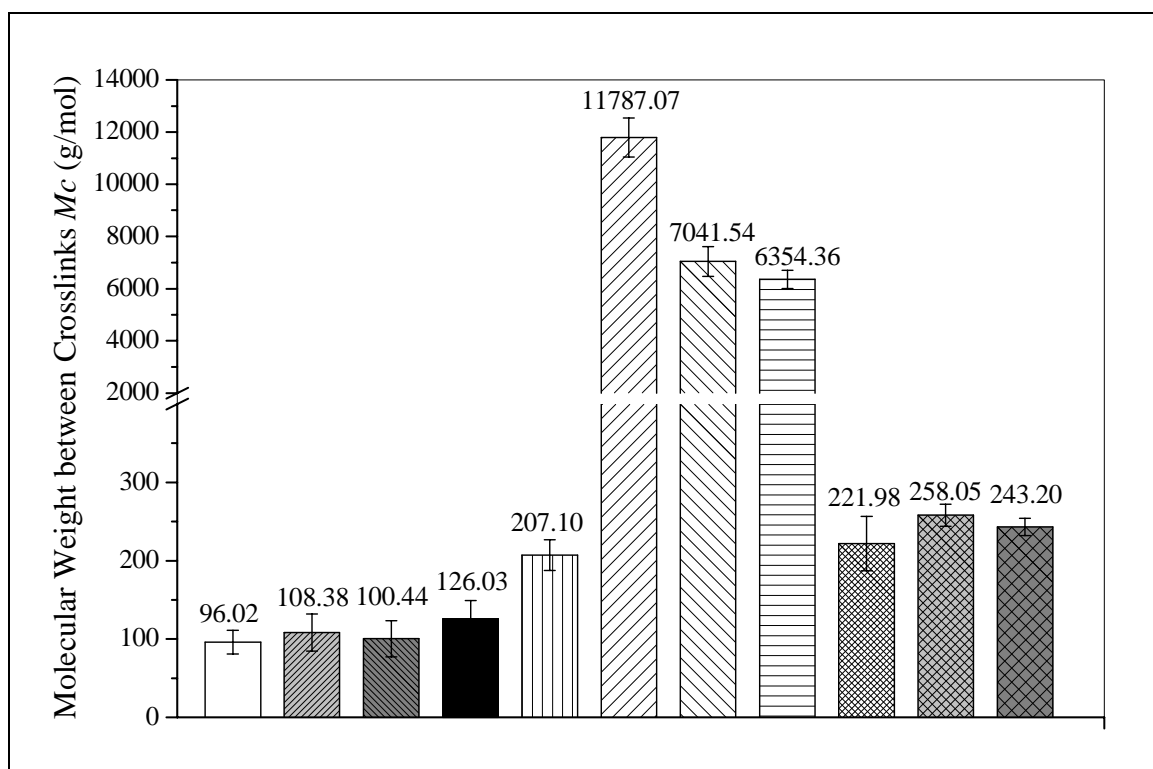


Figure 9. Molecular weight between two adjacent crosslinks for various hydrogel compositions; \square PEGMA200-PEGDMA600 (n=7), ▨ PEGMA200-PEGDMA1000 (n=9), ▩ PEGMA400-PEGDMA600 (n=8), \blacksquare PEGMA400-PEGDMA1000 (n=8), ▧ PEGMA1000-PEGDMA1000 (n=9), ▨ MAA-PEGDMA200 (n=7), ▩ MAA-PEGDMA600 (n=6), ▧ MAA-PEGDMA1000 (n=7), ▨ DMAEM-PEGDMA200 (n=7), ▩ DMAEM-PEGDMA600 (n=6), ▨ DMAEM-PEGDMA1000 (n=6). Each bar represents an average \pm one standard deviation.

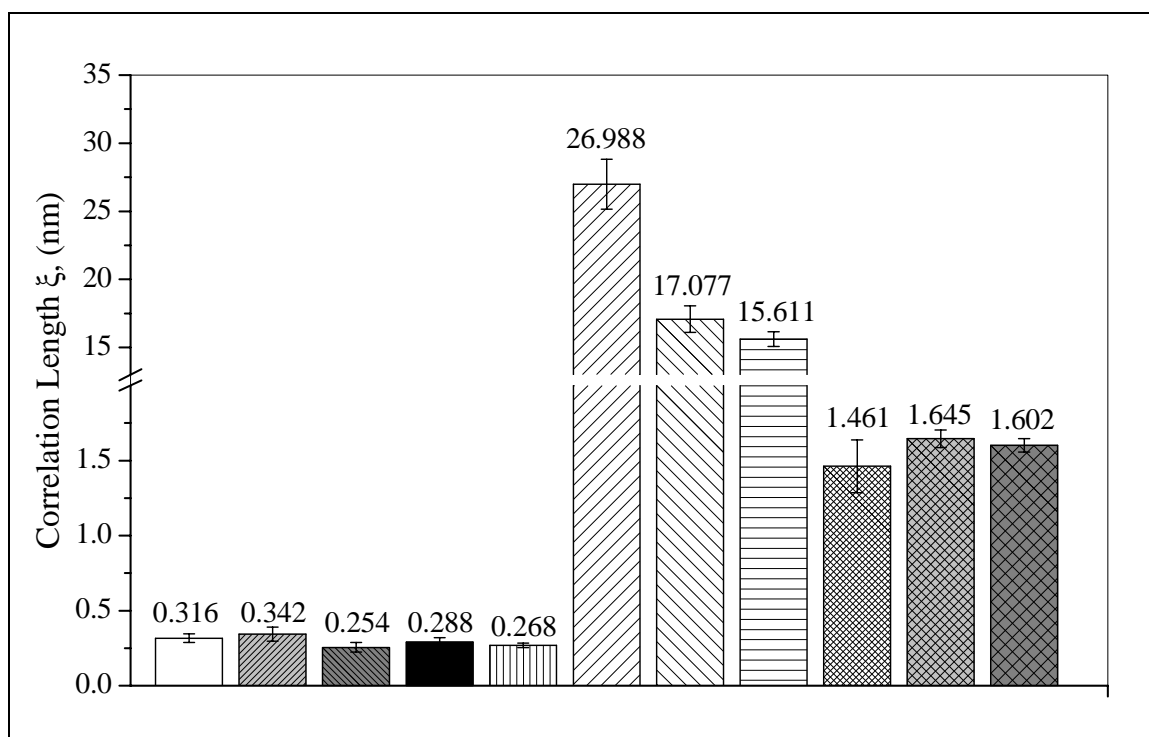


Figure 10. Correlation length (nm) for various hydrogels morphologies; \square PEGMA200-PEGDMA600 (n=7), \square PEGMA200-PEGDMA1000 (n=9), \blacksquare PEGMA400-PEGDMA600 (n=8), \blacksquare PEGMA400-PEGDMA1000 (n=8), \square PEGMA1000-PEGDMA1000 (n=9), \square MAA-PEGDMA200 (n=7), \square MAA-PEGDMA600 (n=6), \square MAA-PEGDMA1000 (n=7), \square DMAEM-PEGDMA200 (n=7), \square DMAEM-PEGDMA600 (n=6), \square DMAEM-PEGDMA1000 (n=6). Each bar represents an average \pm one standard deviation.

6.2 Myoglobin Immobilization through Adsorption

The first method investigated for the immobilization of the hemeproteins was adsorption. This method was employed because is believed to exert a minor effect over the protein functionality when compared with the others existent methods for protein immobilization. The immobilization by adsorption was achieved by placing previously swollen hydrogel disks in a solution of myoglobin from squeletal muscle. After 24 hours of contact between the hydrogels and protein solution, equilibrium was achieved. UV-Vis spectra were collected from the membranes to confirm the presence of the protein. Also, it was possible the determination of the parameter known as partition coefficient to quantify the amount of incorporated protein, as described in section 5.2.4. A spectrophotometry technique was employed to verify the presence of protein inside the networks and to measure the protein concentration in solution. Hemeproteins are characterized by specific absorbance band in their spectrum. Also, the values of the molar extinction coefficient are reported in the literature, which allows the determination of protein concentration in solution.

Figure 11 illustrates the dramatic change experimented in a MAA-PEGDMA200 hydrogel after being in contact with a 0.481mM horse myoglobin solution. The same behavior was observed in MAA based hydrogels with crosslinker length of 600 and 1000. The intense red color of the polymer indicated that a great amount of protein was incorporated inside the hydrogel.



Figure 11. MAA-PEGDMA200 hydrogel after being in contact with a horse myoglobin solution 0.481 mM. Incorporation was performed in deionized water at $T = 4.0^{\circ}\text{C}$.

The UV-Vis spectra of the MAA-PEGDMA hydrogels are displayed in Figure 12. The characteristic Soret band of horse myoglobin appears at 408 nm (see Table 5). This peak can be used to confirm the presence of myoglobin inside the polymer. A comparison between network spectra before and after being in contact with a protein solution showed the appearance of a very broad peak in the range of 300-450 nm. Since this signal is saturated, it is not possible to determine the exact point where this peak is located. However, since MAA-PEGDMA hydrogels without horse myoglobin did not show any peaks in this region of the spectra, the existence of this peak after protein incorporation can be explained as a consequence of the presence of horse myoglobin inside the polymer network.

The myoglobin solution used during incorporation experiments was prepared in deionized water rather than buffer. Experiments performed with myoglobin dissolved in buffer pH 7.0 did not allowed the incorporation of substantial protein amounts inside the polymer due to precipitation. Besides, anionic hydrogels, after 24 hours in contact with myoglobin dissolved in buffer, presented some fissures and rapidly broke during the drying process.

The values of the partition coefficient for MAA-PEGDMA hydrogels are shown in Figure 13. The partition coefficient was higher at smaller crosslinker lengths. The observed result was consistent with the observed values for the correlation length in Figure 9. According to this figure, the space between macromolecular chains was larger at smaller crosslinker length. MAA-PEGDMA200 hydrogels provided more space to accommodate solute molecules when compared to hydrogels formulated with crosslinker

lengths of 600 and 1000. This explains the observed increment in the partition coefficient as an inverse function of the crosslinker length.

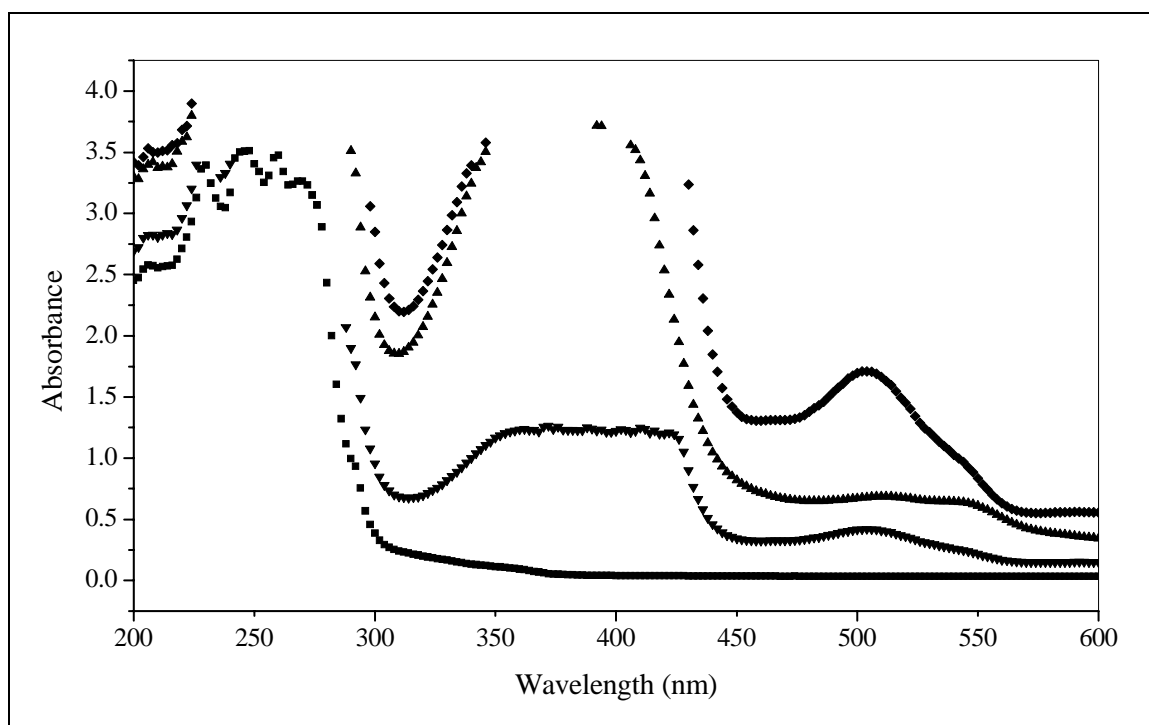


Figure 12. UV-Vis spectra of MAA-PEGDMA hydrogels before and after myoglobin incorporation through adsorption. ■ MAA-PEGDMA without protein, ▲ MAA-PEGDMA200, ▼ MAA-PEGDMA600, and ◆ MAA-PEGDMA1000 after protein incorporation.

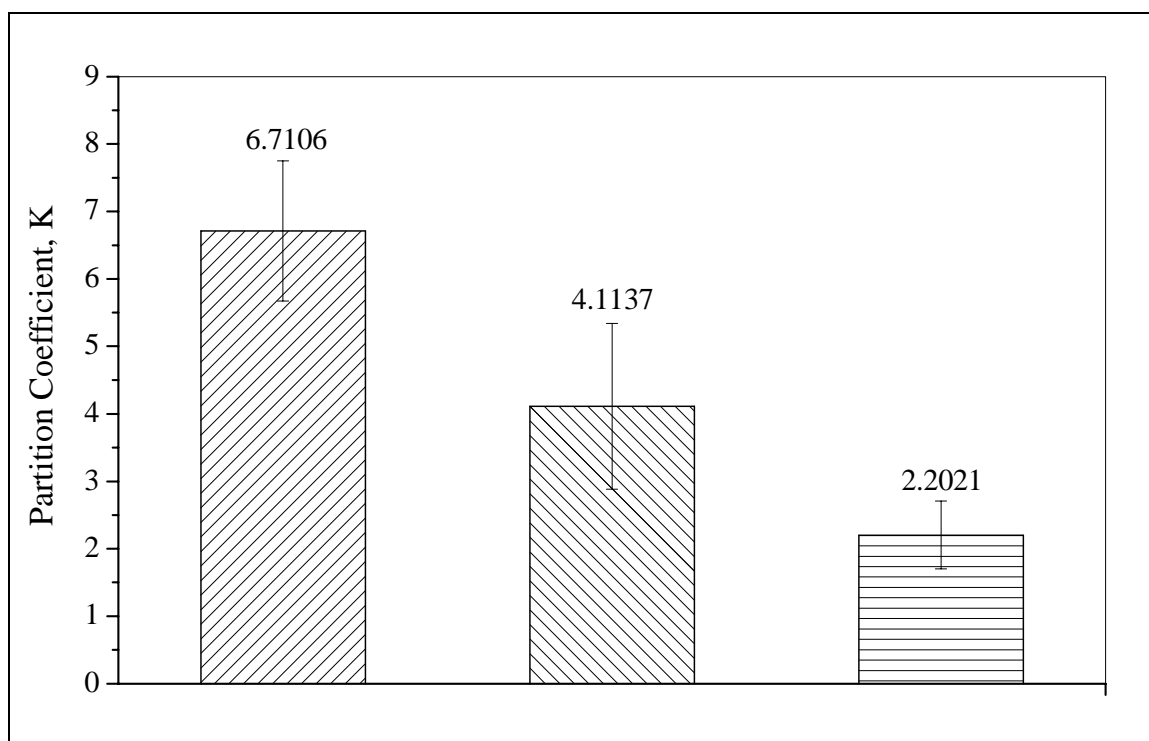


Figure 13. Partition coefficient for MAA-PEGDMA hydrogels for various crosslinker lengths; ▨ MAA-PEGDMA200 (n=6), ▩ MAA-PEGDMA600 (n=6), ▤ MAA-PEGDMA1000 (n=6). Myoglobin dissolved in water, 0.481 mM at $T = 4.0^{\circ}\text{C}$. Each bar represents an average \pm one standard deviation.

For DMAEM-PEGDMA hydrogels the UV-Vis spectra are presented in Figure 14. After being placed in contact with a horse myoglobin solution a defined peak with a maximum at 409 nm could be observed indicating the incorporation of the protein inside the hydrogel. The intensity of the peak increased for those cationic hydrogels with larger crosslinker length.

The results of the partition coefficients for DMAEM-PEGDMA hydrogels are displayed in Figure 15. The partition coefficient for DMAEM-PEGDMA hydrogels diminishes when the crosslinker length increases. This behavior was also observed in MAA-PEGDMA hydrogels. The results obtained for the correlation length of cationic hydrogels were statistically equal for the various morphologies.

The incorporation of horse myoglobin by adsorption inside neutral hydrogels was not possible to achieve. The characteristic peak for myoglobin in UV-Vis spectra after placing the hydrogels in contact with the protein solution was not observed indicating that the protein was not incorporated. Figure 16 illustrates the UV-Vis spectrum for PEGMA200-PEGDMA600 hydrogel before and after being placed in contact with a horse myoglobin solution. The behavior of the others neutral morphologies employed was equivalent. In addition, the initial concentration of the protein solution did not show any change after the partition experiment. Hence, the partition coefficient could not be calculated since this measure is based on the difference in concentration of protein solution before and after the hydrogel is placed in solution.

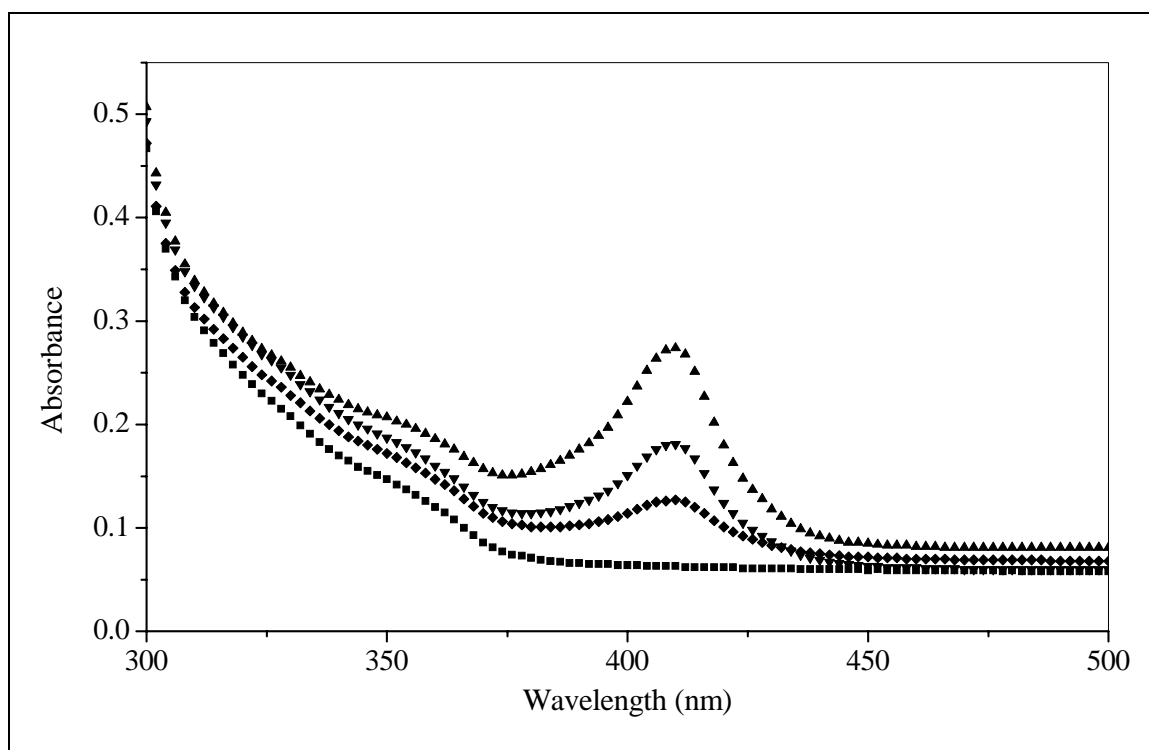


Figure 14. UV-Vis spectra of DMAEM-PEGDMA hydrogels before and after myoglobin incorporation through adsorption, ■ DMAEM-PEGDMA before protein contact, ▲ DMAEM-PEGDMA200, ▼ DMAEM-PEGDMA600, and ◆ DMAEM-PEGDMA1000 after protein contact.

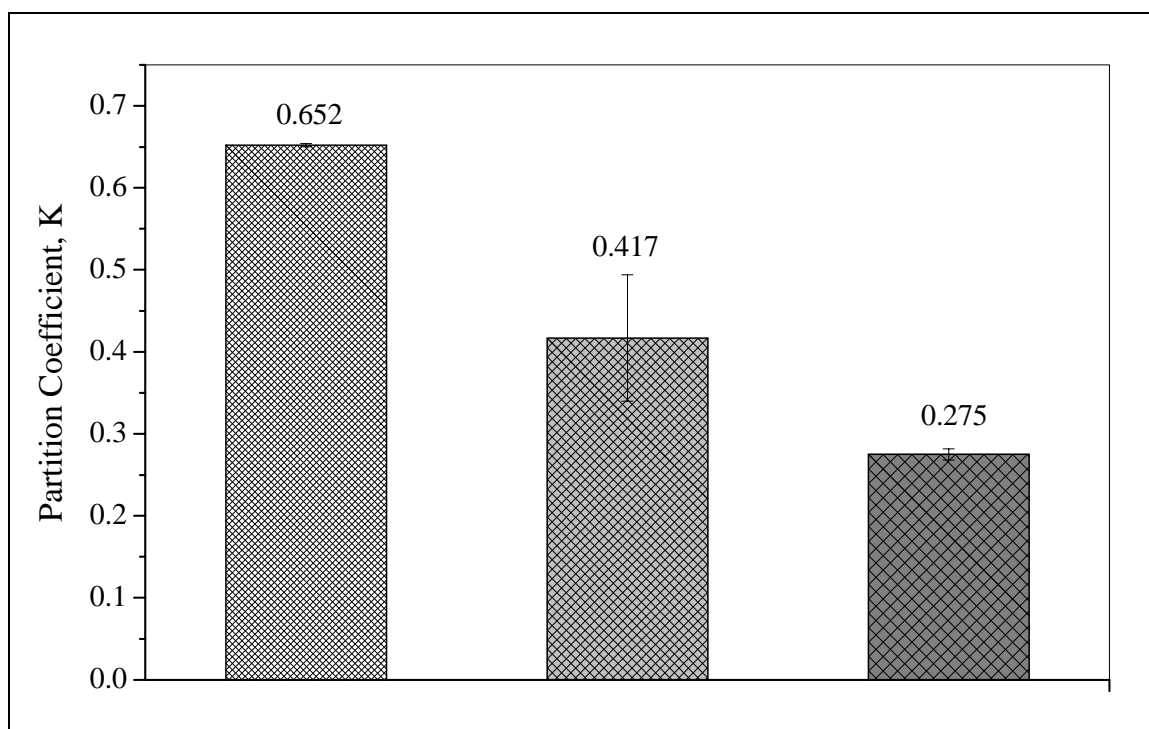


Figure 15. Partition coefficient for DMAEM-PEGDMA hydrogels for various crosslinker lengths, \square DMAEM-PEGDMA200 $n=3$, \blacksquare DMAEM-PEGDMA600 $n=3$, \blacklozenge DMAEM-PEGDMA1000 $n=3$. Myoglobin dissolved in water, 0.257 mM at $T = 4.0^{\circ}\text{C}$. Each bar represents an average \pm one standard deviation.

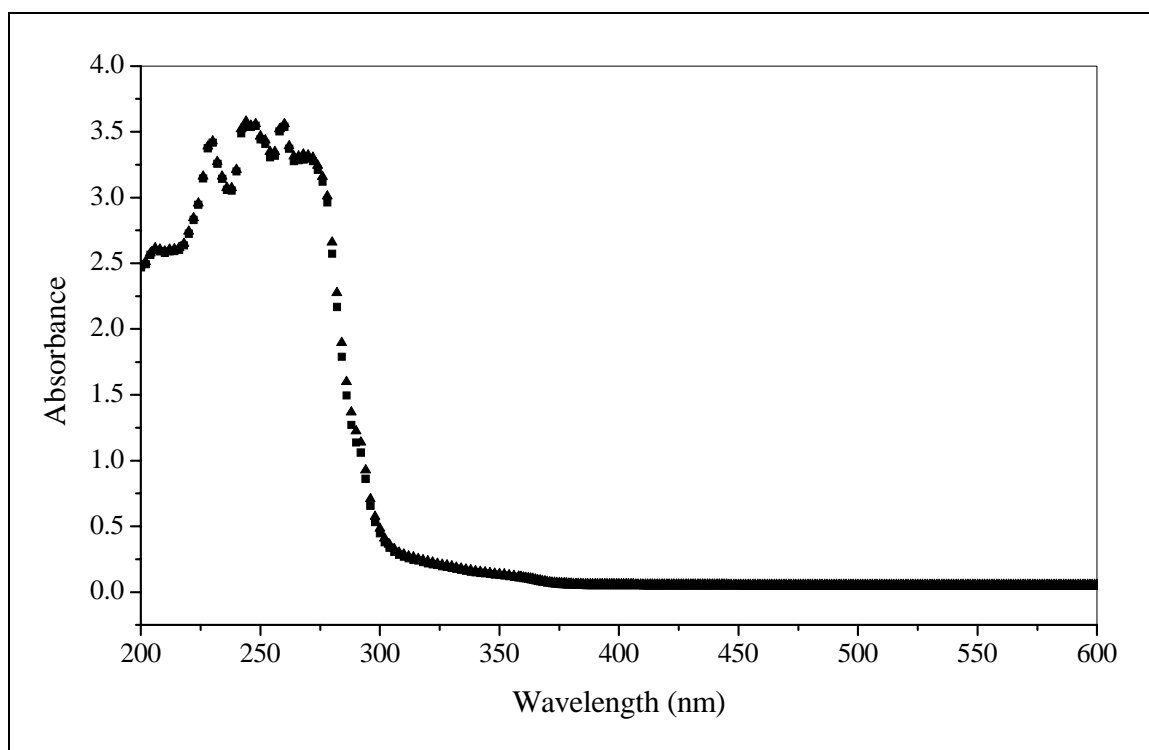


Figure 16. UV-Vis spectra of PEGMA200-PEGDMA600 hydrogels before and after myoglobin incorporation through adsorption, ■ PEGMA200-PEGDMA600 before myoglobin incorporation, ▲ PEGMA200-PEGDMA600 after myoglobin incorporation.

The difficulty in incorporating myoglobin inside PEGMA based hydrogel could be caused by the small correlation length displayed for these polymers as illustrated in Figure 9. The mesh sizes for the neutral hydrogels were not larger than 0.342 nm. The hydrodynamic radius for denaturated horse myoglobin has been reported as 2.04 nm [131]. The smaller correlation length of neutral hydrogels when compared with the protein size could have provoked a size exclusion effect that hindered the incorporation of myoglobin inside PEGMA based hydrogels.

MAA-PEGDMA hydrogels showed the highest capacity to incorporate horse myoglobin through adsorption when compared to cationic and neutral polymers. Interestingly, anionic hydrogels possessed a considerably higher correlation length (15.611-26.988 nm) when compared to the neutral and cationic morphologies. Therefore, MAA based hydrogels had a higher available space for diffusion of myoglobin. In addition, the myoglobin incorporation inside MAA based hydrogels was higher at smaller crosslinker length. Longer crosslinker lengths could create further entanglements than shorter ones. A major quantity of entanglements could produce a decrease in mesh size.

The higher myoglobin incorporation reached in anionic hydrogels could be caused not only by the larger correlation length but also by the interactions between the protein and the moieties of the MAA carrier. Myoglobin is a member of the globular protein family. Globular proteins are characterized by arranging their hydrophobic groups inside the molecule and their hydrophilic groups outside the molecule. One of the hydrophilic groups present in horse myoglobin is histidine. Horse myoglobin has eleven residues of histidine in its bone chain. The pKa of histidine residues is 6.00; over this value it renders protonate [38]. The pKa of MAA is 4.88; over this value it is negatively charged

[27]. In consequence, it is possible that at pH higher than 6.00, ionic interactions between methacrylic acid and histidine residues took place increasing the affinity of myoglobin toward this specific network.

Neutral hydrogels (PEGMA-PEGDMA) did not allow the incorporation of measurable amounts of myoglobin. These types of hydrogels possessed the smallest correlation length when compared to the other morphologies (0.254-0.342 nm). The small existent space between two macromolecular chains did not probably allow the adsorption of myoglobin inside the hydrogels, considering that horse myoglobin radius has been reported as 2.04 nm [131]. The incorporation of horse myoglobin was achieved in cationic hydrogels (DMAEM-PEGDMA). However, a comparison between the partition coefficients of anionic and cationic hydrogels revealed that protein affinity toward cationic hydrogels is approximately 10% of the affinity showed in anionic hydrogels.

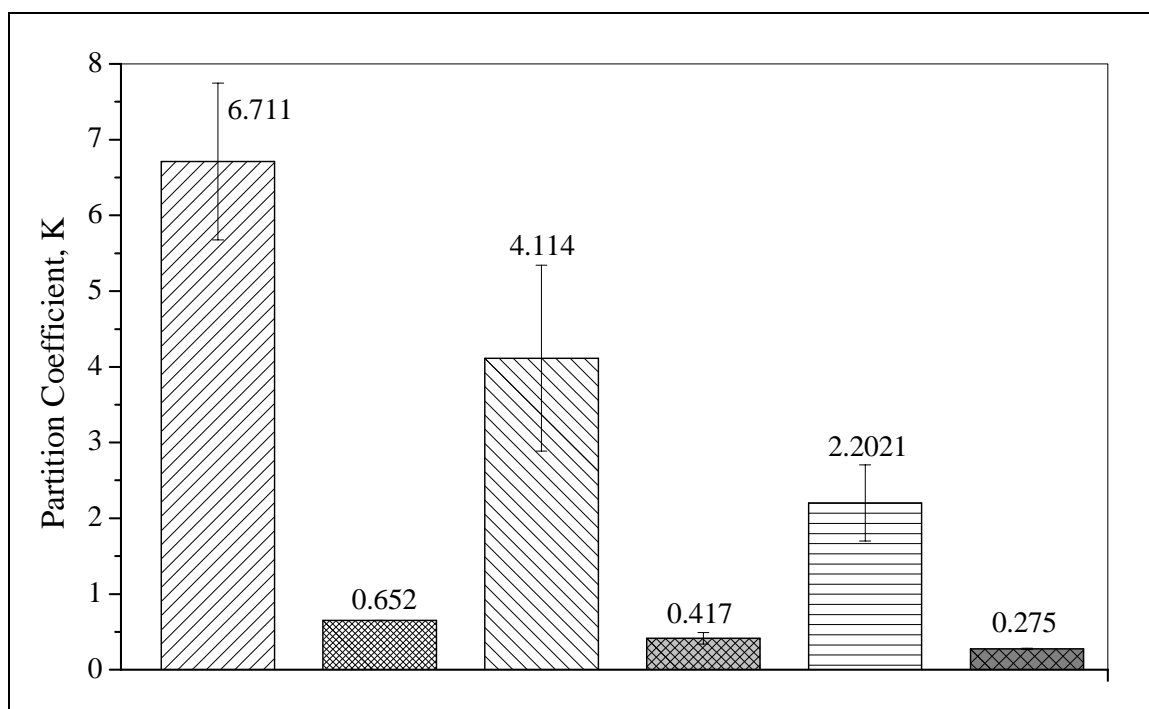


Figure 17. Summary of the partition coefficients for anionic and cationic hydrogels. ▨ MAA-PEGDMA200 (n=6), ▩ DMAEM-PEGDMA200 (n=3), ▧ MAA-PEGDMA600 (n=6), ▦ DMAEM-PEGDMA600 (n=3), ▤ MAA-PEGDMA1000 (n=6), ▣ DMAEM-PEGDMA1000 (n=3). Incorporation was performed in deionized water at $T = 4.0^{\circ}\text{C}$. Each bar represents an average \pm one standard deviation.

6.3 Myoglobin Release after Incorporation by Adsorption

Hydrogels have been extensively used as drug delivery systems since their release behavior can be adapted to specific requirements. Consequently, it was expected that some of the protein incorporated inside the hydrogel would be desorbed in the presence of a buffer solution. By means of release experiments, the amount of protein that remained inside the polymer could be determined. In addition, release experiments allowed the determination of the solute transport mechanism and the diffusion coefficients. Considering that only MAA-PEGDMA hydrogels allowed the incorporation of appreciable amounts of proteins through adsorption, release studies were only performed for anionic networks.

Since methacrylic acid MAA is an anionic polymer that is ionized at pH higher than its pKa, which is 4.88, the release behavior of MAA based hydrogels could be influenced by the pH of the buffer employed during release experiments. To evaluate the effect of pH in the rate of myoglobin release, release experiments were conducted in sodium phosphate buffer (PBS) pH 7.0 and 5.8. Figure 18 presents a plot of the myoglobin fractional release from MAA-PEGDMA hydrogels for various crosslinker lengths at pH 7.0. An increase in the rate of solute transport was observed in hydrogels with shorter crosslinker lengths. For example, it could be noticed that after 10 hours of release the fraction of released protein was inversely related to crosslinker length: 90% for MAA-PEGDMA200 hydrogels, 60% for MAA-PEGDMA600 hydrogels, and 35% for MAA-PEGDMA1000 hydrogels. At longer times, the total release fraction for MAA-

PEGDMA200 and MAA-PEGDMA600 hydrogels was approximately 90% whereas for MAA-PEGDMA1000 hydrogels was approximately 85%. This behavior was found to agree with the mesh size determination. Hydrogels formulated with the shorter crosslinker lengths possessed the higher correlation length, which meant that these networks provided a greater space for solute diffusion when compared with hydrogels having larger crosslinker lengths. Besides, as presented earlier, the myoglobin incorporation degree was superior at shorter crosslinker lengths. As a consequence, a major concentration gradient could be developed between the polymer containing the myoglobin and the buffer solution at hydrogels with shorter crosslinker lengths.

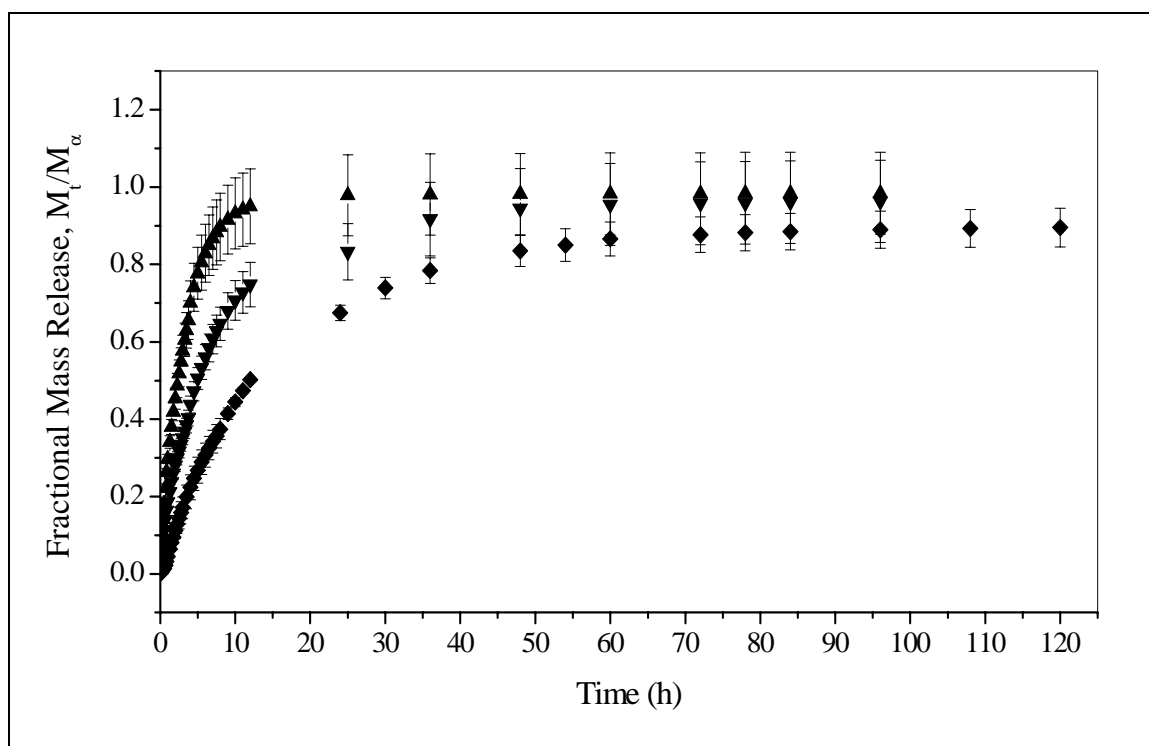


Figure 18. Fractional release of myoglobin incorporated through adsorption in MAA-PEGDMA hydrogels for various crosslinker lengths in PBS at pH = 7.0 at T = 30 °C, ▲ MAA-PEGDMA200 (n=4), ▼ MAA-PEGDMA600 (n=5) and ◆ MAA-PEGDMA1000 (n=3). Each point represents an average \pm one standard deviation.

The use of the general expression of the Stefan's approximation (equation 26) allowed the evaluation of the solute transport mechanism. The data was adjusted with a confidence interval of 95%, and the parameters k and n were calculated. Table 10 presents the results obtained for these two parameters. The values of the diffusional exponent (n) for MAA-PEGDMA hydrogels were found to be in the range of 0.5 to 1.0. According to these results, it can be concluded that anomalous transport occurred during the release of myoglobin from anionic hydrogels (refer to Table 7). Therefore, the transport mechanism is a combination of Fickian diffusion and chain relaxation process. The Fickian diffusion was promoted by the existent concentration gradient between the hydrogel that contained the protein and the buffer solution that was free of protein. The chain relaxation process was caused by the hydrogel swelling. At the beginning, the dry hydrogel was placed in the sodium phosphate buffer solution at pH 7.0. The swelling of the hydrogel produced the movement of the polymer chains which pushed away the protein from the hydrogel.

However, in the case of MAA based hydrogels crosslinked with PEGDMA200 and PEGDMA600, the value of the diffusional exponent (n) is closer to 0.5 (corresponding to Fickian diffusion) than the value obtained for hydrogels crosslinked with PEGDMA1000. Based on these results, anionic hydrogels crosslinked with PEGDMA200 and PEGDMA600 displayed a solute transport mechanism where the Fickian diffusion had a significant influence. In contrast, the value of the diffusional exponent for MAA-PEGDMA1000 hydrogels was closer to 1.0 (corresponding to relaxation controlled). This value suggested that solute transport mechanism of MAA-PEGDMA1000 hydrogels was strongly dominated by chain relaxation.

Since the myoglobin transport mechanism through MAA-PEGDMA hydrogels showed contributions from Fickian diffusion and chain relaxation processes, the dual model proposed by Berens and Hopfenbers was employed to estimate the diffusion coefficients. This model takes in to consideration the influence of these two factors over the solute transport (refers to section 2.4.2). Also, the application of this model allowed considering the contributions of Fickian diffusion and chain relaxation to the transport process. By means as, the trends observed through the evaluation of the diffusional exponent were confirmed.

Table 11 presents the results obtained with the Berens and Hopfenbers model. These results obtained for the Fickian and chain relaxation contributions indicated that the solute transport is the result of a coupling between the two contributions which confirmed the aforementioned analysis from the diffusional exponent values. According to the results, Fickian diffusion contributed in a higher proportion to the solute transport in anionic morphologies. However, the chain relaxation contribution increased in hydrogels with larger crosslinker lengths.

The values obtained for the diffusion coefficient substantiated the behavior observed for myoglobin release from anionic hydrogels. The diffusion coefficient increased for hydrogels with shorter crosslinker lengths. This result agreed with release experiments where the amount of myoglobin released was higher for MAA based hydrogels constructed with shorter crosslinker lengths.

Two reasons could explain the results obtained through the evaluation of the diffusional exponent and the application of the Berens and Hopfenbers model. The correlation length and the amount of incorporated myoglobin were higher at shorter

crosslinker lengths. A larger correlation length could provide a larger space for diffusion facilitating the myoglobin transport from the hydrogel to the buffer solution. Besides, as the amount of protein incorporated inside the polymer networks became higher the concentration gradient increased which could induce Fickian diffusion.

Table 10. Values of the parameters n and k of the Stefan's approximation for myoglobin incorporated through adsorption in MAA-PEGDMA hydrogels with various crosslinker lengths. Experiments were performed in PBS at pH = 7.0 and T = 30 °C.

	k , characteristic constant of the polymer/solute system	n , diffusional exponent.
MAA-PEGDMA200 (97:3 molar ratio, 1:1 dilution rate)	0.29402 ± 0.00191	0.61677 ± 0.00736
MAA-PEGDMA600 (97:3 molar ratio, 1:1 dilution rate)	0.18087 ± 0.00224	0.62374 ± 0.01029
MAA-PEGDMA1000 (97:3 molar ratio, 1:1 dilution rate)	0.05904 ± 0.00277	0.91782 ± 0.02788

Table 11. Diffusion coefficients for myoglobin incorporated through adsorption in MAA-PEGDMA hydrogels with various crosslinker lengths evaluated using the Berens and Hopfenbers model. Experiments were performed in PBS at pH = 7.0 and T = 30 °C.

	ϕ_F , contribution of Fickian diffusion	ϕ_R , contribution of chain relaxation	D (cm ² / s), the diffusion coefficient
MAA-PEGDMA200 (97:3 molar ratio, 1:1 dilution rate)	$0.9319 \pm 2.1963 \times 10^{-4}$	$0.0681 \pm 2.1963 \times 10^{-4}$	$7.7647 \times 10^{-9} \pm 9.3886 \times 10^{-11}$
MAA-PEGDMA600 (97:3 molar ratio, 1:1 dilution rate)	$0.9005 \pm 1.820 \times 10^{-3}$	$0.0995 \pm 1.820 \times 10^{-3}$	$3.4037 \times 10^{-9} \pm 5.4707 \times 10^{-11}$
MAA-PEGDMA1000 (97:3 molar ratio, 1:1 dilution rate)	$0.8555 \pm 4.9936 \times 10^{-3}$	$0.1444 \pm 4.9936 \times 10^{-3}$	$1.6818 \times 10^{-9} \pm 1.2439 \times 10^{-11}$

Release experiments were also conducted in sodium phosphate buffer (PBS) at pH 5.8. MAA-PEGDMA200 hydrogels did not have the adequate mechanical strength to resist the test and broke after 10 minutes of buffer contact. Even though anionic hydrogels crosslinked with PEGDMA600 and PEGDMA1000 lasted until the end of the release experiments, these membranes developed some fissures at their edges during the test.

Figure 19 presents the myoglobin fractional mass release for MAA hydrogels crosslinked with PEGDMA600 and PEGDMA1000. Compared with the release degree obtained at pH 7.0, the amount of protein released from both morphologies drastically diminished when PBS buffer pH 5.8 was used. The amount of protein released from anionic hydrogels was approximately 10% for MAA-PEGDMA200 and 1% for MAA-PEGDMA1000 polymer networks. The pKa value of methacrylic acid is 4.88. At pH 5.8 the polymer is still collapsed due to the closeness of the pH buffer to the pKa value, and did not allowed a substantial protonation of the polymer network. The collapsed polymer state could hinder the myoglobin diffusion from the anionic hydrogels. In contrast, MAA hydrogels at pH 7.0 are highly swelled. Highly swollen hydrogels allows greater solute transport due to the large amounts of unbound water [73].

A similar analysis to the one performed for release studies at pH 7.0 was completed for release studies at pH 5.8. First, applying the general expression of Stefan's approximation, the diffusional exponent (n) was evaluated. The results obtained are shown in Table 12. The value of the diffusional exponent for MAA hydrogels crosslinked with PEGDMA600 and PEGDMA1000 were in the range of 0.5 to 1.0 indicating that the transport mechanism is a combination of Fickian diffusion and chain

relaxation. Afterward, the Berens and Hopfenbers model was used to evaluate the contributions of each transport mechanisms, results are displayed in Table 13. Both morphologies were markedly influenced by chain relaxation mechanism. It could be observed that the chain relaxation contribution was increased at larger crosslinker lengths. The value of the contribution parameter was 0.89 for MAA-PEGDMA600 and 0.99 for MAA-PEGDMA1000. The aforementioned results indicated that for MAA-PEGDMA1000 hydrogels, the myoglobin transport was almost completely due to chain relaxation mechanism.

The diffusion coefficient was on the order of magnitude of 10^{-9} cm²/s for MAA-PEGDMA600 and 10^{-11} cm²/s for MAA-PEGDMA1000 hydrogels. It should be noticed that MAA hydrogels crosslinked with PEGDMA1000 only released approximately 1% of the myoglobin previously incorporated. Diffusion coefficients of myoglobin released at pH 5.8 were smaller when compared to the values obtained for myoglobin released at pH 7.0

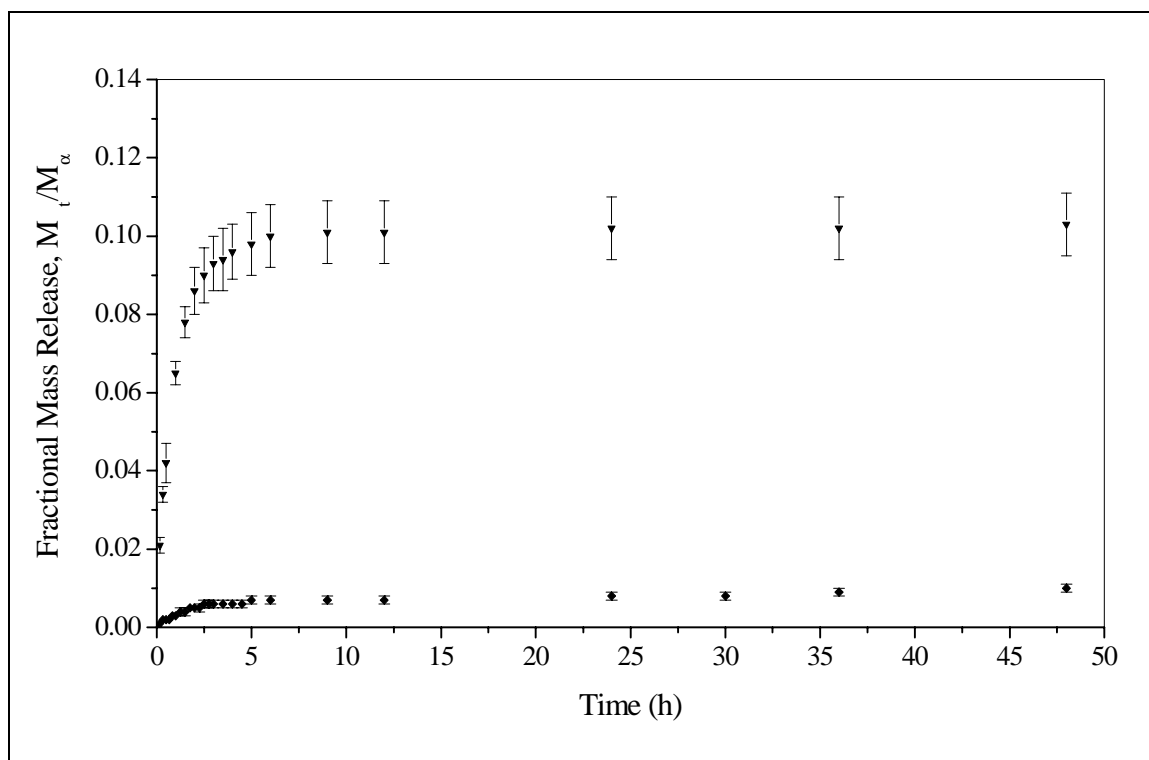


Figure 19. Fractional release of myoglobin incorporated through adsorption in MAA-PEGDMA hydrogels for various crosslinker lengths in PBS at pH = 5.8 at T = 30 °C, ▼ MAA-PEGDMA600 (n=3) and ◆ MAA-PEGDMA1000 (n=3). Each point represents an average \pm one standard deviation.

Table12. Values of the parameters n and k of the Stefan's approximation for myoglobin incorporated through adsorption in MAA-PEGDMA hydrogels with various crosslinker lengths. Experiments were performed in PBS at pH = 5.8 and T = 30 °C.

	k , characteristic constant of the polymer/solute system	n , diffusional exponent.
MAA-PEGDMA600 (97:3 molar ratio, 1:1 dilution rate)	0.06143 ± 0.00128	0.53438 ± 0.03207
MAA-PEGDMA1000 (97:3 molar ratio, 1:1 dilution rate)	0.00333 ± 0.00004	0.68215 ± 0.02134

Table 13. Diffusion coefficients for myoglobin incorporated through adsorption in MAA-PEGDMA hydrogels with various crosslinker lengths evaluated using the Berens and Hopfenbers model. Experiments were performed in PBS at pH = 5.8 and T = 30 °C.

	ϕ_F , contribution of Fickian diffusion	ϕ_R , contribution of chain relaxation	D (cm ² / s), the diffusion coefficient
MAA-PEGDMA600 (97:3 molar ratio, 1:1 dilution rate)	$0.1011 \pm 1.8937 \times 10^{-4}$	$0.8988 \pm 1.8937 \times 10^{-4}$	$1.0995 \times 10^{-9} \pm 1.1575 \times 10^{-10}$
MAA-PEGDMA1000 (97:3 molar ratio, 1:1 dilution rate)	$0.0061 \pm 2.7060 \times 10^{-4}$	$0.9939 \pm 2.7060 \times 10^{-4}$	$7.6023 \times 10^{-11} \pm 4.3082 \times 10^{-12}$

6.4 Myoglobin Immobilization through Entrapment

Encouraging results were obtained for myoglobin incorporation by the adsorption technique inside MAA-PEGDMA hydrogels. However, the higher the incorporation, the higher the release rate as approximately 90% of the incorporated protein was lost. Therefore, immobilization by entrapment was investigated. Entrapment consists in the construction of a three-dimensional network around the protein. As a consequence, this technique was expected to minimize protein release. The same polymer morphologies studied for immobilization by adsorption were considered for entrapment.

To perform the protein entrapment, the solvent fraction of the polymerization solution corresponding to deionized water was replaced by the myoglobin solution. The amount of protein incorporated by entrapment in anionic hydrogels was substantially lower than the amount incorporated by adsorption in these types of polymers. Figure 20 depicts a comparison between the amounts of myoglobin incorporated in MAA hydrogels by both methods. It could be observed that the entrapment technique only allowed the incorporation of approximately 1% of the myoglobin incorporated by adsorption. However the diameter of the disks used to incorporated myoglobin by adsorption were 7/16" larger than disks obtained after myoglobin entrapment.

In the case of MAA based hydrogels, the contact between myoglobin and the polymerization solution produced a change in the characteristic peak of myoglobin. As illustrated in Figure 21, the peak of myoglobin that appeared at 409 nm was immediately displaced to 400 nm after being in contact with the polymerization solution of MAA-

PEGDMA200. After polymerization was performed, the peak appeared at 395 nm. The same result was obtained for polymerization solutions of MAA-PEGDMA600 and MAA-PEGDMA1000. Besides, the addition of sodium dithionite to the polymerization solution containing myoglobin did not produce any change in the oxidation state of the protein. Sodium dithionite is typically used to reduce heme proteins from metaquo state (Fe^{III}) to deoxy state (Fe^{II}). The formerly mentioned result indicated that the polymerization solution had a detrimental effect on myoglobin. This effect could be caused for one of the components that constituted the polymerization solution or for the combination of the individual effects of each component. The polymerization solution was composed of methacrylic acid (MAA) as monomer, polyethylene glycol dimethacrylate (PEGMA) as crosslinker agent, and a solution of ethanol and deionized water as solvent. Proteins are very sensitive to pH changes and MAA has a very low pH. PEGMA is frequently used to precipitate proteins in separation techniques. Furthermore, non-ionic polymers such as PEGMA have shown a little tendency to denature proteins [133]. Also, proteins can be denatured in the presence of alcohols [27]. Exposure to a low pH, contact with a possible precipitating agent, and solvent could have caused myoglobin inactivation.

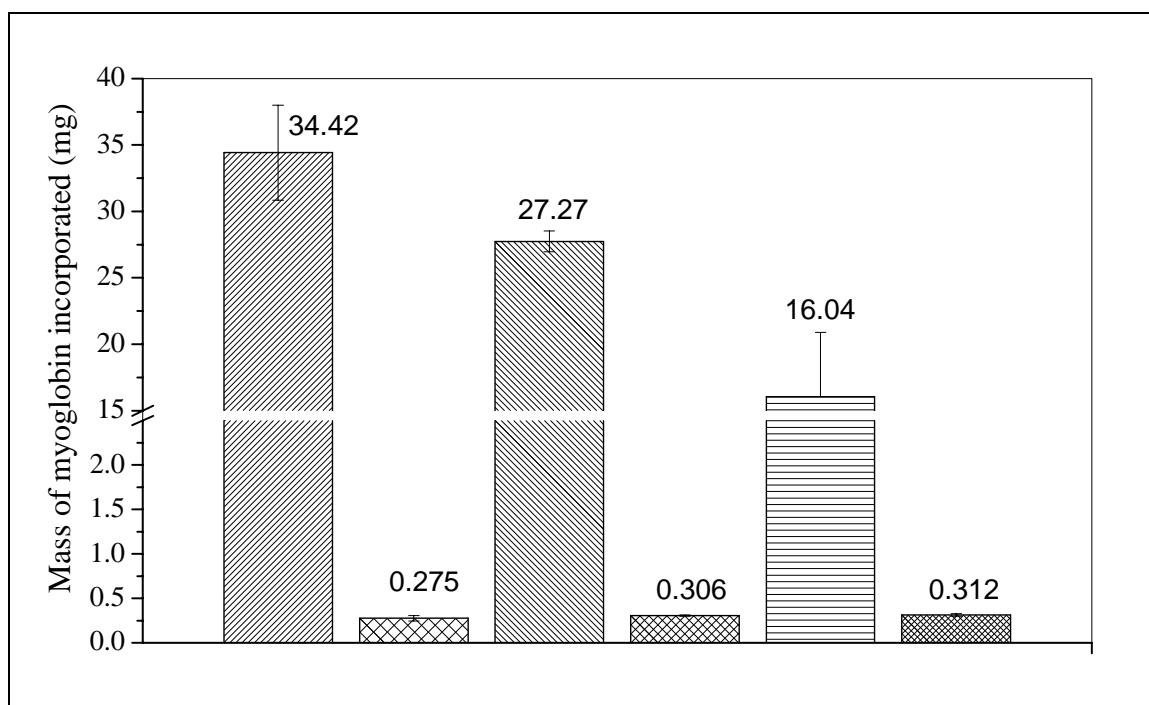


Figure 20. Comparison between the amount of myoglobin incorporated inside MAA based hydrogels with various crosslinker lengths by adsorption and entrapment. ▨ adsorbed Mb in MAA-PEGDMA200 (n=6), ▩ entrapped Mb in MAA-PEGDMA200 (n=5), ▪ adsorbed Mb in MAA-PEGDMA600 (n=6), ▫ entrapped Mb in MAA-PEGDMA600 (n=5), ▬ adsorbed Mb in MAA-PEGDMA1000 (n=6), ▭ entrapped Mb in MAA-PEGDMA1000 (n=5). Each bar represents an average \pm one standard deviation.

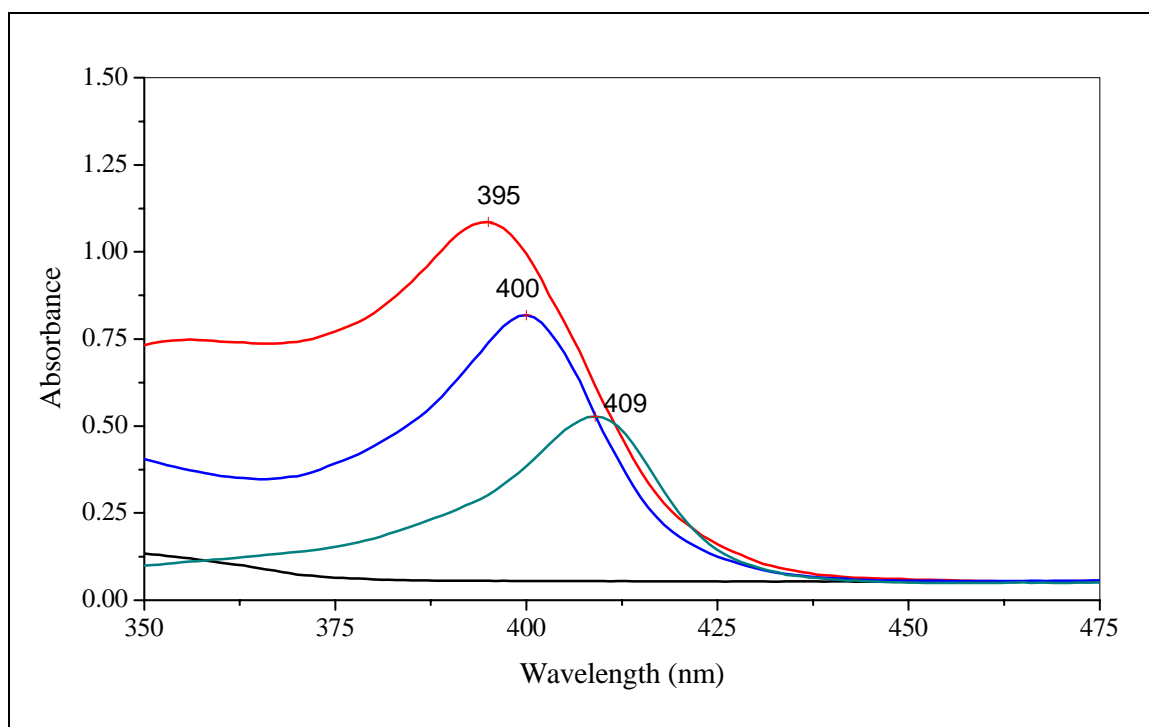


Figure 21. Effect of MAA-PEGDMA200 polymerization solution over Soret characteristic peak of horse myoglobin. — Spectrum of MAA-PEGDMA200 polymerization solution without myoglobin, — spectrum of free myoglobin in metaquo state, — spectrum of MAA-PEGDMA200 polymerization solution immediately after addition of Mb, — spectrum of MAA-PEGDMA200 containing myoglobin after polymerization.

Placing myoglobin in PEGMA-PEGDMA polymerization solutions caused rapid precipitation of the protein. Even though precipitation was perceptible to the naked eye, images taken with an inverse light microscope (Olympus, Melville NY) allowed a closer observation of myoglobin precipitation. Figure 22 shows the aggregation of horse myoglobin in the presence of PEGMA200-PEGDMA600 and PEGMA1000-PEGDMA1000 polymerization solutions. A similar phenomenon was observed for the various neutral polymerization solutions employed.

Neutral hydrogels had a 1:1 monomer-crosslinker molar ratio and 1:1 dilution rate. The effect of the polymers and the ethanol over myoglobin were examined individually. The precipitation of myoglobin in presence of ethanol occurred faster than in presence of PEGMA-PEGDMA solutions. One minute after the contact between ethanol and myoglobin, small agglomerates of protein could be observed. One minute later, the extension and the size of the aggregates significantly increased (see Figure 23). In the case of PEGMA-PEGDMA solutions, the formation of agglomerates occurred slower and in a lower proportion than with ethanol. The aggregates observed in the presence of the monomer and crosslinker solution were more difficult to visualize and had a small dimension when compare with those presented in ethanol (see Figure 24).

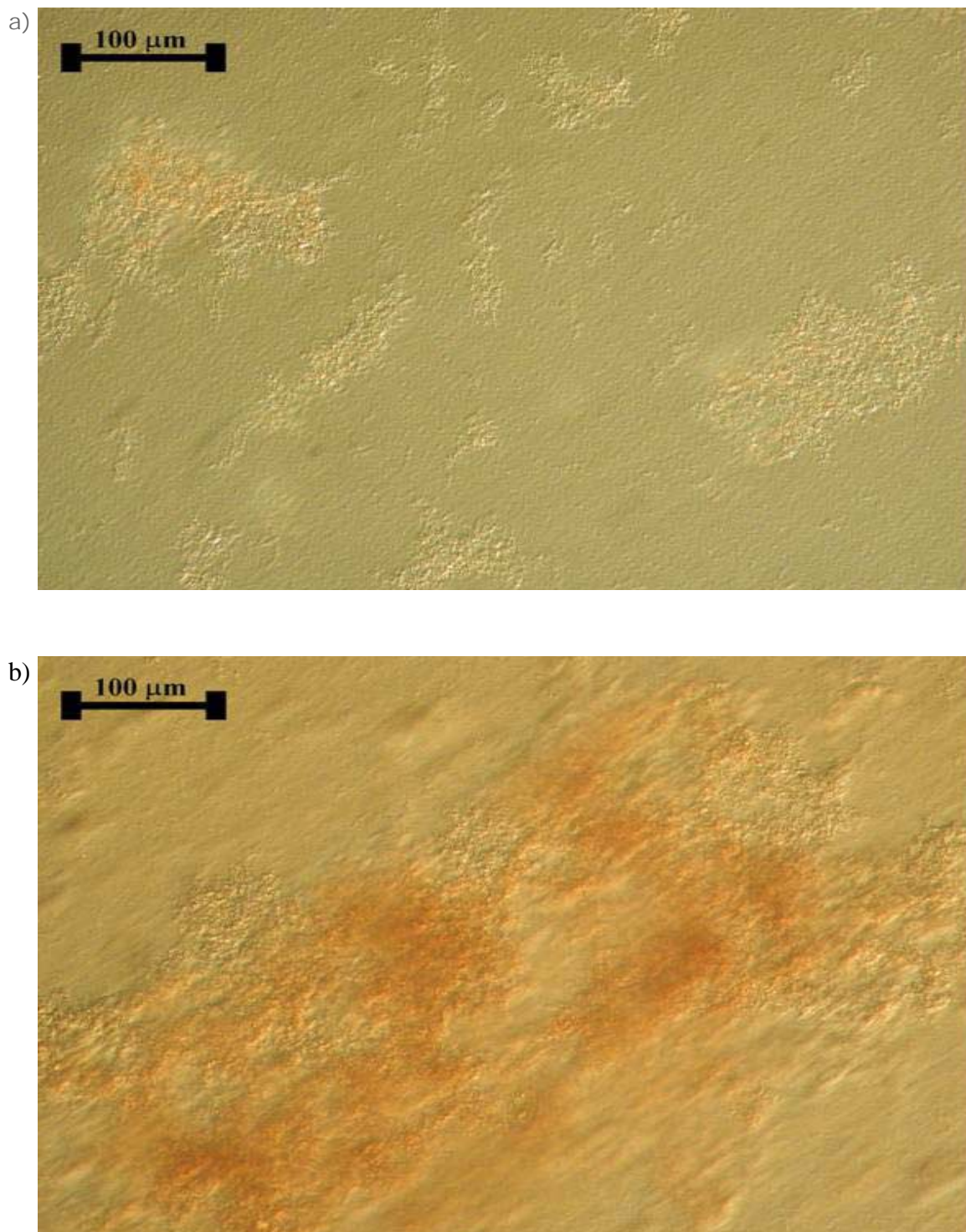


Figure 22. Precipitating effect of PEGMA-PEGDMA polymerization solutions over myoglobin after 10 minutes of contact, a) PEGMA200-PEGDMA600, b) PEGMA1000-PEGDMA1000, 1:1 monomer crossliker molar ratio and 1:1 dilution rate.

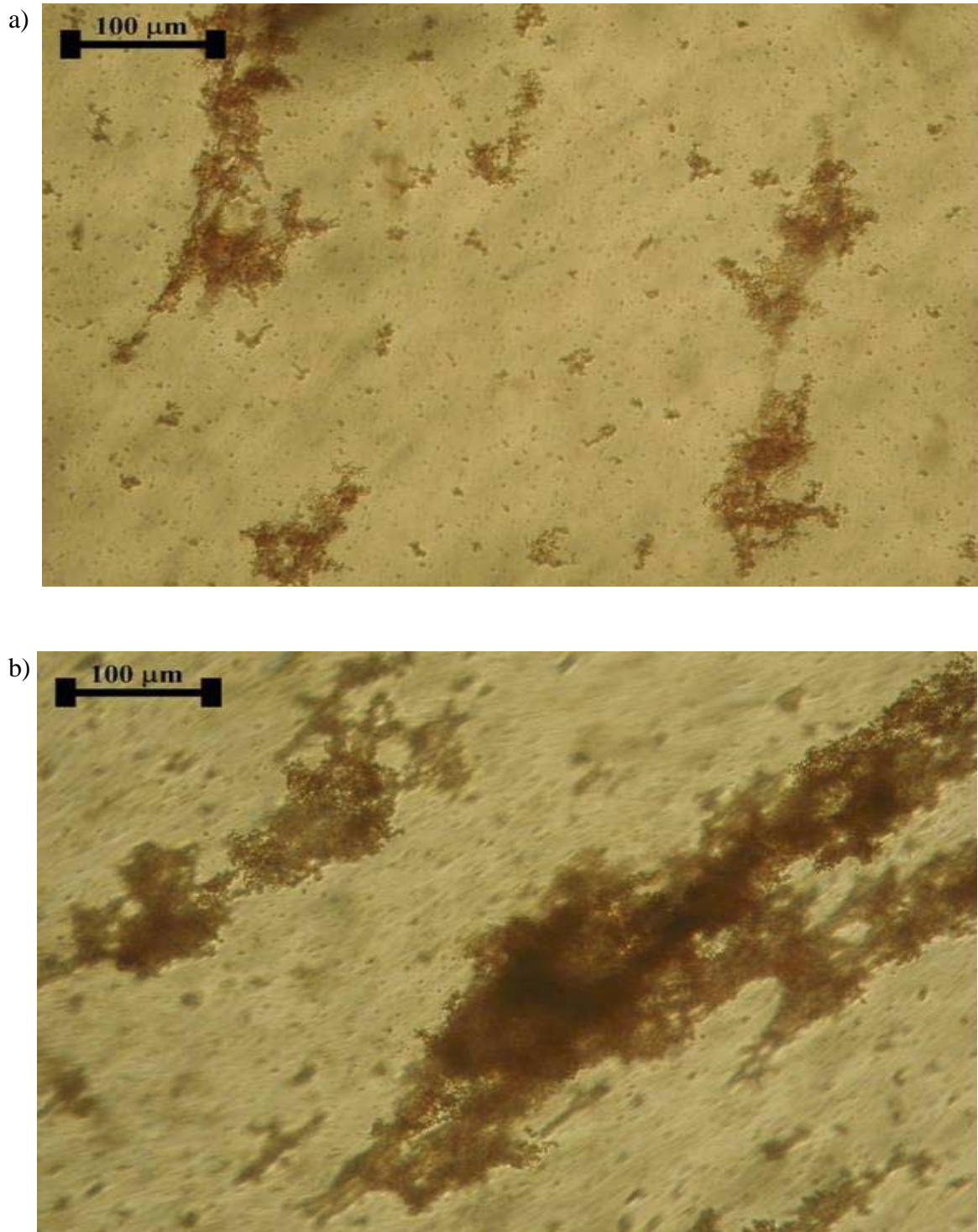


Figure 23. Precipitating effect of ethanol over myoglobin a) after 1 minute of contact, b) after 2 minutes of contact.

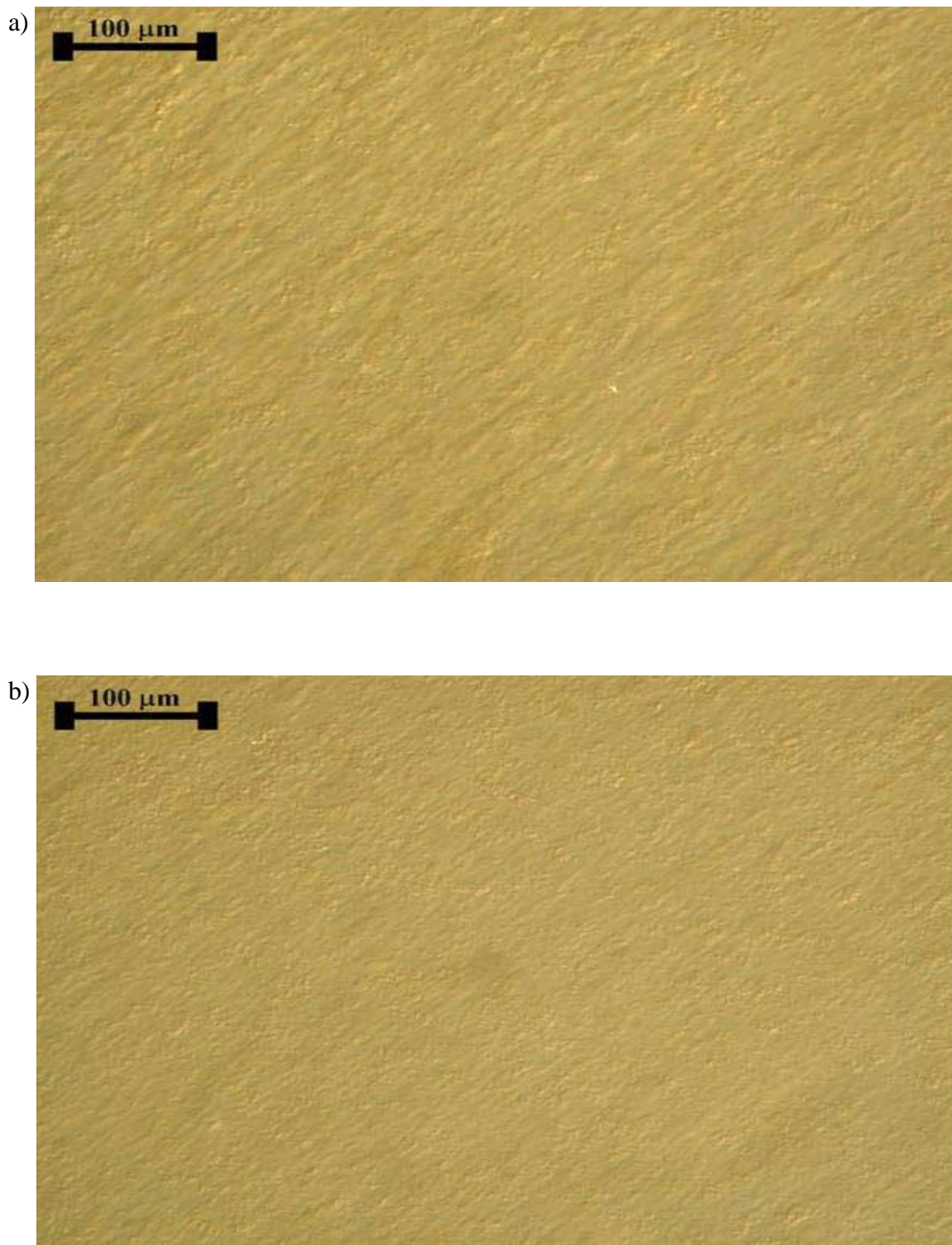


Figure 24. Precipitating effect of PEGMA-PEGDMA solutions over myoglobin after 10 minutes of contact a) PEGMA200-PEGDMA600, b) PEGMA1000-PEGDMA1000.

In neutral polymerization solutions, polyethylene glycol monomethacrylate was used as a monomer with tethered chain molecular weights of 200, 400 and 1000 g/mol. The crosslinker employed was polyethylene glycol dimethacrylate that possessed PEG chains with molecular weights of 200, 600 and 1000 g/mol. Similar to MAA based hydrogel, the solvent used in the preparation of PEGDMA hydrogels was a 1:1 weight solution of ethanol and deionized water. The contact of myoglobin with PEG could be promoting its precipitation since PEG is frequently used in protein fractional precipitation. This protein separation technique takes advantage of PEG properties to reduce protein solubility according to protein size. Moreover, similar to ethanol and other precipitating agents, polyethylene glycol has a slight tendency to denature proteins [132 – 134]. Consequently, the agglomeration of myoglobin observed in PEGMA polymerization solutions could be the result of the precipitating and denaturing effects that PEG and ethanol have showed over proteins.

Myoglobin agglomeration was also observed when it was placed in contact with polymerization solutions of cationic hydrogels (see Figure 25). Like neutral polymerization solutions, the myoglobin agglomeration in cationic polymerization mixtures was more noticeable when the solutions contained ethanol when compared to solutions containing only DMAEM as monomer and PEGDMA as crosslinker (see Figure 26). Once more, the interaction of polyethylene glycol and ethanol with the protein could be the cause of myoglobin precipitation. As mentioned above, PEG and ethanol have been reported to produce precipitation and denaturation of proteins.

The detrimental effects over myoglobin structure caused by methacrylic acid at lower pH, precipitating and denaturing effects of polyethylene glycol and ethanol did

not allow the utilization of the various polymer morphologies studied to immobilized this hemeprotein through the entrapment technique.

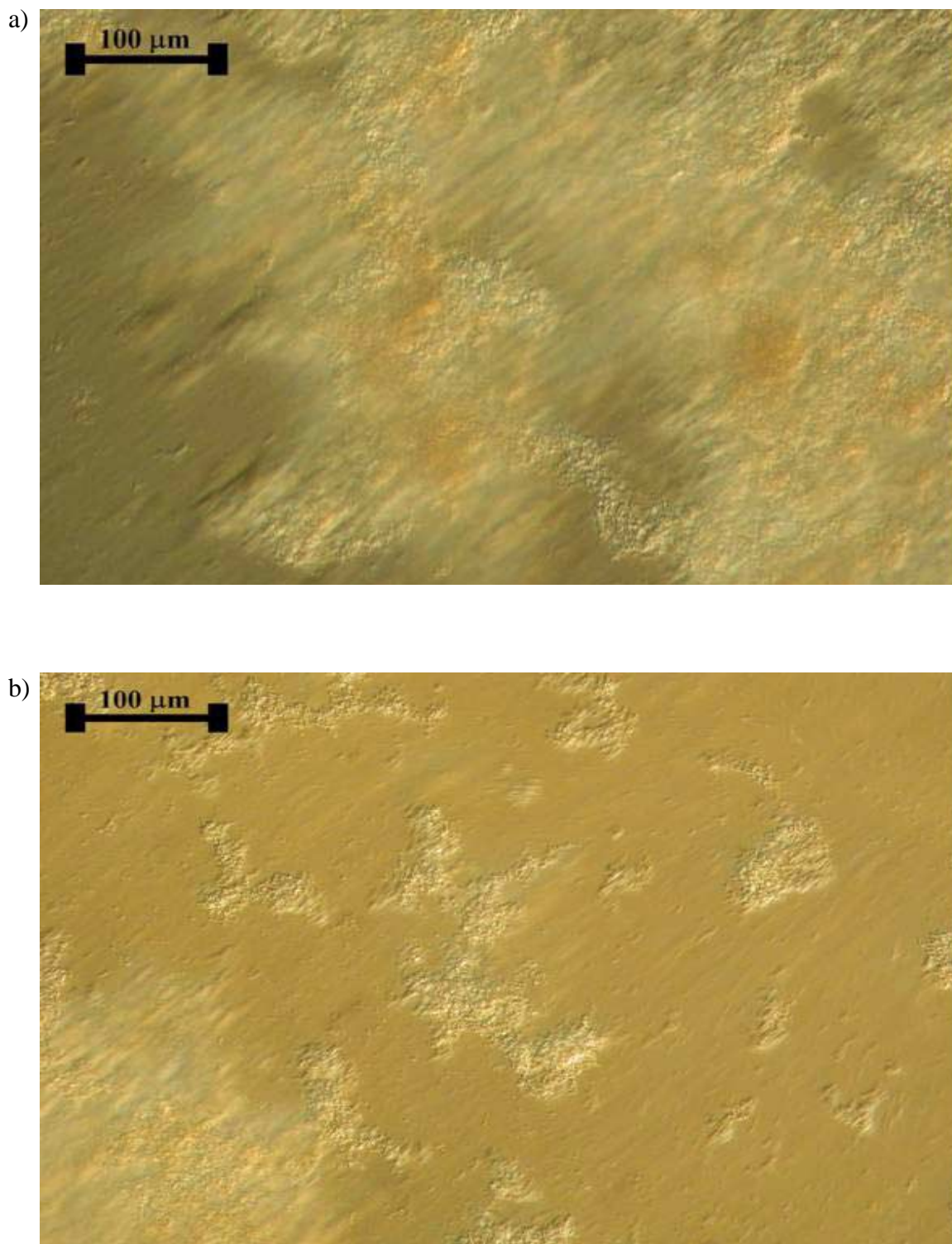


Figure 25. Precipitating effect of DMAEM-PEGDMA polymerization solutions containing ethanol over myoglobin after 10 minutes of contact, a) DMAEM-PEGDMA600, b) DMAEM-PEGDMA1000.

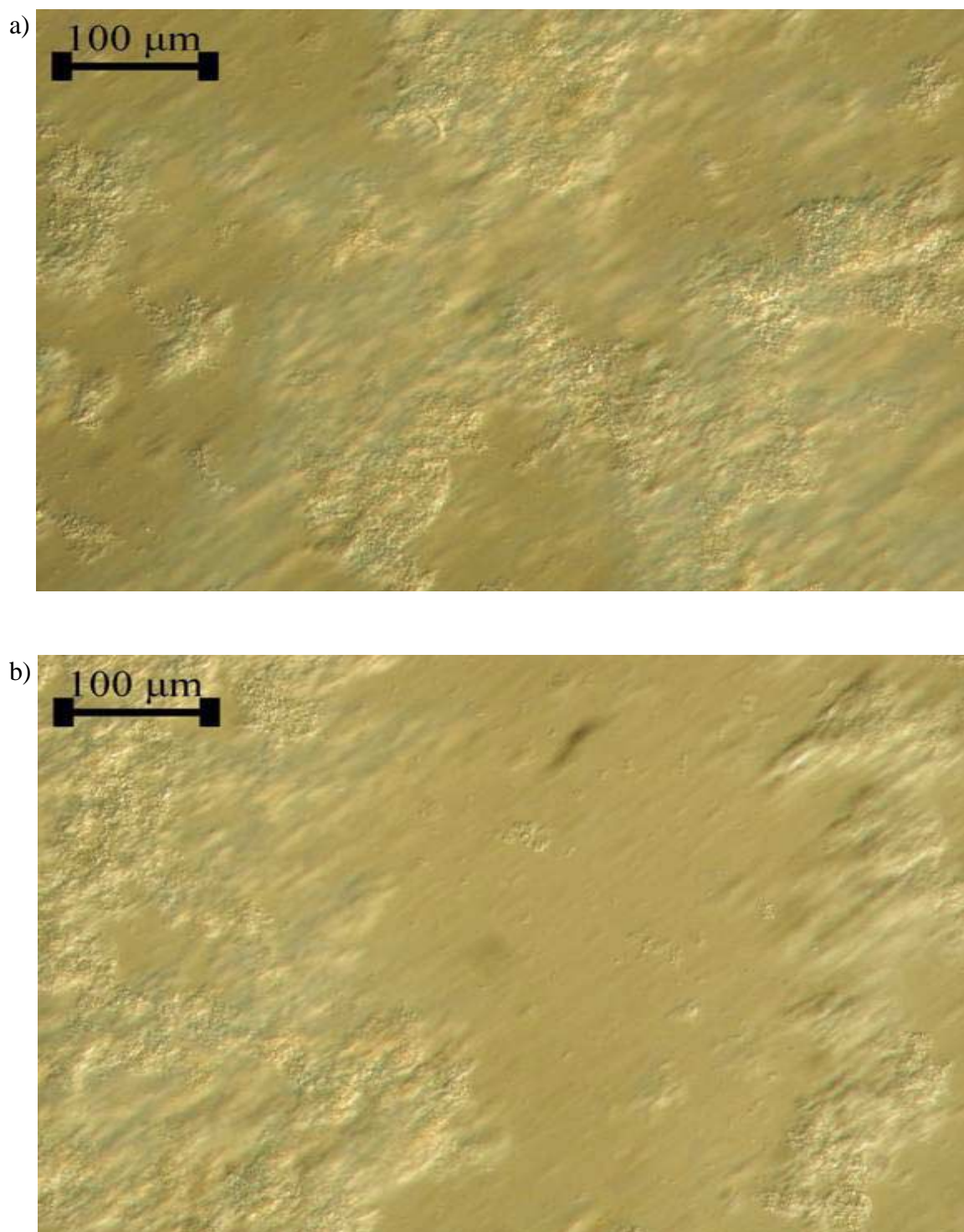


Figure 26. Precipitating effect of DMAEM-PEGDMA solutions over myoglobin after 10 minutes of contact a) DMAEM-PEGDMA600, b) DMAEM-PEGDMA1000.

6.5 Myoglobin Release after Incorporation by Entrapment

The release behavior of myoglobin incorporated by entrapment in MAA based hydrogels was investigated to determine the amount of protein that remained inside the polymer network and to evaluate the solute transport mechanism and diffusion coefficients. Still, the incorporation of myoglobin through entrapment in MAA based hydrogels showed a loss in the protein biological activity.

The myoglobin fractional release behavior is illustrated in Figure 27. The three anionic morphologies employed behaved in a similar manner during myoglobin release. No statistical differences were observed. The evaluation of the diffusional exponent (n) (equation 26) confirmed this trend (see Table 14). The value of this parameter in MAA based hydrogels was around 0.95 for all the three crosslinker lengths of polyethylene glycol dimethacrylate considered. This result indicated that the transport mechanism of myoglobin incorporated by entrapment inside MAA hydrogels coupled Fickian diffusion and chain relaxation. However, the nearness of the values obtained to 1 suggested the possibility that chain relaxation phenomenon strongly dominated the transport of myoglobin.

Afterwards, the Berens and Hopfenbers model was utilized to estimate the Fickian and chain relaxation contributions to solute transport and to evaluate the diffusion coefficients (see Table 15). The chain relaxation contribution was approximately 0.80 for the anionic hydrogels investigated. The prior value corroborated the assumption made from the diffusional exponent (n) result that chain relaxation mechanism controlled the

myoglobin transport from MAA hydrogels. The diffusion coefficients for myoglobin incorporated by entrapment inside MAA hydrogels were in the magnitude order of 10^{-11} cm^2/s . They were two magnitude orders lower when compared with the release at the same conditions of pH and temperature of myoglobin incorporated by adsorption inside the same hydrogel morphologies. The incorporation through entrapment hindered the diffusion of the protein from the polymer structure since the network was built around the protein during the polymerization process.

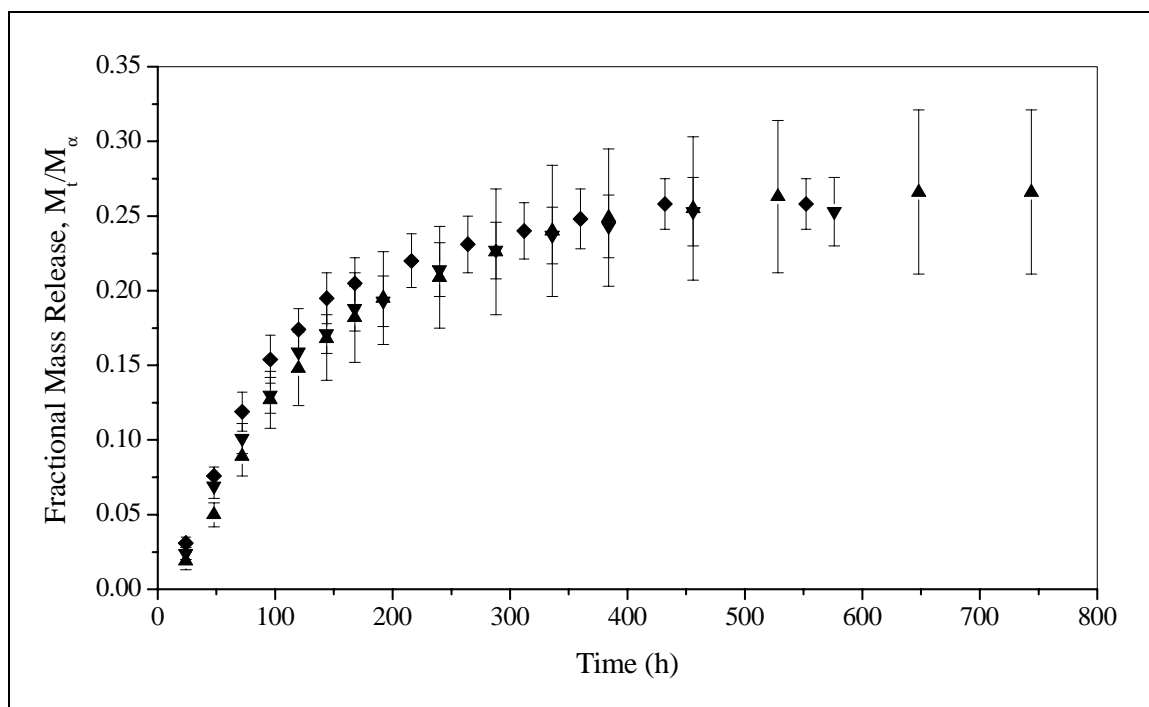


Figure 27. Fractional release of myoglobin incorporated through entrapment in MAA-PEGDMA hydrogels for various crosslinker lengths in PBS at pH = 7.0 at T = 30 °C, ▲ MAA-PEGDMA200 (n=5), ▼ MAA-PEGDMA600 (n=5) and ◆ MAA-PEGDMA1000 (n=5). Each point represents an average \pm one standard deviation.

Table 14. Values of the parameters n and k of the Stefan's approximation for myoglobin incorporated through entrapment in MAA-PEGDMA hydrogels with various crosslinker lengths. Experiments were performed at PBS at pH = 7.0 and T = 30 °C.

	k , characteristic constant of the polymer/solute system	n , diffusional exponent.
MAA-PEGDMA200 (97:3 molar ratio, 1:1 dilution rate)	0.00155 ± 0.00071	0.94164 ± 0.09514
MAA-PEGDMA600 (97:3 molar ratio, 1:1 dilution rate)	0.00137 ± 0.00049	0.99578 ± 0.078
MAA-PEGDMA1000 (97:3 molar ratio, 1:1 dilution rate)	0.0020 ± 0.00086	0.94153 ± 0.09495

Table 15. Diffusion coefficients for myoglobin incorporated through entrapment in MAA-PEGDMA hydrogels with various crosslinker lengths evaluated using the Berens and Hopfenbers model. Experiments were performed at PBS at pH = 7.0 and T = 30 °C.

	ϕ_F , contribution of Fickian diffusion	ϕ_R , contribution of chain relaxation	D (cm ² / s), the diffusion coefficient
MAA-PEGDMA200 (97:3 molar ratio, 1:1 dilution rate)	$0.2010 \pm 4.2789 \times 10^{-3}$	$0.7990 \pm 4.2789 \times 10^{-3}$	$2.2245 \times 10^{-11} \pm 1.5101 \times 10^{-12}$
MAA-PEGDMA600 (97:3 molar ratio, 1:1 dilution rate)	$0.1736 \pm 5.9042 \times 10^{-3}$	$0.8264 \pm 5.9042 \times 10^{-3}$	$3.4343 \times 10^{-11} \pm 9.3681 \times 10^{-13}$
MAA-PEGDMA1000 (97:3 molar ratio, 1:1 dilution rate)	$0.1861 \pm 3.8082 \times 10^{-3}$	$0.8139 \pm 3.8082 \times 10^{-3}$	$3.2871 \times 10^{-11} \pm 6.3542 \times 10^{-13}$

6.6 Myoglobin Activity Studies after Incorporation by Adsorption

The capacity of myoglobin to perform reactions with its specific ligands was initially tested after its incorporation in MAA based hydrogels and later after release experiments. In the case of activity studies carried out immediately after myoglobin incorporation, the great amount of protein contained inside the hydrogels did not allow the accurate detection of the characteristic peaks that appears at the Soret band. Consequently, the characteristic peaks that typically appear at the Q band were used to follow the changes in the oxidation state and to verify the binding of carbon monoxide. Typically, the intensity of the peaks appearing in the Q band is approximately 10% of the intensity shown for the peaks that appears at Soret band. The spectral properties of myoglobin in ferrous and ferric state are listed in Table 4 and Table 5.

The activity tests involved the change in the myoglobin oxidation state from metaquo myoglobin (Fe^{III}) to deoxy state (Fe^{II}) using sodium dithionite and the reaction with carbon monoxide. The distinctive peaks at Q band for myoglobin in metaquo state are located at 502 and 630 nm. Myoglobin in the deoxy state normally displays a peak at 560 nm. The binding between myoglobin and carbon monoxide could be verified by the appearance of the characteristic peaks of the complex at 540 and 579 nm. These values were used to confirm the occurrence of the reactions.

Figures 28, 29 and 30 present the effect of the addition of sodium dithionite over myoglobin oxidation state. From these three figures, it could be observed that the spectra

of the different hydrogel morphologies containing myoglobin displayed two peaks located in the region where the characteristic peaks should appear for myoglobin in metaquo state. The peaks appeared at 504.6 and 633 nm for MAA-PEGDMA200, 503.2 and 632.6 nm for MAA-PEGDMA600, and 505.2 and 632.6 nm for MAA-PEGDMA1000.

After the addition of sodium dithionite, the disappearance was noticed through time of the two aforementioned peaks and the formation of a new peak. This new peak was located at 552 nm for MAA-PEGDMA200, 551.2 nm for MAA-PEGDMA600 and 552.4 nm for MAA-PEGDMA1000. The formation of this peak indicated that a change in the oxidation state from Fe^{III} to Fe^{II} occurred in myoglobin incorporated inside MAA based hydrogels. It should be noticed that the peaks corresponding to metaquo myoglobin did not completely disappear implying that some myoglobin inside the hydrogel was still in metaquo state. The presence of some myoglobin in metaquo state could have influenced the fact that the peak corresponding to deoxy myoglobin appeared almost 8 nm before from its common value.

After myoglobin reduction to deoxy state, the hydrogel membranes were placed in contact with carbon monoxide. Their behavior is illustrated in Figures 31, 32 and 33. The interaction of CO and MAA loaded hydrogels produced the gradual disappearance of 560nm peak. Also, the formation could be observed over the course of time of two peaks at 539 and 574.4 nm for MAA-PEGDMA200, 541.8 and 578.4 nm for MAA-PEGDMA600, and 542 and 576.4 nm for MAA-PEGDMA1000. The peaks displayed after the contact with CO were near to the characteristic values that account for the

formation of the carboxy-myoglobin complex. The presence of both peaks confirmed the capacity of myoglobin to bind carbon monoxide.

Myoglobin that had been incorporated inside MAA based hydrogels was able to be reduced from metaquo state (Fe^{III}) to deoxy state (Fe^{II}) by the addition of sodium dithionite. The reduced myoglobin loaded hydrogels were capable of binding carbon monoxide and showed the characteristic peaks. These results indicated that myoglobin loaded MAA hydrogels retained the biological activity immediately after immobilization processes was performed.

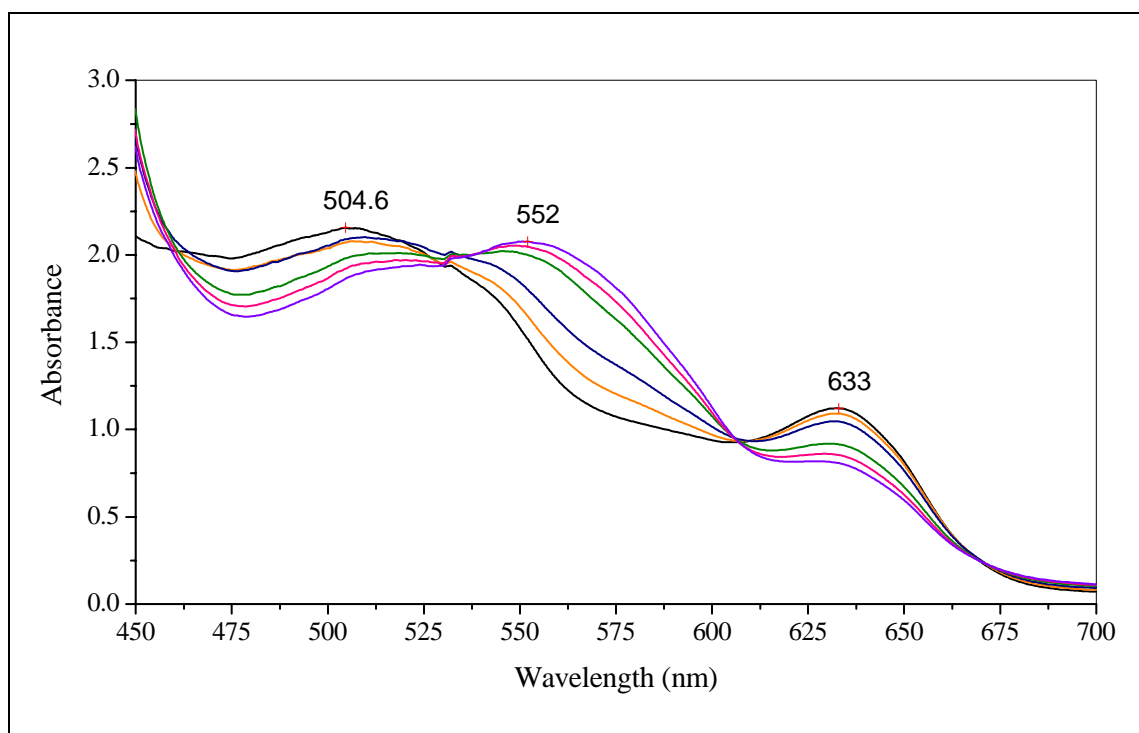


Figure 28. Effect of the addition of sodium dithionite over the spectroscopic properties of myoglobin incorporated in MAA-PEGDMA200 hydrogels before release, — spectrum before addition of sodium dithionite, spectra after addition of sodium dithionite: — t=0 min, — t=5 min, — t=10 min, — t=20 min, and — t=30 min.

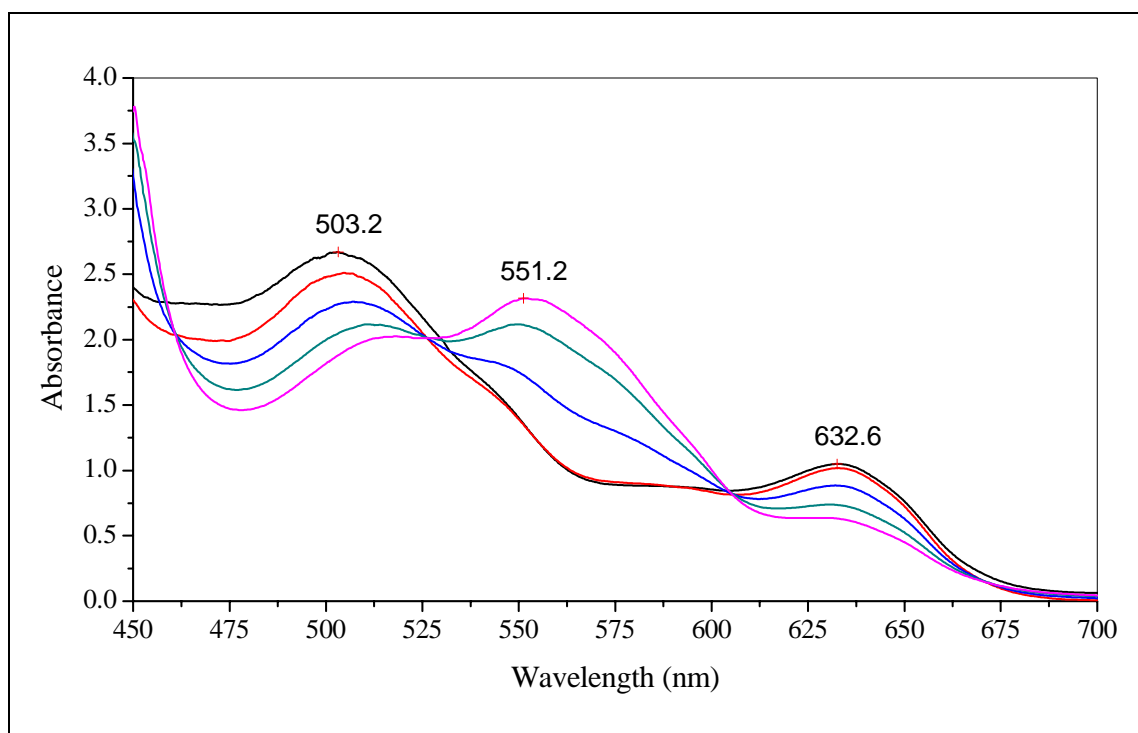


Figure 29. Effect of the addition of sodium dithionite over the spectroscopic properties of myoglobin incorporated in MAA-PEGDMA600 hydrogels before release, — spectrum before addition of sodium dithionite, spectra after addition of sodium dithionite: — t=0 min, — t=10 min, — t=30 min, — t=45 min.

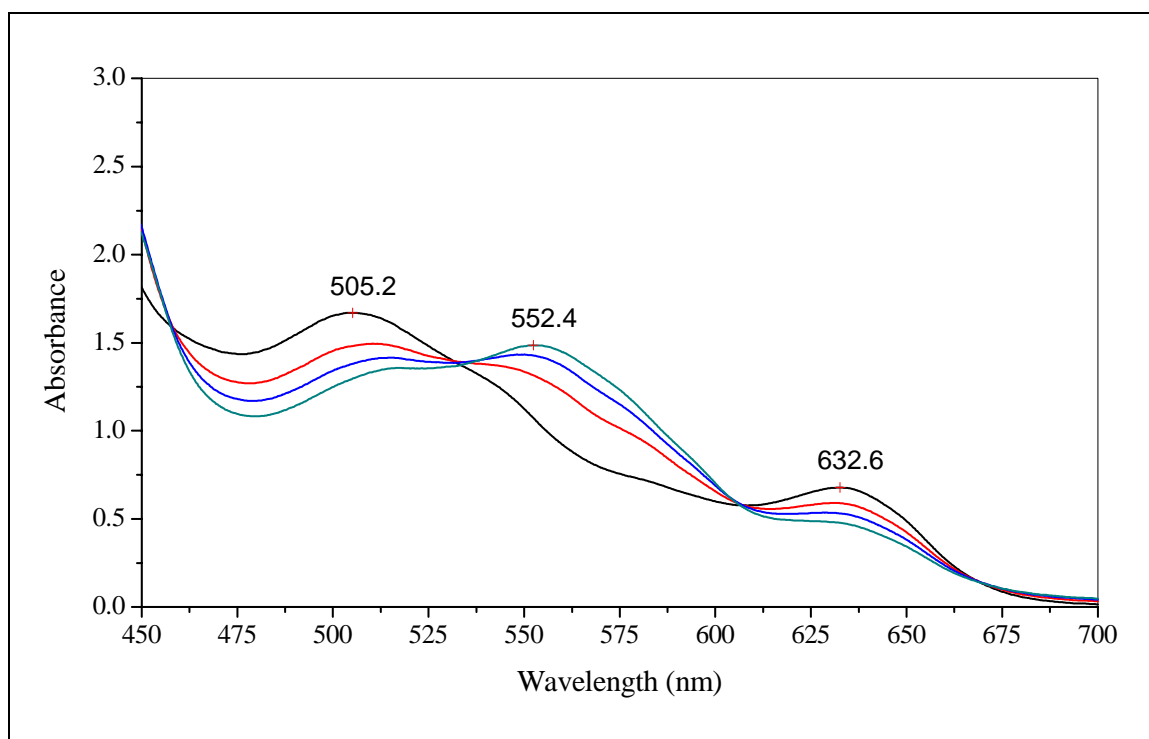


Figure 30. Effect of the addition of sodium dithionite over the spectroscopic properties of myoglobin incorporated in MAA-PEGDMA1000 hydrogels before release, — spectrum before addition of sodium dithionite, spectra after addition of sodium dithionite: — t=0 min, — t=5 min, — t=10 min.

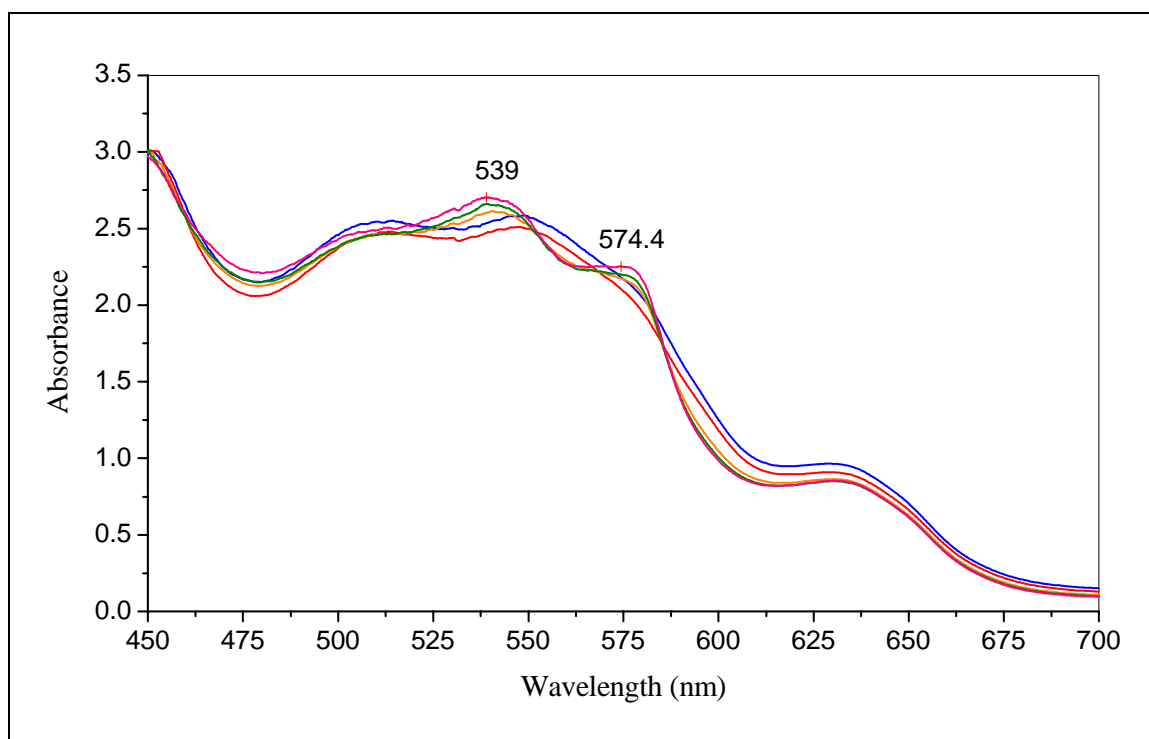


Figure 31. Effect of the contact with carbon monoxide over the spectroscopic properties of reduced myoglobin incorporated in MAA-PEGDMA200 hydrogels before release, — spectrum before addition of CO, spectra after addition of CO: — 0.5 cm³ CO t=5 min, — 1.0 cm³ CO t=5 min, — 1.0 cm³ CO t=10 min, — 1.0 cm³ CO t=20 min.

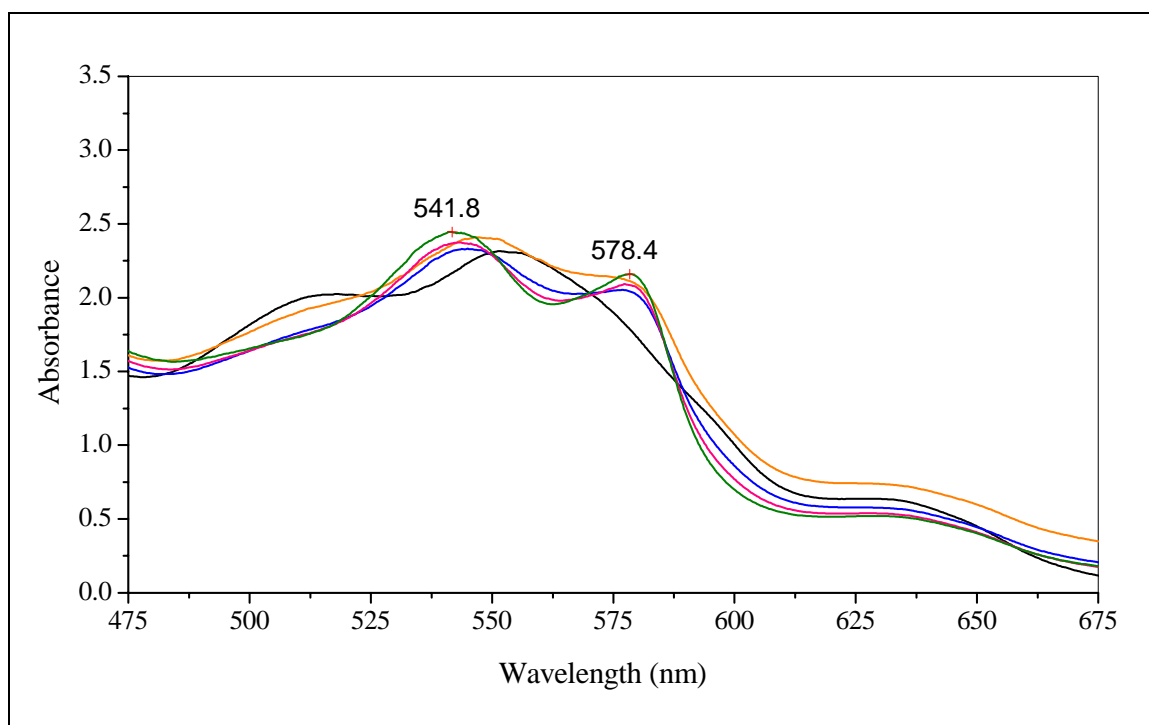


Figure 32. Effect of the contact with carbon monoxide over the spectroscopic properties of reduced myoglobin incorporated in MAA-PEGDMA600 hydrogels before release, — spectrum before addition of CO, spectra after addition of CO: — 0.5 cm³ CO t=0 min, — 0.5 cm³ CO t=5min, — 0.5 cm³ CO t=10 min, — 1.0 cm³ CO t=5 min.

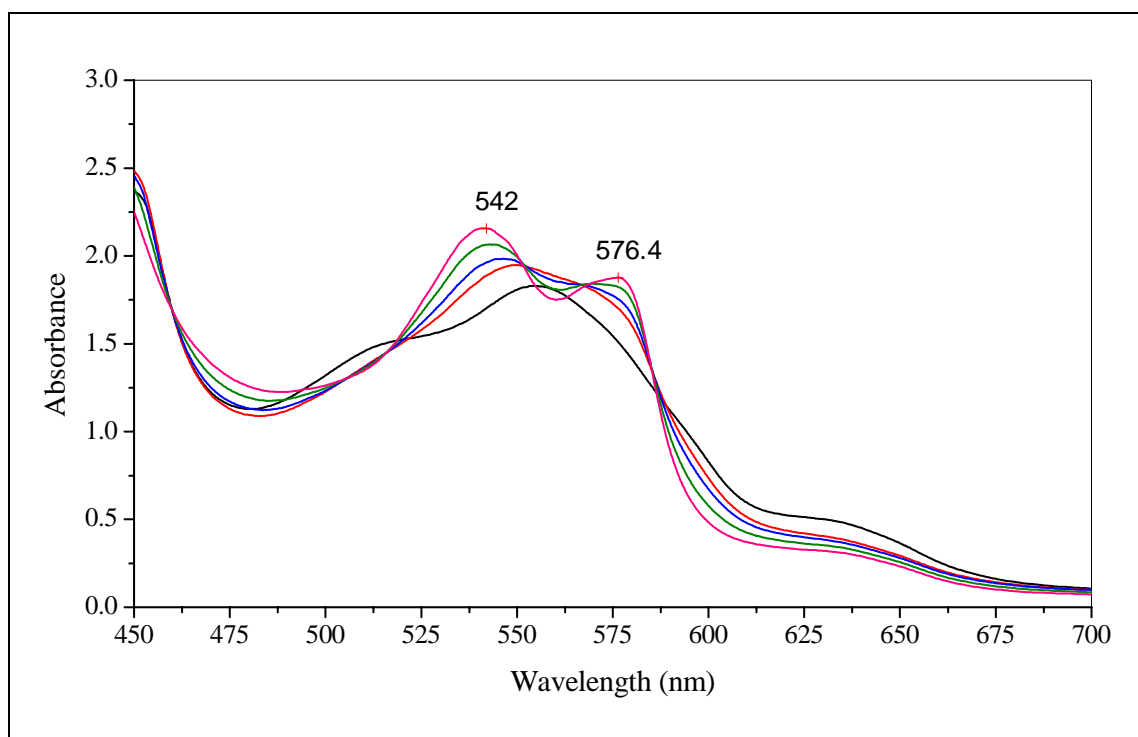


Figure 33. Effect of the addition of carbon monoxide over the spectroscopic properties of reduced myoglobin incorporated in MAA-PEGDMA1000 hydrogels before release, — spectrum before addition of CO, spectra after addition of CO: — 1.0 cm³ CO t=0 min, — 1.0 cm³ CO t=10 min, — 1.5 cm³ CO t=10 min, — 1.5 cm³ CO t=30 min.

After release experiments were completed, the same abovementioned procedure was followed to verify the biological activity of myoglobin permanently encapsulated inside the hydrogel. For release experiments carried out at pH 7.0, the peaks displayed in the Soret band were used to monitor the changes in spectral properties. The significant amount of protein released, almost 85% for all anionic morphologies used, produced a decrease in the intensity of the peaks observed at Soret band. Normally, peaks at the Soret band for myoglobin in metaquo and deoxy state are located at 408 and 435 nm respectively. The carboxy-myoglobin complex shows a peak in the Soret band at 425 nm. The appearance of these peak values were used to corroborate the occurrence of the reactions.

Figures 34, 35, and 36 correspond to MAA-PEGDMA200, MAA-PEGDMA600, and MAA-PEGDMA1000 respectively after release in PBS at pH 7.0 and show the effect over myoglobin spectral properties resulting from the exposure to sodium dithionite and carbon monoxide.

In the case of MAA based hydrogels with crosslinker lengths of 200 and 600, the spectra taken after conclusion of the release experiment showed a peak which was displayed at 409.2 nm. The characteristic peak of metaquo myoglobin typically appears at 408 nm. The interaction with sodium dithionate produced the disappearance of the peak at 409.2 nm and a new peak was observed at 430.2 nm for MAA-PEGDMA200 and 432.4 nm for MAA-PEGDMA600. Comparing with the characteristic values of metaquo and deoxy state, the observed change in spectroscopic properties indicated that protein permanently immobilized inside MAA-PEGDMA200 and MAA-PEGDMA600 hydrogels changed its oxidation state from metaquo to deoxy.

Hydrogels containing reduced myoglobin were placed in contact with carbon monoxide. In the presence of carbon monoxide, the spectra of hydrogels containing myoglobin showed the vanishing of the peak corresponding to deoxy myoglobin. The formation of a new a peak at 422.8 nm for MAA-PEGDMA200 and 423 for MAA-PEGDMA600 was also observed. This peak around 423 nm indicated the binding of myoglobin and carbon monoxide. The capacity of the myoglobin remaining inside MAA-PEGDMA200 and MAA-PEGDMA600 hydrogels after release experiments to be reduced by sodium dithionate and to bind carbon monoxide indicated the retention of myoglobin biological activity. After adsorption incorporation was performed, hydrogels were dried. The myoglobin release from MAA based hydrogels at pH 7.0 and 30 °C took around 4 days. Even after being dried and placed in buffer solution for more than 4 days, myoglobin inside MAA-PEGDMA200 and MAA-PEGDMA600 hydrogels demonstrated the ability to perform typical reactions of hemeproteins.

MAA hydrogels crosslinked with PEGDMA1000 also displayed changes in their spectroscopic properties after being in contact with sodium dithionite and carbon monoxide (Figure 36). However, the values of the peaks obtained were distant from the characteristic peaks reported in literature. After the addition of sodium dithionite, MAA-PEGDMA1000 containinig hydrogels showed the displacement of the peak corresponding to metaquo state from 409.4 nm to 420.6 nm. The characteristic peak of deoxy state that should have appeared after the addition of sodium dithionite is typically located at 435 nm. Then, the contact with carbon monoxide produced displacement of the peak at 420.6 nm to 417.6 nm. The literature has reported that the peak of the carboxy-myoglobin complex appears at 425 nm. The changes in spectroscopic properties

indicated that myoglobin performed reactions due to the contact with sodium dithionite and carbon monoxide. Nevertheless, the differences between the peaks obtained and the values reported in literature suggested the possibility that the release process in MAA-PEGDMA1000 hydrogels could have a detrimental effect over myoglobin structure.

In the case of release studies conducted at pH 5.8, the activity tests after release indicated that any change in myoglobin spectroscopic properties occurred after the contact with sodium dithionite. From this result, it could not be categorically concluded that the protein contained inside the hydrogels was not biologically active. Probably, MAA based hydrogels at pH 5.8 were still collapsed impeding the diffusion of sodium dithionite inside the hydrogel and avoiding the protein reduction.

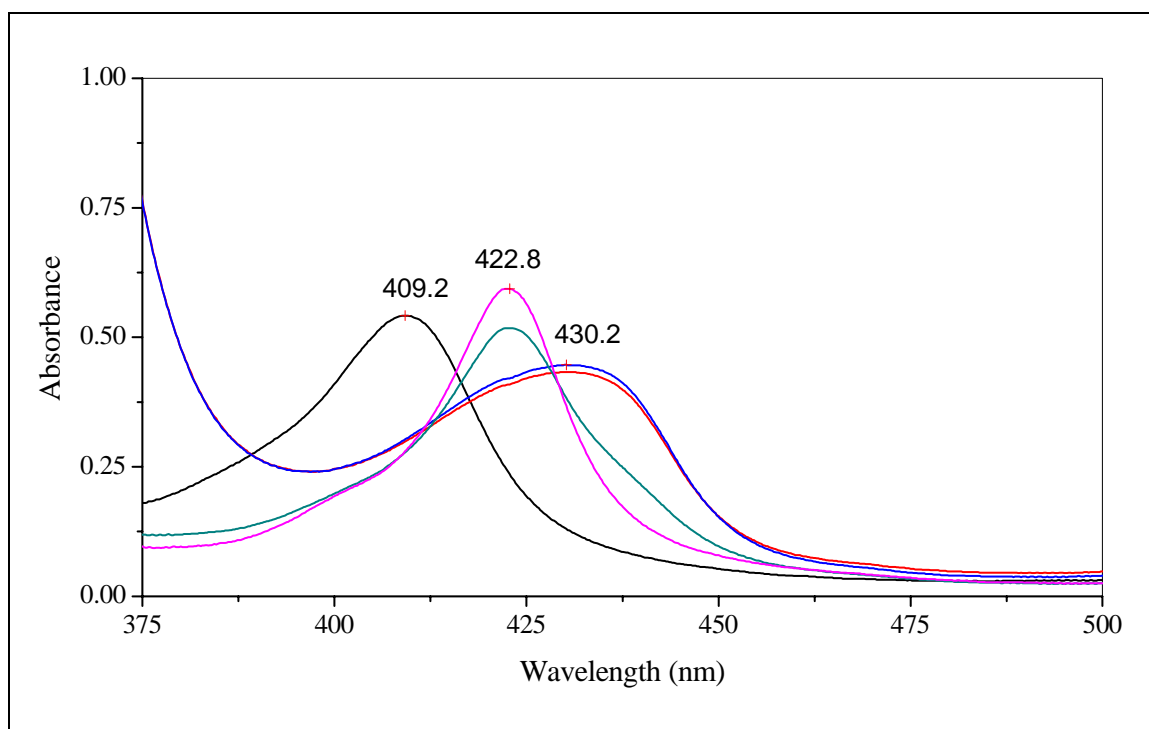


Figure 34. Effect of sodium dithionite and carbon monoxide over the spectroscopic properties of myoglobin incorporated in MAA-PEGDMA200 hydrogels after release, — spectrum before dithionite and CO, spectra after addition of sodium dithionite: — t=0 min, — t=5 min, spectra after CO — 0.5 cm³ CO t=0 min, — 0.5 cm³ CO t=0 min.

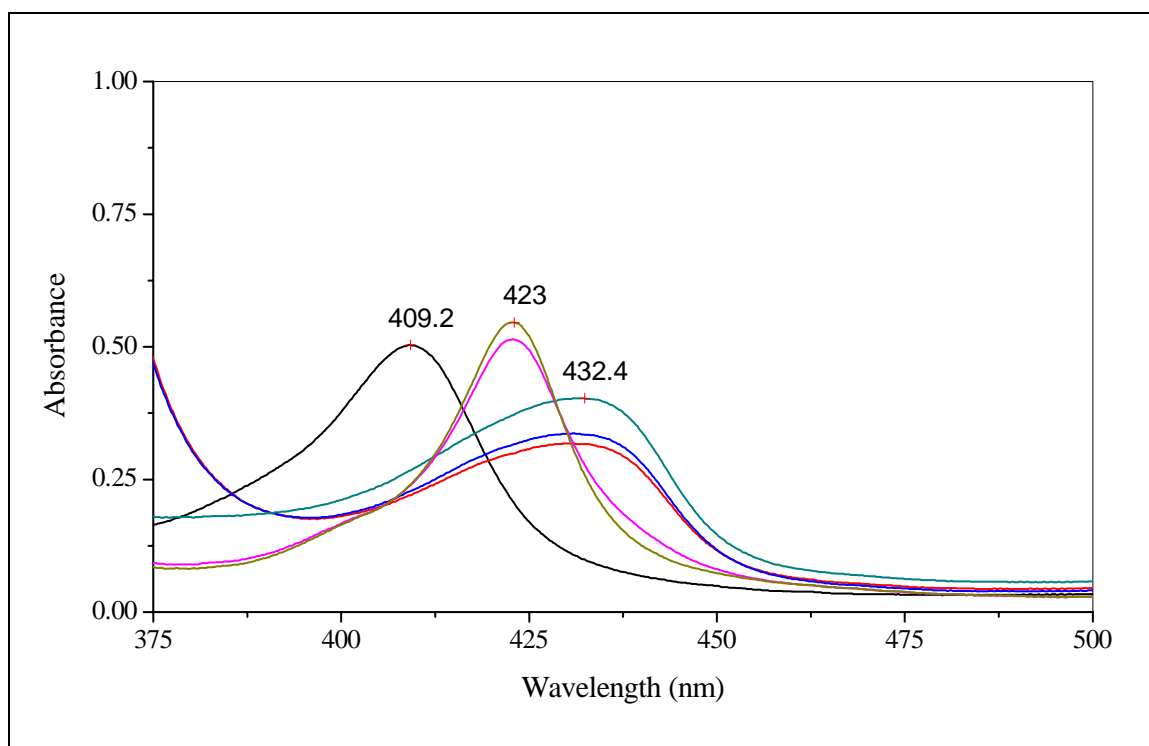


Figure 35. Effect of sodium dithionite and carbon monoxide over the spectroscopic properties of myoglobin incorporated in MAA-PEGDMA200 hydrogels after release, — spectrum before dithionate and CO, spectra after addition of sodium dithionate: — t=0 min, — t=5 min, — t=10 min, spectra after CO: — 0.5 cm³ CO t=0 min and, — 0.5 cm³ CO t=5 min.

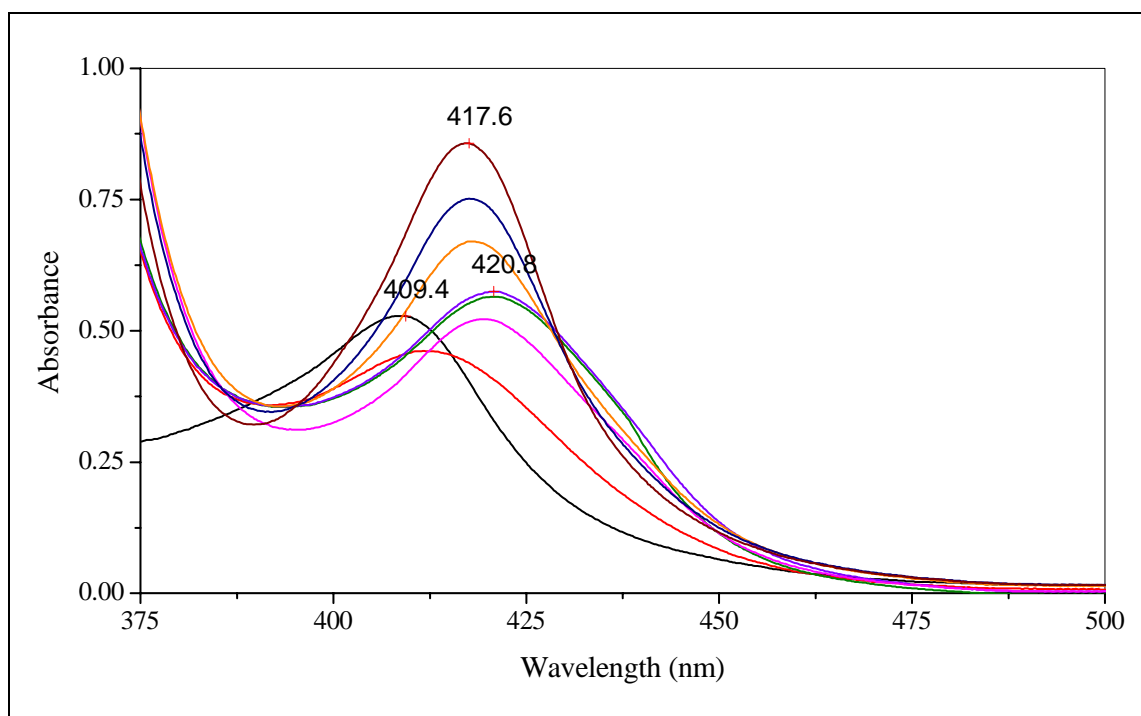


Figure 36. Effect of sodium dithionite and carbon monoxide over the spectroscopic properties of myoglobin incorporated in MAA-PEGDMA1000 hydrogels after release, — spectrum before dithionate and CO, spectra after addition of sodium dithionate: — t=0 min, — t=5 min, — t=10 min, spectra after CO: — 0.5 cm³ CO t=0 min, — 0.5 cm³ CO t=5 min, — 0.5 cm³ CO t=10 min, and — 1.0 cm³ CO t=5 min.

6.7 Hemoglobin I Immobilization through Adsorption

Considering that the more promising results of myoglobin immobilization through adsorption were obtained for anionic hydrogels, these polymer networks were used as support for the incorporation by adsorption of hemoglobin I (HbI) from *Lucina pectinata*. The amount of HbI incorporated inside MAA based hydrogels was significantly lower when compared with the amount of myoglobin adsorbed in the same polymer morphologies (Figure 37). The isolation of HbI from *Lucina pectinata* clams was a process that took a long time and a small amount of protein was obtained. Thus, the concentration of hemoglobin I in the solution employed to perform the incorporation was lower when compared to myoglobin solution utilized in adsorption experiments.

The low concentration of hemoglobin I solution employed during the immobilization experiments of adsorption could explain the small incorporation degree. Nevertheless, the possibility could not be neglected that the interactions developed between Hemoglobin I and the anionic network did not promote the protein incorporation in the same mode as myoglobin-polymer interactions.

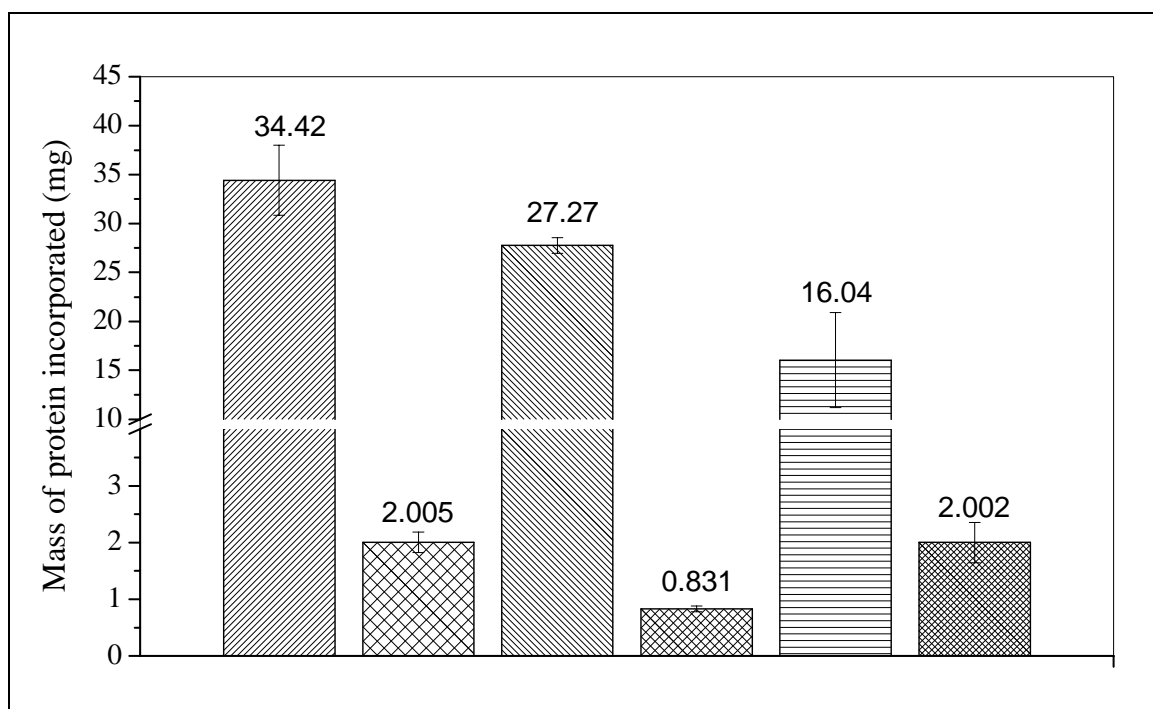


Figure 37. Comparison between the amount of myoglobin and hemoglobin I incorporated by adsorption inside MAA based hydrogels with various crosslinker lengths, ▨ Mb in MAA-PEGDMA200 (n=6), ▩ HbI in MAA-PEGDMA200 (n=6), ▪ Mb in MAA-PEGDMA600 (n=6), ▫ HbI in MAA-PEGDMA600 (n=6), ▬ Mb in MAA-PEGDMA1000 (n=6), ▭ HbI in MAA-PEGDMA1000 (n=6). Each bar represents an average \pm one standard deviation.

6.8 Hemoglobin I Activity Studies after Incorporation by Adsorption

The biological activity of hemoglobin I from *Lucina pectinata* after being incorporated by adsorption inside MAA based hydrogels was studied. The stronger affinity of hemoglobin I toward hydrogen sulfide has been widely reported in literature [13, 41]. The capability to act as a natural receptor for hydrogen sulfide has made hemoglobin I an important object of study. Consequently, the activity of hemoglobin I was analyzed using a solution of hydrogen sulfide to determine the capacity of the protein immobilized to bind this highly toxic compound.

Figure 38 presents the results obtained during the realization of the activity test of hemoglobin I incorporated inside MAA-PEGDMA200 hydrogels. Similar results were achieved for MAA-PEGDMA600 and MAA-PEGDMA1000 hydrogels. The spectrum of the hydrogel after the incorporation of hemoglobin I had a peak at 407.8 nm. The characteristic peak of metaquo hemoglobin I in the Soret band is reported to be located at 407 nm. Subsequently, the contact of the hydrogel containing HbI with a hydrogen sulfide solution produced the appearance of a peak at 426.2 nm. Typically, the sulfide-hemoglobin I complex displays a peak at 426 nm. Therefore, hemoglobin I immobilized by adsorption in anionic networks was able to bind hydrogen sulfide indicating that the protein biological activity was not affected during immobilization process.

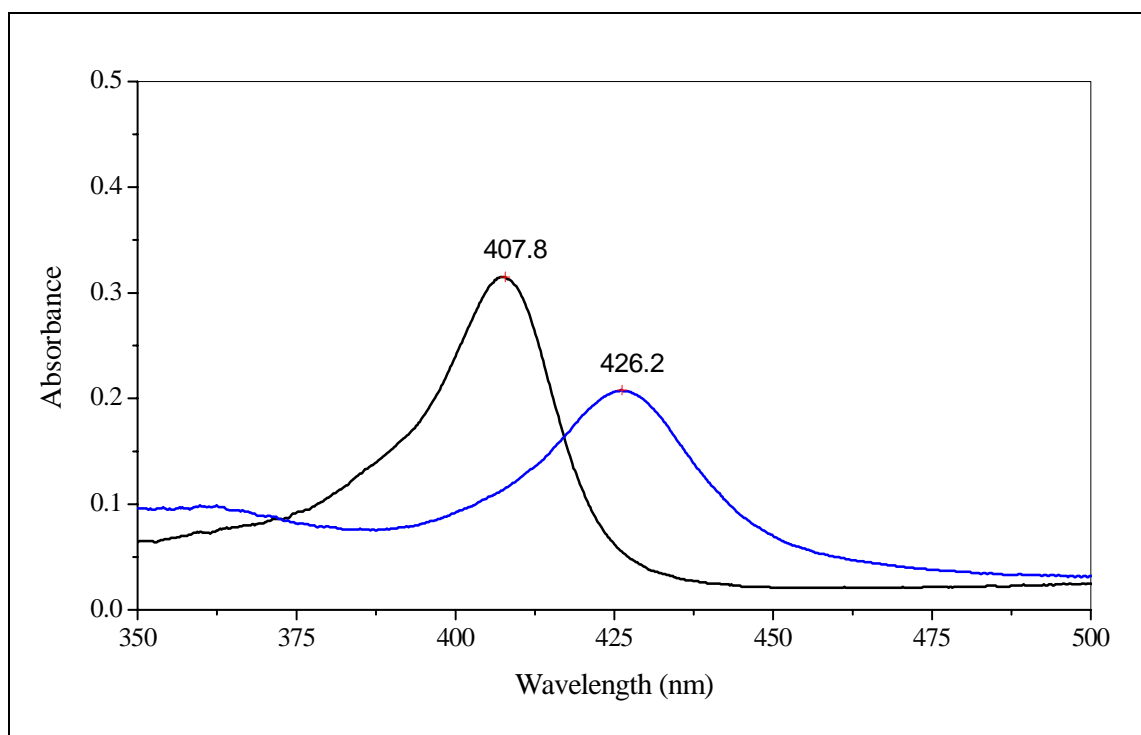


Figure 38. Effect of the contact with a hydrogel sulfide solution over the spectroscopic properties of hemoglobin I incorporated in MAA-PEGDMA200 hydrogels, — spectrum of MAA-PEGDMA200 hydrogel containing HbI, — spectrum after 1 minute of contact with hydrogen sulfide solution.

Chapter Seven

Conclusions

Several investigations have been pursuing a suitable manner to immobilize heme proteins. The changes in spectroscopic properties displayed for heme proteins in the presence of specific ligands make them excellent candidates to be used as recognition elements in biosensor technology. This project focused on the application of hydrophilic polymer networks as immobilization support for horse myoglobin and hemoglobin I from *Lucina pectinata*. Hemoglobin I from *Lucina pectinata* was investigated due to its particular strong affinity toward hydrogen sulfide. This special feature makes HbI appropriate to be used as a recognition element for hydrogen sulphide, a very toxic compound. Horse myoglobin was also studied not only because it is commercially available but also because it shows affinity to other interesting molecules such as oxygen, carbon monoxide, cyanide and nitric oxide. To immobilize these proteins inside hydrogel networks two techniques were considered, adsorption and entrapment. The effect of immobilization method over protein behavior was analyzed for various morphologies.

The highest myoglobin incorporation degree through adsorption immobilization technique was achieved in MAA based hydrogels. Cationic hydrogels also allowed the myoglobin incorporation by adsorption. However, the affinity of horse myoglobin toward DMAEM based hydrogels was approximately 10% of the affinity showed toward MAA based hydrogels. Neutral hydrogels did not adsorb any measurable amount of myoglobin.

An inverse relationship between the crosslinker length and amount of myoglobin incorporated was noticed for methacrylic acid hydrogels. Hydrogels synthesized with a larger crosslinker length incorporated a smaller protein amount than hydrogels with a shorter crosslinker length. Measurements of the correlation length supported this behavior. The correlation length in MAA hydrogels diminished when the crosslinker length increased.

Even though methacrylic acid hydrogels allowed the highest myoglobin incorporation by adsorption, these hydrogels also permitted the release of the previously incorporated protein. The rate of release was highly influenced by the pH of the buffer used as release media. For release experiments performed at pH 7.0, anionic hydrogels released almost 90% of the loaded protein. MAA-PEGDMA200 hydrogels permitted the highest protein release. The rate of release diminished when the crosslinker length increased. The evaluation of the solute transport mechanism evidenced that the coupling between Fickian diffusion and chain relaxation phenomenon led to myoglobin release. The Fickian diffusion played a more determinant role in myoglobin transport than chain relaxation mechanism. Fickian diffusion contribution was in the range of 0.9319 to 0.8555 for the anionic morphologies. However, the chain relaxation contribution was

increased at larger crosslinker length. The diffusion coefficients for MAA based hydrogels at PBS buffer pH 7.0 were in the magnitude order of 10^{-9} cm²/s, and they increased as crosslinker lengths diminished.

The increase in chain relaxation contribution and diffusion coefficients for myoglobin loaded MAA hydrogels as function of crosslinker lengths could be due to the correlation length. The anionic polymers employed were classified as microporous polymers since their correlation length is in the range of 10 to 100 nm. According to literature, the solute transport mechanism is typically due to diffusion and convection in microporous hydrogels [82, 83]

As aforementioned, an inverse relation was also observed between the mesh size and the crosslinker length. Consequently, hydrogels formulated with short crosslinker lengths provided a greater space of diffusion facilitating myoglobin release. The enlargement in the crosslinker length produced a decrease in the correlation length which meant a small space for solute diffusion. The reduction in the diffusion could hinder Fickian diffusion making chain relaxation contribution more relevant for hydrogels with larger crosslinker. In addition, the amount of protein incorporated inside hydrogels was higher for polymers with shorter crosslinker lengths. The concentration gradient responsible for Fickian diffusion was reduced as the crosslinker length increased.

At lower pH, the mechanical strength of the polymer networks declined. For that reason, only myoglobin loaded MAA-PEGDMA600 and MAA-PEGDMA1000 were able to perform release experiments at pH 5.8. However, all the morphologies developed fissures during the course of the test. The amount of myoglobin released from anionic hydrogels in PBS buffer at pH 5.8 was significantly lower than at pH 7.0. The

myoglobin fractional mass released was approximately 10% for MAA-PEGDMA600 and 1% for MAA-PEGDMA1000. Even though the pKa of methacrylic acid is 4.88, MAA hydrogels were not as highly swelled at pH 5.8 than at pH 7.0. The solute transport is facilitated in highly swollen hydrogels due to large amounts of unbound water [73].

The evaluation of the solute transport mechanism evidenced that the chain relaxation phenomena almost dominated myoglobin release at pH 5.8. The chain relaxation contribution was 0.891 for MAA-PEGDMA600 and 0.994 for MAA-PEGDMA1000. The diffusion coefficients for myoglobin loaded MAA hydrogels were in the order of magnitude of 10^{-9} cm²/s for hydrogels crosslinked with PEGDMA600 and 10^{-11} cm²/s for PEGDMA1000. The diminishing in the diffusion coefficients for release performed at pH 5.8 agreed with the experimental observations.

The biological activity of myoglobin immobilized through adsorption was investigated. Myoglobin loaded various anionic morphologies displayed changes in its spectroscopic properties before and after release experiments at pH 7.0 were performed. The proximity of the peaks displayed by myoglobin after reduction of the oxidation state and binding of carbon monoxide was similar to what was reported in literature and confirmed the activity retention after immobilization. Therefore, myoglobin was capable of overcoming the adsorption over the polymer network, drying and release process without suffering a significantly loss of its biological activity. In the case of myoglobin permanently encapsulated after release at pH 7.0 in MAA-PEGDMA1000, the peaks depicted were distant from the values established. The aforementioned could indicate that myoglobin immobilization process in MAA-PEGDMA1000 could have some detrimental effects over protein structure.

Myoglobin remaining inside the polymer network after release experiments performed at pH 5.8 did not show any change in its spectroscopic properties after being in contact with sodium dithionite and carbon monoxide. MAA hydrogels at pH 5.8 were not highly swelled. Probably, at this low pH the network had not overwhelmed the collapsed state hindering the occurrence of the reactions.

The immobilization of myoglobin was also investigated using the entrapment technique. The myoglobin incorporation through entrapment was not possible in PEGMA-PEGDMA and DMAEM-PEGDMA hydrogels. The contact between myoglobin and polymerization solutions of neutral and cationic polymers produced protein precipitation. The formation of protein aggregates was more notorious when the polymerization solutions contained ethanol when compared with the effect produced for monomer and crosslinker mixtures. The protein precipitation could be caused by the influence of polyethylene glycol and ethanol.

The contact of myoglobin with the polymerization solutions of MAA based hydrogels did not produce protein precipitation. However a displacement in the myoglobin characteristic peak at Soret band was observed immediately after the protein was in contact with the polymerization solution from 408 nm to 400 nm. After the polymerization of the network the peak was observed to appear at 390 nm. No spectroscopic changes were observed after the addition of sodium dithionate to the polymerization solution containing myoglobin. The low pH of the anionic polymerization solutions could be adversely affecting the protein structure.

The entrapment of myoglobin inside anionic polymers allowed the incorporation of lower amounts of myoglobin when compared with the amount loaded by adsorption.

Nevertheless, the amount of protein released from hydrogels during release experiments was also small. Approximately, 30% of the protein was released. The immobilization by entrapment was performed during the polymerization process permitting the construction of the polymer network around the protein which could hinder the solute transport. The behavior of the various anionic morphologies during release was very similar showing a marked influence of the relaxation process over myoglobin transport. The diffusion coefficients of myoglobin incorporated by entrapment were in the magnitude order of 10^{-11} cm²/s. A reduction of two magnitude orders were noticed when compared with the diffusion coefficients of myoglobin incorporated by adsorption in the same hydrogel morphologies.

Considering that the best results for the myoglobin immobilization were obtained by adsorption in MAA based hydrogels, the immobilization of hemoglobin I from *Lucina pectinata* was performed in a similar manner. The amount of HbI incorporated inside anionic hydrogels was considerably lower than myoglobin loaded in these polymer configurations. The abovementioned could be caused by the low hemoglobin I concentration in the solution used during incorporation process. However, the possibility could not be overlooked that myoglobin and hemoglobin I developed different interactions with the anionic polymer used as support. Hemoglobin I evidenced to be biologically active after its incorporation inside MAA hydrogels. The HbI loaded MAA-PEGDMA hydrogels was able to bind hydrogen sulfide.

In agreement with the results obtained, the best results for myoglobin immobilization were achieved by adsorption technique inside MAA-PEGDMA hydrogels. The myoglobin adsorption in anionic morphologies allowed the incorporation

of the highest amounts of protein. Myoglobin loaded MAA-PEGDMA hydrogels showed to maintain the biological activity immediately after incorporation was performed. Anionic morphologies allowed the release of approximately 90% of the protein previously loaded at pH 7.0. Nonetheless, the myoglobin remaining inside anionic hydrogels maintain its biological activity. The aforesaid indicated that myoglobin incorporated inside MAA-PEGDMA hydrogels was able to successfully overcome the adsorption into the polymer, the polymer drying, and the release process without undergoing a significant unfavorable effect over its biological activity.

REFERENCES

1. J. A. Kramer. Hydrogen Sulfide detectors and determination. *Turbomachinery International*, 30-32 (1992)
2. G. Schlavon and G. Zotti. Electrochemical detection of trace hydrogen sulfide in gaseous samples by porous silver electrodes supported on ion-exchange membranes (solid polymer electrolytes). *Anal. Chem.*, 67, 318-323 (1995)
3. A. A. Cardoso, H. Liu and P. K. Dasgupta. Fluorometric fiber optic drop sensor for atmospheric hydrogen sulfide. *Talanta*, 44, 1099-1106 (1997)
4. M. S. Legator, C. R. Singleton, D. L. Morris and D. L. Philips. Health effects from chronic low-level exposure to hydrogen sulfide. *Arch. Environ. Health*, 56(2), 123-131 (2001)
5. D. C. Fuller and A. J. Suruda. Occupationally related hydrogen sulfide deaths in the United States from 1984-1994. *J. Occup. Environ. Med.*, 42(9), 939-942 (2000)
6. A. R. Hirsch. Hydrogen sulfide exposure without loss of consciousness: chronic effects in four cases. *Toxicol. Ind. Health*, 18, 51-61 (2002)
7. M. M. F. Choi and P. Hawkins. Development of an optical hydrogen sulphide sensor. *Sens. Actuators B*, 90, 211-215 (2003)
8. N. S. Lawrence, J. Davis and R. G. Compton. Analytical strategies for the detection of sulfide: a review. *Talanta*, 52, 771-784 (2000)
9. M. L. Ferrer, F. Del Monte, C. Reyes Mateo, J. Gomez and D. Levy. Denaturation and leaching study of horseradish peroxidase encapsulated in sol-gel matrices. *J. Sol-Gel Sci. Technol.*, 26, 1169-1172 (2003)
10. W. Jin and J. D. Brennan. Properties and applications of proteins encapsulated within sol-gel derived materials. *Anal. Chim. Acta*, 461, 1-36 (2002)
11. A. Boffi, M. Rizzi, F. Monacelli and P. Ascenzi. Determination of H₂S solubility via the reaction with ferric hemoglobin I from the bivalve mollusk *Lucina pectinata*. *Biochim. Biophys. Acta*, 1523, 206-208 (2000)
12. D. W. Krauss and J. B. Wittenberg. Hemoglobins of the *Lucina pectinata*/Bacteria symbiosis. I. Molecular properties, kinetics and equilibria of reactions with ligands. *J. Biol. Chem.*, The American Society for Biochemistry and Molecular Biology, Inc., 265(27), 16043-16053 (1990)

13. R. Gretchen-Leon, H. Munier-Lehmann, O. Barzu, V. Baudin-Creuzza, R. Pietri, J. Lopez-Garriga and C. L. Cadilla. High-level production of recombinant sulfide-reactive hemoglobin I from *Lucina pectinata* in *Escherichia coli*. High yields of fully functional holoprotein synthesis in the BLi5 *E. coli* strain. *Protein Express. Purif.*, 38, 184-195 (2004)
14. A. P.F. Turner. *Yearbook of Science and Technology*. McGraw-Hill, New York, 40-42 (1999)
15. D. R. Trévenot, K. Toth, R. A. Durst and G. S. Wilson. Electrochemical Biosensors: Recommended Definitions and Classification. *Pure Appl. Chem Pure Appl. Chem.*, 71(12), 2333-2348, (1999)
16. K. E. Chung, E. H. Lan, M. S. Davidson, B. S. Dunn, J. S. Valentine and J. I. Zink. Measurement of dissolve oxygen in water using glass-encapsulated myoglobin. *Anal Chem.*, 67, 1505-1509 (1995)
17. D. J. Blyth, J. W. Aylott, D. J. Richardson and D. A. Russell. D. J. Blyth, J. W. Aylott, D. J. Richardson and D. A. Russell. Sol-gel encapsulation of metalloproteins for the development of optical biosensors for nitrogen monoxide and carbon monoxide. *The Analyst*, 120(11), 2725-2730 (1995)
18. P.M. Douglass, S. Daunert, J. D. Patel and L.G. Bachas. Biologically inspired, intelligent muscle material for sensing and responsive delivery of Countermeasures. *International Conference on Environmental Systems (ICES2000)*, Toulouse, France, July 10-13, 2000.
19. A. I. Kestner. Immobilized Enzymes. *Russ. Chem. Rev.*, 43(8), 690-705 (1974)
20. A. Mulchandani and K. R. Rogers, (eds). *Methods in Biotechnology: Enzyme and Microbial Biosensors*. Humana Press, New Jersey (1998)
21. J. M. S. Cabral and J. F. Kennedy. *In Protein Immobilization, Fundamental and Applications*; Taylor, R.F., Ed; Marcel Dekker, Inc.: New York, 1991; Chapter 3, pp 74.
22. J. M. S. Cabral and J. F. Kennedy. *In Thermostability of Enzymes*, M. N. Gupta ed., Narosa, New Delhi, 1993, pp 162.
23. A. S. Hoffman. Hydrogels for biomedical applications. *Adv. Drug Deliv. Rev.*, 43, 3-12, (2002)
24. Y. Qiu, K. Park. Environment-sensitive hydrogels for drug delivery. *Adv. Drug Deliver. Rev.*, 53 321-339 (2001)

25. N.A. Peppas, P. Bures, W. Leobandung, H. Ichikawa. Hydrogels in pharmaceutical formulations. *Eur. J. Pharmaceut. Biopharm.*, 50, 27-46 (2000)
26. N. A. Peppas. Hydrogels and drug delivery. *Curr. Opin. Colloid Interface Sci.*, 2, 531-537 (1997)
27. UNEP Publications. Methacrylic acid. SIDS Profile Summary. CAS N^o: 79-31-4
28. D. Hariharan, N.A. Peppas. Characterization, dynamic swelling behaviour and solute transport in cationic networks with applications to the development of swelling-controlled release systems. *Polym. J.*, 37(1), 149 (1995)
29. J. M. Harris (ed). *Poly(ethylene glycol) Chemistry: Biotechnical and Biomedical Applications*. Plenum Press, New York (1992)
30. A. E. Eroglu, M. Volkan and O. Yavuz Ataman. Fiber optic sensors using novel substrates for hydrogen sulfide determination by solid surface fluorescence. *Talanta*, 53, 89-101 (2000)
31. R. J. Russell, A. C. Axel, K. L. Shields, M. V. Pishko. Mass transfer in rapidly photopolymerized poly(ethylene glycol) hydrogels used for chemical sensing. *Polymer*, 42, 4893-4901 (2001)
32. D. H. Dawson, G. S. Henshaw and D. E. Williams, Description and characterization of a hydrogen sulfide gas sensor based on Cr_{2-y} Ti_yO_{3+x}. *Sens. Actuators B*, 26-27, 76-80 (1995)
33. T. L. Royster Jr., D. Chatterjee, G. R. Paz-Pujalt and C. A. Marrese. Fabrication and evaluation of thin-film solid-state sensors for hydrogen sulfide detection. *Sens. Actuators B*, 53, 155-162 (1998)
34. N. Miura, Y. Yan, G. Lu and N. Yamazoe. Sensing characteristics and mechanism of hydrogen sulfide sensor using stabilized zirconia and oxide sensing electrode. *Sens. Actuators B*, 34, 367-372 (1996)
35. E. Antonini and M. Brunori. *Hemoglobin and Myoglobin in their reactions with ligands*. Frontiers of Biology, North-Holland Publishing Company, Amsterdam, Vol 21, (1971)
36. S. Otsuka and T. Yamanaka. *Metalloproteins, Chemical Properties and Biological Effects, Bioactive Molecules*, Volume 8, Elsevier (1988)
37. S. Dewilde, E. Angelini, L. Kiger, M. C. Marden, M. Beltramini, B. Salvato. L. Moens. Structure and function of the globin and globin gene from the Antarctic mollusc *Yoldia eightsi*. *Biochem. J.*, 370, 245 (2003)

38. D. L. Nelson, M. M. Cox. *Lehninger Principles of Biochemistry*. Worth Publishers, (2000)
39. L. A. Moran, K. G. Scrimgeour, H. R. Horton, R. S. Ochs and J. D. Rawn. *Biochemistry*, Prentice Hall (1994)
40. M. Rizzi, J. B. Wittenberg, A. Coda, M. Fasano, P. Ascenci and M. Bolognesi. Structure of the sulfide-reactive Hemoglobin from the clam *Lucina pectinata*. *J. Mol. Biol.*, 244, 86-99 (1994)
41. M. Rizzi, J. B. Wittenberg, A. Coda, P. Ascenzi, M. Bolognesi. Structural bases for sulfide recognition in *Lucina pectinata* Hemoglobin I. *J. Mol. Biol.*, 258(1), 1-5 (1996)
42. J. Cerda, Y. Echevarria, E. Morales and J. Lopez-Garriga. Resonance Raman studies of the heme-ligand active site of Hemoglobin I from *Lucina pectinata*. *Biospectroscopy*, 5, 289-301 (1999)
43. D. W. Krauss and J. B. Wittenberg. Hemoglobins of the *Lucina pectinata*/Bacteria symbiosis. II. An electron paramagnetic resonance and optical spectral study of the ferric proteins. *J. Biol. Chem.*, The American Society for Biochemistry and Molecular Biology, Inc., 265(27), 16054-16059 (1990)
44. F. M. Antommattei-Perez, T. Rosado-Ruiz, C. Cadilla and J. Lopez-Garriga. The cDNA-derived amino acid sequences of hemoglobin I. from *Lucina pectinata*. *J. Protein Chem.*, 18(8), 831-836 (1999)
45. T. Rosado-Ruiz, F. M. Antommattei-Perez, C. L. Cadilla and J. Lopez-Garriga. Expresión and Purification of Recombinant Hemoglobin I from *Lucina pectinata*. *J. Protein Chem.*, 20(4), 311-315 (2001)
46. J. Helbing, L. Bonacina, R. Pietri, J. Bredenbeck, P. Hamm, F. van Mourik, F. Chaussard, A. Gonzalez-Gonzalez, M. Chergui, C. Ramos-Alvarez, C. Ruiz and J. Lopez-Garriga. Time-resolved visible and infrared study of the cyano complexes of myoglobin and of Hemoglobin I from *Lucina pectinata*. *Biophys. J.*, 87, 1881-1891 (2004)
47. L. Estrada. *Immobilization of Hemoglobin I from Lucina Pectinata in Tetramethylorthosilicate (TMOS) Gels*, Ms Thesis, Chemical Department Puerto Rico University, Mayagüez (2001)
48. P. Gemeiner. *In Enzyme Engineering: Immobilized Biosystems*. P. Gemeiner (ed), Ellis Horwood Limited (1992)
49. L. Gao, Q. Gao, Q. Wang, S. Peng and J. Shi. Immobilization of hemoglobin at the galleries of layered niobate $\text{HfCa}_2\text{Nb}_3\text{O}_{10}$. *Biomaterials*, 26, 5267-5275 (2005)

50. M. P. J. Kierstan, M.P. Coughlan. *In Protein Immobilization Fundamentals and Applications*; Taylor, R. F., Ed.; Marcel Dekker, Inc. (1991)
51. C. O. Fagain. *In: Stabilizing Protein Function*. C. O. Fagain (ed), Berlin, (1997)
52. M. T. Reetz. Entrapment of biocatalysts in hydrophobic sol-gel materials for use in organic chemistry. *Advanced Materials*, 9, 943-954 (1997)
53. M. Carena and F. M. Veronese. Entrapment of biomolecules into hydrogels obtained by radiation-induced polymerization. *J. Control. Release*, 29, 187-193 (1994)
54. W. Tischer and F. Wedekind. Immobilized Enzymes: Methods and Applications. *Biocatalysis-From Discovery to Application*. 200, 95-126 (1999)
55. L. J. Blum, P. R. Coulet, (eds). *Biosensor Principles and Applications*. Marcel Dekker, New York (1991)
56. S. Cosnier. Biomolecule immobilization on electrode surfaces by entrapment or attachment to electrochemically polymerized films. A review. *Biosen. Bioelectron.*, 14, 443-456 (1999)
57. I. Karube and Y. Nomura. Enzyme sensors for environment analysis. *J. Mol. Catal. B: Enzym.*, 10, 177-181 (2000)
58. B. M. Paddle. Biosensors for chemical and biological agents of defense interest. *Biosen. Bioelectron.*, 11(11), 1079-1113 (1996)
59. Y. Liu and T. Yu. Polymers and enzyme biosensors. *Rev. Macromol. Chem. Phys.*, C37(3), 459-500 (1997)
60. J. C. Salamone, (ed). *Concise Polymeric Materials Encyclopedia*. CRC Press LLC (1999)
61. J. F. Liang, Y. T. Li and V. C. Yang. Biomedical applications of immobilized enzymes. *J. Pharm. Sci.*, 89(8), 979-990 (2000)
62. J. D. Newman, L.J. Tigwell, P. J. Warner and A. P. F. Turner. Biosensors: boldly going into the new millennium. *Sensor Rev.*, 21(4), 268-271 (2001)
63. A. P.F. Turner. Biosensors: sense and sensitivity. *Science Magazine*, 290, 1315-1317 (2000)
64. S. J. Alcock and A. P. F. Turner. Continuous analyte monitoring to aid clinical practice. *IEEE Eng. Med Biol.*, 13(3), 319-325 (1994)

65. M. J. Dennison, A. P. F. Turner. Biosensors for environmental monitoring. *Biotechnol. Adv.*, 13(1), 1-12 (1995)
66. K. J. M. Sandström and A. P. F. Turner. Biosensors in air monitoring. *J. Environ. Monit.*, 1, 293-298 (1999)
67. W. E. Hennink and C. F. van Nostrum. Novel crosslinking methods to design hydrogels. *Adv. Drug Deliver. Rev.*, 54, 13-36 (2002)
68. M. Morishita, A. M. Lowman, K. Takayama, T. Nagai and N. A. Peppas. Elucidation of the mechanism of incorporation of insulin in controlled release systems based on complexation polymers. *J. Control. Release*, 81, 25-32 (2002)
69. C. L. Bell and N. A. Peppas. Water, solute and protein diffusion in physiologically responsive hydrogels of poly(methacrylic acid-g-ethylene glycol). *Biomaterials*, 17, 1203-1218 (1996)
70. N. A. Peppas, Y. Huang, M. Torres-Lugo, J. H. Ward and J. Zhang. Physicochemical foundations and structural design of hydrogels in medicine and biology. *Annu. Rev. Biomed. Eng.*, 02, 9-29 (2000)
71. N. A. Peppas and A. R. Khare. Preparation, structure and diffusional behavior of hydrogels in controlled release. *Adv. Drug Deliver. Rev.*, 11, 1-35 (1993)
72. L.M. Schwarte, K. Podual and N.A. Peppas. Cationic hydrogels for controlled release of proteins and other macromolecules. *American Chemical Society*, 3, 56-66 (1998)
73. M. T. am Ende, D. Hariharan D and N. A. Peppas. Factors influencing drug and protein transport and release from ionic hydrogels. *React. Polym.*, 25, 127-137 (1995)
74. K. Podual, F. J. Doyle III and N. A. Peppas. Glucose-sensitive of glucose oxidase-containing cationic copolymer hydrogels having poly(ethylene glycol) grafts. *J. Controlled Release*, 67, 9-17 (2000)
75. P. J. Flory. Statistical mechanics of swelling of network structures. *J. Chem. Phys.*, 18(1), 108-111 (1950)
76. L. Brannon-Peppas and N. A. Peppas. Equilibrium swelling behavior of pH-sensitive hydrogels. *Chem. Eng. Sci.*, 46(3), 715-722 (1991)
77. P. J. Flory and J. Rehner. Statistical mechanics of cross-linked polymer networks II. Swelling. *J. Chem. Phys.*, 11(11), 521-526 (1943)

78. N. A. Peppas and E. W. Merrill. Crosslinked poly(vinyl alcohol) hydrogels as swollen elastic networks. *J. Appl. Polym. Sci.*, 21, 1763-1770 (1977)
79. N. A. Peppas. *Hydrogels in medicine and pharmacy applications*. CRC Press: Boca Raton, Florida, vol. 1 (1987)
80. A. Katchalsky and I. Michaeli. Polyelectrolyte gels in salt solutions. *J. Polym. Sci.*, 15, 69-86 (1955)
81. J. Ricka and T. Tanaka. Swelling of ionic gels: Quantitative performance of the Donnan theory. *Macromolecules*, 17, 2916-2921 (1984)
82. M. T. am Ende and N. A. Peppas. Transport of ionizable drugs and proteins in crosslinked Poly(acrylic acid) and Poly(acrylic acid-co-2-hydroxyethyl methacrylate) hydrogels. II. Diffusion and release studies. *J. Control. Release*, 48, 47-56 (1997)
83. L. Masaro and X. X. Zhu. Physical models of diffusion for polymer solutions, gels and solids. *Prog. Polym. Sci.*, 24, 731-775 (1999)
84. J. Crank. *The mathematics of diffusion*. 2nd edition, Oxford University Press, New York (1975)
85. M. T. am Ende and Mikos AG. Diffusion-controlled delivery of proteins from hydrogels and other hydrophilic systems. *Protein Delivery: Physical Systems*. Edited by Sanders and Hendren. Plenum Press, New York (1997)
86. M. C. Thimmegowda, P. D. Sathyanarayana, G. Shariff, M B. Ashalatha, R. Ramani and C. Ranganathaiah. A free volume microprobe study of water sorption in a contact tens polymer. *J. Biomater. Sci. Polymer Edn.*, 13(12), 1295-1311 (2002)
87. D. J. Ensore, H. B. Hopfenberg, V. T. Stannett and A. R. Berens. Effect of prior sample history on n-hexane sorption in glassy polystyrene microspheres. *Polymer*, 18, 1105-1110 (1977)
88. A. R. Berens and H. B. Hopfenberg. Diffusion and relaxation in glassy polymer powders: 2. Separation of diffusion and relaxation parameters. *Polymer*, 19, 489-496 (1978)
89. A. R. Berens. Diffusion and relaxation in glassy polymer powders: 1. Fickian diffusion of vinyl chloride in poly(vinyl chloride). *Polymer*, 18, 697-704 (1977)
90. D. J. Ensore, H. B. Hopfenberg and V. T. Stannett. Effect of particle size on the mechanism controlling n-hexane sorption in glassy polystyrene microspheres. *Polymer*, 18, 793-800 (1977)

91. E. W. Merrill, K. A. Dennison and C. Sung. Partitioning and diffusion of solutes in hydrogels of poly(ethylene oxide). *Biomaterials*, 14(15), 1117-1126 (1993)
92. M. Torres-Lugo and N. A. Peppas. Molecular Design and in Vitro Studies of Novel pH-Sensitive Hydrogels for the Oral Delivery of Calcitonin. *Macromolecules*, 32, 6646-6651 (2000)
93. S. W. Kim, Y. H. Bae and T. Okano. Hydrogels: swelling, drug loading, and release. *Pharm. Res.*, 9(3), 283-290 (1992)
94. B. Kim, N. A. Peppas. Analysis of molecular interactions in poly(methacrylic acid-g-ethylene glycol) hydrogels. *Polymer*, 44, 3701-3707 (2003)
95. C. L. Bell and N. A. Peppas. Modulation of drug permeation through interpolymer complexed hydrogels for drug delivery applications. *J. Control. Release*, 39, 201-207 (1996)
96. A. M. Mathur, K. F. Hammonds, J. Klier and A. B. Scranton. Equilibrium swelling of poly(methacrylic acid-g-ethylene glycol) hydrogels. Effect of swelling medium and synthesis conditions. *J. Control. Release*, 54, 177-184 (1998)
97. M. Schwartz, H. Guterman and J. Kost. Electrical properties of glucose-sensitive hydrogels: Swelling and conductivity relationships. *J. Biomed. Mater. Res.*, 41, 65-70 (1998)
98. P. Gupta, K. Vermani and S. Garg. Hydrogels: from controlled release to pH-responsive drug delivery. *Drug Discov. Today*, 7(10), 569-579 (2002)
99. K. Y. Lee and D. J. Mooney. Hydrogels for Tissue Engineering. *Chem. Revs.*, 101, 1869-1879 (2001)
100. S. Herber, W. Olthuis and P. Bergveld. A swelling hydrogel-based P_{CO2} sensor. *Sens. Actuators, B*, 91, 378-382 (2003)
101. S. Brahim, D. Narinesingh and A. Guiseppi-Elie. Bio-smart hydrogels: co-joined molecular recognition and signal transduction in biosensor fabrication and drug delivery. *Biosen. Bioelectron.*, 17, 973-981 (2002)
102. A. E. F. Nassar, W. S. Willis and J. Rusling. Electron transfer from electrodes to myoglobin: facilitated in surfactant films and blocked by absorbed biomacromolecules. *Anal. Chem.*, 67, 2386-2392 (1995)
103. H. Ma, N. Hu and J. F. Rusling. Electroactive myoglobin films grown layer-by-layer with poly(styrenesulfonate) on pyrolytic graphite electrodes. *Langmuir*, 16, 4696-4975 (2000)

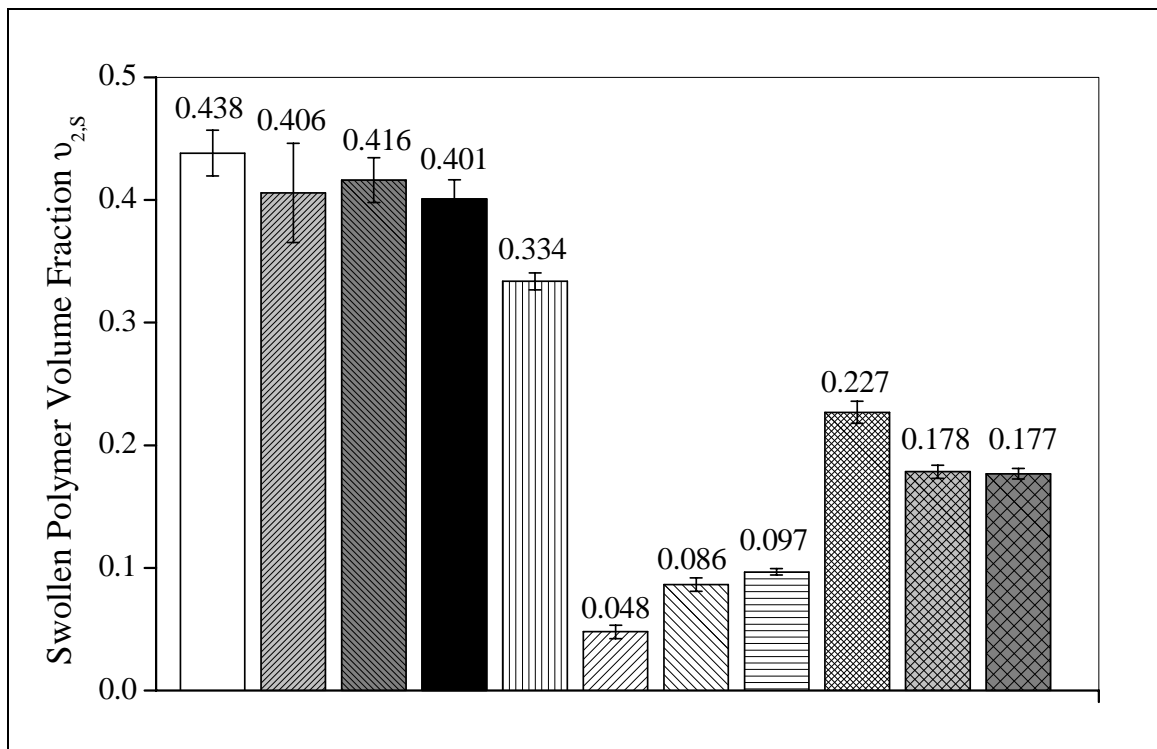
104. R. S. Freire, C. A. Pessoa, L. D. Mello and L. T. Kubota. Direct electron transfer: an approach for electrochemical biosensors with higher selectivity and sensitivity. *J. Braz. Chem. Soc.*, 14(2), 230-243 (2003)
105. H. Lu, Z. Li and N. Hu. Direct voltammetry and electrocatalytic properties of catalase incorporated in polyacrylamide hydrogel films. *Biophys. Chem.*, 104, 623-632 (2003)
106. N. Hu. Direct electrochemistry of redox proteins or enzymes at various film electrodes and their possible applications in monitoring some pollutants. *Pure Appl. Chem.*, 73(12), 1979-1991 (2001)
107. C. Fan, H. Wang, S. Sun, D. Zhu, G. Wagner and G. Li. Electron-transfer reactivity and enzymatic activity of hemoglobin in a SP Sephadex membrane. *Anal. Chem.*, 73, 2850-2854 (2001)
108. H. Y. Gu, A. M. Yun and H. Y. Chen. Direct electron transfer and characterization of hemoglobin immobilized on a Au colloid-cysteamine-modified gold electrode. *J. Electrochem. Chem.*, 516, 119-126 (2001)
109. S. Liu, Z. Dai, H. Y. Chen and H. X. Ju. Immobilization of hemoglobin on zirconium dioxide nanoparticles for preparation of a novel hydrogen peroxide biosensor. *Biosen. Bioelectron.*, 19, 963-969 (2004)
110. H. Y. Gu, A. M. Yu, S. S. Yuan, H. Y. Chen. Amperometric nitric oxide biosensor based on the immobilization of the hemoglobin on a nanometer-sized gold colloid modified Au electrode. *Anal. Lett.*, 35(4), 647-661 (2002)
111. X. Xu, S. Liu, B. Li and H. Ju. Disposable nitrite sensor based on hemoglobin-colloid gold nanoparticle modified screen-printed electrode. *Anal. Lett.*, 36(11), 2427-2442 (2003)
112. L. Shen, R. Huang and N. Hu. Myoglobin in polyacrylamide hydrogel films: direct electrochemistry and electrochemical catalysis. *Talanta* 56, 1131-1139 (2002)
113. J. F. Rusling. Enzyme bioelectrochemistry in cast biomembrane-liked films. *Acc. Chem. Res.*, 31, 363-369 (1998)
114. X. Chen, N. Hu, Y. Zeng, J. F. Rusling and J. Yang. Ordered electrochemically active films of hemoglobin, didodecyldimethylammonium ions and clay. *Langmuir*, 15, 7022-7030 (1999)
115. R. Huang and N. Hu. Direct voltammetry and electrochemical catalysis with horseradish peroxidase in polyacrylamide hydrogel films. *Biophys. Chem.*, 104, 199-208 (2003)

116. H. Sun, N. Hu and H. Ma. Direct electrochemistry of hemoglobin in polyacrylamide hydrogel films on pyrolytic graphite electrodes. *Electroanal.*, 12(13), 1064-1070 (2000)
117. S. Liu and H. X. Ju. Nitrite reduction and detection at a carbon paste electrode containing hemoglobin and colloidal gold. *Analyst*, 128, 1420-1424 (2003)
118. S. Liu, Z. Dai, H. Chen and H. Ju. Immobilization of hemoglobin on zirconium dioxide nanoparticles for preparation of a novel hydrogen peroxide biosensor. *Biosen. Bioelectron.*, 19, 963-969 (2004)
119. B. A. McCool, R. Cashion, G. Karles and W. J. DeSisto. Silica encapsulated hemoglobin and myoglobin powders prepared by an aqueous fast-freezing technique. *J. Non-Cryst. Solids*, 333, 143-149 (2004)
120. N. Shibayama and S. Saigo. Fixation of the quaternary structures of human adult hemoglobin by encapsulation in transparent porous silica gels. *J. Mol. Biol.*, 251, 203-209 (1995)
121. E. H. Lan, B. C. Dave, J. M. Fukuto, B. Dunn, J. I. Zink and J. S. Valentine. Synthesis of sol-gel encapsulated heme proteins with chemical sensing properties. *J. Mater. Chem.*, 9, 45-53 (1999)
122. B. C. Dave, J. M. Miller, B. Dunn, J. S. Valentine and J. I. Zink. Encapsulation of proteins in bulk and thin film sol-gel matrices. *J. Sol-Gel Sci. Technol.*, 8, 629-634 (1997)
123. M. F. McCurley, G. J. Bayer and S. A. Glazier. A fluorescence assay for dissolved oxygen using sol-gel encapsulated myoglobin and an analogy to the inner filter effect. *Sens. Actuators B*, 35-36, 491-496 (1996)
124. L. Chen, Z. Tian and Y. Du. Synthesis and pH sensitivity of carboxymethyl chitosan-based polyampholyte hydrogels for protein carrier matrices. *Biomaterials*, 25, 3725-3732 (2004)
125. J. E. Elliott, M. Macdonald, J. Nie, C. N. Bowman. Structure and swelling of poly(acrylic acid) hydrogels: effect of pH, ionic strength, and dilution on the crosslinked polymer structure. *Polymer*, 45, 1503-1510 (2004)
126. M. B. Mellott, K. Searcy and M. V. Pishko. Release of protein from highly cross-linked hydrogels of poly(ethylene glycol) diacrylate fabricated by UV polymerization. *Biomaterials*, 22, 929-941 (2001)
127. B. Amsden. Solute diffusion in hydrogels. An examination of the retardation effect. *Polym. Gels Netw.*, 6, 13-43 (1998)

128. P. van de Wetering, A. T. Metters., R. G. Schoenmakers and J. A. Hubbell. Poly(ethylene glycol) hydrogels formed by conjugate addition with controllable swelling, degradation, and release of pharmaceutically active proteins. *J. Controlled Release*, 102, 619-627 (2005)
129. S. H. Gehrke, L. H. Uhden and J. F. McBride. Enhanced loading and activity retention of bioactive proteins in hydrogel delivery systems. *J. Control. Release*, 55, 21 (1998)
130. B. Jeong, A. Gutowska. Lessons from nature: stimuli-responsive polymers and their biomedical applications. *Trends Biotechnol.*, 20, 305-311 (2002)
131. H. Zhou. Dimensions of denatured protein chains from hydrodynamic data. *J. Phys. Chem. B*, 106, 5769-5775 (2002)
132. M. Guo and G. Narsimhan. Solubility of Globular Proteins in Poly- charide solutions. *Biotechnol. Prog.*, 7, 54-59 (1991)
133. R. Guo and G. Narsimhan. Phase Diagram for the Mixture of Globular Proteins and Uncharged Polymers. *Paper presented at the IFT Annual Meeting.*, June 25-29, Atlanta, GA (1994)
134. J. M. Harris and S. Zalipsky, In: *Chemistry and Biological Applications of Polyethylene glycol*. ACS Books, Washington, D.C., (1997)
135. K. Nakamura, R. J. Murray, J. I. Joseph, N. A. Peppas, M. Morishita and A. L. Lowman. Oral insulin delivery using P(MAA-g-EG) hydrogels: effects of network morphology on insulin delivery characteristics. *J. Controlled Release*, 95, 589-599 (2004)

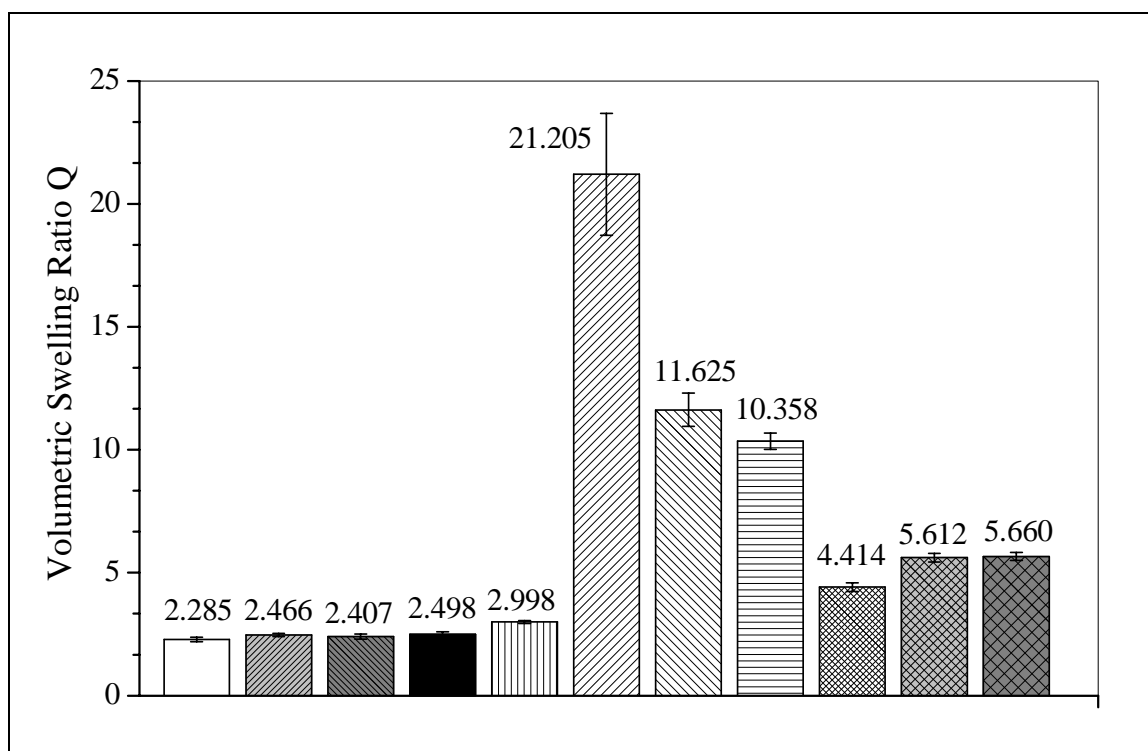
APPENDIX 1

Polymer volume fraction in the swollen state for various hydrogel compositions; □ PEGMA200-PEGDMA600 (n=7), ▨ PEGMA200-PEGDMA1000 (n=9), ▩ PEGMA400-PEGDMA600 (n=8), ■ PEGMA400-PEGDMA1000 (n=8), ▤ PEGMA1000-PEGDMA1000 (n=9), ▧ MAA-PEGDMA200 (n=7), ▨ MAA-PEGDMA600 (n=6), ▩ MAA-PEGDMA1000 (n=7), ▪ DMAEM-PEGDMA200 (n=7), ▫ DMAEM-PEGDMA600 (n=6), ▬ DMAEM-PEGDMA1000 (n=6). Each bar represents an average \pm one standard deviation.



APPENDIX 2

Volumetric swelling ratio for various hydrogel compositions; □ PEGMA200-PEGDMA600 (n=7), ▨ PEGMA200-PEGDMA1000 (n=9), ▩ PEGMA400-PEGDMA600 (n=8), ■ PEGMA400-PEGDMA1000 (n=8), ▤ PEGMA1000-PEGDMA1000 (n=9), ▦ MAA-PEGDMA200 (n=7), ▧ MAA-PEGDMA600 (n=6), ▨ MAA-PEGDMA1000 (n=7), ▩ DMAEM-PEGDMA200 (n=7), ▪ DMAEM-PEGDMA600 (n=6), ▫ DMAEM-PEGDMA1000 (n=6). Each bar represents an average \pm one standard deviation.



APPENDIX 3

Kinetic constants and efficiency of the initiator 1-Hydroxy cyclohexyl phenyl ketone.

	k_p , propagation kinetic constant	k_t , termination kinetic constant	k_d , decay kinetic constant	f , efficiency
1-Hydroxy cyclohexyl phenyl ketone	670 L/(mol-s)	0.0165 s ⁻¹	2.1x10 ⁶ L/(mol-s)	0.5
Reference	[69]	[69]	[69]	[69]

APPENDIX 4

Values of the different polymer parameters used for the calculation of the molecular weight between crosslinks.

Parameters	Value	Reference
$\chi_{1,MAA}$, Flory-Huggins polymer-water interaction parameter	0.499	[69]
$\chi_{1,DMAEM}$, Flory-Huggins polymer-water interaction parameter	0.22	[135]
$\chi_{1,PEGDMA}$, Flory-Huggins polymer-water interaction parameter	0.55	[69]
$C_{n,MAA}$, Flory characteristic ratio of the polymer	14.66	[69]
$C_{n,DMAEM}$, Flory characteristic ratio of the polymer	11	[135]
$C_{n,PEGMA}$, Flory characteristic ratio of the polymer	3.8	[69]
V_1 , molar volume of water	18 cm ³ /mol	[69]
l , length of the bond along the polymer backbone	0.154 nm	[69]